Summer 7-30-2019

Changes in Mammalian Abundance Through the Eocene-Oligocene Climate Transition in the White River Group of Nebraska, USA

Robert Gillham
University of Nebraska - Lincoln, rgillham2@huskers.unl.edu

Changes in Mammalian Abundance Through the Eocene-Oligocene Climate Transition in the White River Group of Nebraska, USA

By

Robert B. Gillham

A THESIS

Presented to the Faculty of
The Graduate College at the University of Nebraska
In Partial Fulfillment of Requirements
For the Degree of Master of Science

Major: Geosciences
Under the Supervision of Professor Ross Secord

Lincoln, NE
August, 2019

Changes in Mammalian Abundance Through the Eocene-Oligocene Climate Transition in the White River Group of Nebraska, USA

Robert B. Gillham M.S.
University of Nebraska, 2019
Advisor: Ross Secord

Marine records show major cooling during the Eocene-Oligocene Climate Transition (EOCT). Most proxy studies in the White River Group suggest drying across the EOCT, and some suggest cooling. The lower resolution continental record has hindered a direct correlation of the marine climate record to Nebraska. I explore various correlation schemes and what they imply for faunal changes. This study compiles and analyzes data from 4,875 specimens in the University of Nebraska State Museum (UNSM) collection to test the hypothesis that climate change across the Eocene-Oligocene (E-O) boundary caused significant abundance changes in mammals. A series of binning schemes was created. One binning scheme followed previously established lithological zones, two schemes were based on average sediment accumulation rates, and three more were created by applying a cubic spline curve to published $^{206}Pb/^{238}U$ zircon ash dates. For the purpose of correlating the marine and Toadstool sections, I constructed a high-resolution (±0.5 m) carbon isotope stratigraphy across the E-O boundary using fossil enamel from the oreodont *Merycoidodon*. Results show that turnover in taxonomic abundance occurs throughout the study interval and is not concentrated across the EOCT. The largest pulse of faunal change and largest abundance changes for the most common taxa, *Merycoidodon* and the horse *Mesohippus*, slightly predate the EOCT. This raises the possibility that climate change began earlier in the continental interior than indicated by the marine benthic oxygen isotope record. Chord distance analyses reveal that the faunal composition of Orellan zones are more similar to

one another than they are to the faunas of Chadron zones. This similarity is likely caused by the extinction, or near extinction, of Chadron taxa like *Megacerops* around the EOCT. Despite the lack of significant change in evenness, numerous taxa underwent extended changes in relative abundance through time. *Archaeotherium,* a water-dependent artiodactyl, decreased in relative abundance through time just as *Poebrotherium*, a water-independent camelid, increased in abundance through time. Changes in the relative abundances of *Poebrotherium* and *Archaeotherium* are consistent with a drier environment beginning in EOCT. The level of water-dependence in other taxa is less clear, and their changes in abundance cannot be confidently explained through diet, dentition, body mass, or locomotion.

DEDICATION

Dedicated to my wife, Kathleen Gillham, who has made every day of our time here even better and to the best family anyone could ask for.

TABLE OF CONTENTS

LIST OF FIGURES

PAGE

LIST OF TABLES

PAGE

APPENDIX FIGURES

APPENDIX TABLES

INTRODUCTION

Numerous authors have studied climate change across the Eocene-Oligocene boundary in both the marine (Zanazzi et al., 2007, 2009; Cramer et al., 2009; Galeotti et al., 2016; Zhang et al., 2017; Śliwińska et al., 2019) and terrestrial realms (Pearson et al., 2008; Zanazzi and Kohn, 2008; Sheldon, 2009; Hooker et al., 2010; Xiao et al., 2010; Boardman and Secord, 2013; Zhang and Guo, 2014). Studies have generally concluded that major climate change occurred at high latitudes, but efforts to calculate temperature change precisely have been hampered as marine oxygen isotope ratios are vulnerable to changes ice sheet volume (Zachos et al., 2001; Ivany et al., 2006; Petersen et al., 2015). Simultaneously, proxies for continental climate in North America have yielded disparate results, with interpretations ranging from minor to major cooling (Wolfe, 1978, 1992, 1994; Sheldon, 2009; Sheldon and Retallack, 2004; Zanazzi et al., 2007). Continental studies also vary from showing no appreciable change in precipitation to a marked drying signal (Clark et al., 1967; Terry, 2001; Sheldon and Retallack, 2004; Zanazzi et al., 2007, 2009; Boardman and Secord, 2013). Nevertheless, most studies have found that drying (Clark et al., 1967; Terry, 2001; Sheldon and Retallack, 2004; Boardman and Secord, 2013) and an unresolved amount of cooling occurred.

The impact that this climate shift had on terrestrial mammalian faunas in the White River Group is also controversial. Several taxa go extinct at or near the Eocene-Oligocene boundary, including the graviportal brontotheres, which were by far the largest mammals living in North America at that time. The magnitude of faunal turnover at the boundary, however, may not have been above background levels. Prothero (1994), Prothero and Heaton (1996), and Prothero (1999) argued that a 13 °C drop in temperate occurred across the boundary but that it had no significant effect on North America mammalian turnover. However, all current estimates of

cooling are much smaller than 13 °C. While none of these studies performed a rigorous faunal turnover analysis, the number of taxa that go extinct at or near the boundary appears to be small relative to the number that cross the boundary.

In a more recent study of faunal change, Alroy et al. (2000) measured a dozen variables, including standing diversity, per-lineage origination and extinction rates, total turnover, net diversification, change in proportional representation of major orders, and the mean, standard deviation, skewness, and kurtosis of body mass. These authors divided the Cenozoic record randomly into 1 million-year bins with no consideration for established divisions of time such as epochs, land-mammal ages, or biozones. They found no consistent correlation between climate and any of the various faunal dynamics tested. Consequently, the EOCT did not fall out as an interval of significant faunal turnover. They concluded that factors like within-lineage competition and logistic diversity dynamics were more important drivers of mammal evolution than climate (Alroy et al., 2000). Because of the coarse nature of this study, however, and their random choice of bins, their study could have homogenized any interesting biological signals across the EOCT.

Although mammalian faunal turnover in the White River Group across the EOCT does not appear to have been significant, with 62 out of 70 species persisting across the EOCT (Prothero and Heaton, 1996), a switch to drier and possibly cooler climate might be expected to favor some taxa and result in abundance changes. To test whether there were significant changes in relative abundance across the EOCT, I compiled data for 24 mammalian genera that cross the EOCT from 4,875 specimens curated in the University of Nebraska State Museum (UNSM). I explored the use of different binning schemes. Taxa were assigned to bins corresponding to specific stratigraphic intervals of equal chronologic length and analyses were conducted to test

for abundance changes. I also tested for changes in the evenness of faunal distributions using Simpson-D and Shannon H diversity indices (Shannon, 1948; Simpson, 1949; Allen et al., 2009). With the aim of better correlating the marine climate record (Galeotti et al., 2016) to the section in Toadstool Geological Park, I also constructed a high-resolution record of $\delta^{13}C$ values from the enamel of the common oreodont *Merycoidodon*. This record allowed me to use local lithologic zones created by Schultz and Stout (1955) and create new stratigraphic intervals (bins) for this study on the basis of the inferred climatic shifts. I then used these zones and bins to more rigorously test for a mammalian response to climate change across the EOCT.

STRATIGRAPHIC SETTING AND PALEOCLIMATIC CONTEXT

Lithostratigraphy

The White River Formation/Group on the High Plains has been studied since the mid-19th century (Leidy, 1848; Owen, 1848, 1850). Lithostratigraphic, biostratigraphic, tephrostratigraphic, and magnetostratigraphic intervals within the unit were defined and redefined over time. Most currently, the White River has been assigned group rank in South Dakota and Nebraska, and formation rank in Colorado and Wyoming. This is despite thicker stratigraphic intervals in Wyoming. The White River Group (WRG) contains the Chamberlain Pass, Chadron, and Brule formations (LaGarry 1998, Terry 1998). These formations, in turn, have members within them that vary regionally. The best exposures of White River rocks are in Nebraska, South Dakota, and Wyoming. The WRG contains an abundance of well-preserved vertebrate fossils and represents one of the best preserved and most complete Cenozoic fossil sequences in the world. Faunal sequences in the WRG are the basis for three North American

Land Mammal ages (NALMAs): the Chadronian (latest Eocene), Orellan (early Oligocene), and Whitneyan ("middle" Oligocene) (Emry et al., 1987; Prothero and Emry, 2004).

The Chadron Formation chiefly consists of greenish channel-fill sandstones, and overbank siltstones, and it also contains rare lacustrine limestones (Schultz and Stout, 1955; Clark and Beerbower, 1967; Evans and Welzenbach, 1998). It contains a large proportion of fluvially reworked volcaniclastic sediment (Swinehart et al., 1985).

Schultz and Stout (1955) divided the Chadron Formation into lithologic units named A, B, and C, in ascending stratigraphic order (Fig. 1). Chadron A is a brightly-colored conglomerate that contains blocks of reworked Pierre Shale and is only exposed in limited areas. This stratigraphic interval is also referred to as the Yoder Beds (Schultz and Stout, 1955), and it was later grouped within the Chamberlain Pass Formation (Terry 1998, Terry and LaGarry 1998). The overlying Chadron B interval was further divided into B1-B4 by a series of marker beds such as ashes, paleosols, gypsum, and limestones (Fig. 1) by Terry and LaGarry (1998). The lowest part of Chadron B, mostly the B1 subunit, was renamed the Peanut Peak Member, while the rest of Chadron B, C, and Orella A units from Schultz and Stout (1955) were combined in the Big Cottonwood Creek Member by Terry and LaGarry (1998).

The common marker beds in the Cottonwood Creek Member are ash beds referred to as "the purplish-white" beds or "purple white" (PW) beds by Schultz and Stout (1955). These beds actually have no purplish tint, but Schultz and Stout were wearing rose-tinted sunglasses when describing them (George Corner, University of Nebraska State Museum, personal communication). There are five "purple-white" ash beds in total, with the fifth being the lowest and the first the highest. The first purple-white ash layer is more commonly referred to as the "Upper Purple White" or UPW. The second purple white is most often called the "Lower Purple

White" or LPW. Together the UPW and LPW form the boundaries of Chadron C. The other purple-white layers form the boundaries of Chadron B1-B4, while the Third Purple White marks the base of B4 and the top of B3. The Fourth Purple White marks the base of B3 and the top of B2. Finally, the Fifth Purple White marks the base of base of B2 and the top of B1.

The Brule Formation conformably overlies the Chadron Formation (LaGarry, 1998), and like the latter, it contains abundant primary airfall and fluvially reworked ash in an upward-increasing trend (Retallack, 1983; Clark and Beerbower 1967; Swinehart et al 1985). Schultz and Stout (1955) divided the Brule Formation into the Orella and Whitney members. They subdivided the Orella member into Orella A, B, C, and D zones, in ascending stratigraphic order (Fig. 1). On the basis of its lithology, Orella A is now considered to be a part of the Big Cottonwood Creek Member of the Chadron Formation (Terry and LaGarry, 1998). Orella A is a green to buff claystone that consists of the inclusive, 10 m stratigraphic interval from the UPW and upward to the base of the lower nodular layer (LNL) of Schultz and Stout (1955). The LNL is sometimes referred to as the first nodular layer or the lowest nodules of Orella B in the UNSM collection field notes and Schultz and Stout (1955). Orella B extends from the LNL and ends at the Upper Nodular Layer just under 15 m higher (Schultz and Stout, 1955). Like Orella A, Orella B is mostly green to buff claystones, but with many nodules, concretions, and sandstones mixed in as well. Orella C is composed of laminated brown claystone and siltstone with a thick complex of channel cuts that in some places descend into lower parts of the Orella member (Schultz and Stout, 1955). The upper boundary of Orella C was referred to as "bench" or "the bench" in Schultz and Stout (1955) but has now been recognized as the Serendipity Ash (LaGarry, 1998). Orella C is typically about 21m in thickness in most places but can be locally as thick as 44.5m (Schultz and Stout, 1955). Finally, Orella D is composed of brown to buff

claystones and siltstones and contains several nodule layers. The White Bed once marked the boundary between the Orella and Whitney members. The White Bed is also referred to as "the White Nodule Layer", "the White Zone", "Highest of the Channel Sandstones" or simply "X" in Schultz and Stout and the UNSM collections of the White River Room. LaGarry, (1998), redefined the upper boundary of the Orella Member as 2.5-5.0 m below the White Bed rather than right on it.

Geochronology

The most recent $^{40}Ar/^{39}Ar$ dates suggested that the Chadronian normal magnetozone correlates with chron C16n (35.89-35.71 Ma), the late Chadronian normal magnetozone with chron C15n (35.29-35.00 Ma), the early Orellan normal magnetozone with chron C13n (33.71-33.16 Ma), and the late Whitneyan with chron C12n (31.03-30.59 Ma) (Prothero, 1996; Ogg, 2012). However, there is uncertainty of up to several meters in the magnetochrons stratigraphic placement (D. Terry written communication) that could alter the ages calculated from the Prothero (1996) work.

Sahy et al. (2015), examined Prothero's work and determined that the $^{40}Ar/^{39}Ar$ dates were lower in precision and accuracy with an unknown bias to be roughly one million years older than U-Pb zircon dates. Recently, Sahy et al. (2017) have also moved the age of the E-O boundary to 34.09 ± 0.08 Ma. A cubic spline curve that includes both the new Sahy et al. (2015) and Prothero (1996) magnetozone dates shows that there is great inconsistency in results between the two. This is probably due to the higher accuracy of the Sahy et al. (2015) dates coupled with the uncertain placement of the magnetochrons.

Numerous revised $^{206}Pb/^{238}U$ zircon dates were recently published by Sahy et al. (2015) for ashes in the White River Group of Nebraska. Upper Whitney Ash = 30.908 ± 0.021 Ma; Lower Whitney Ash = 31.777 ± 0.012 Ma; Serendipity Ash = 33.414 ± 0.035 Ma; and the Upper Purple White (UPW) = 33.919 ± 0.033.

Thus, age control is well-distributed throughout the unit, however, there is a disjunction between these $^{206}Pb/^{238}U$ zircon dates and the widely cited $^{40}Ar/^{39}Ar$ dates of Prothero and Swisher (1992) needs to be corrected in future work the Toadstool magnetostratigraphy was revised by

Paleoclimate and Paleoenvironments

Leaf-margin analyses using fossils from the Florissant Fossil Beds National Monument, Colorado (MacGinitie, 1953), and costal floras ranging from Alaska to the Mississippi embayment suggest a large-scale cooling of ~7-8 °C across the Eocene-Oligocene boundary in North America (Wolfe, 1978, 1992, and 1994). However, the Florissant flora is a single point in time and its elevation (and accuracy of its MAT estimate) has been much debated. Additionally, the costal floras used to reconstruct temperature could very well yield different estimates than superposed floras from the continental interior. Unfortunately, macrofloras are apparently not preserved in the classic White River Orellan sites in Nebraska and Wyoming, which contain the E-O boundary. Also, problems associated with the replication of results from leaf-margin analyses have been recognized since these classic studies (e.g., Kowalski, 2003).

Another climate proxy suggested a mean annual decrease in temperature of ~7.1 ± 3.1 °C across the E-O boundary in the White River Group of Nebraska of the EOCT utilized based on $\delta^{18}O$ values from local fossil bone and mammalian tooth enamel (Zanazzi et al., 2009). The

enamel $\delta^{18}O$ values did not change significantly but values in the bone, which were assumed to be diagenetically reset to groundwater within 20-50 thousand years after burial, increased across the boundary by ~1.5‰. However, this approach assumes that mammals were drinking from water with the same $\delta^{18}O$ values as the water that formed the diagenetically altered bone carbonate. This assumption cannot be demonstrated. Post-burial groundwater can have very different values than surface water and is prone to evaporation. It is also difficult to precisely time when alteration occurs (Sheldon, 2009) and alteration may be incomplete. Sheldon (2009), noted that an increase in aridity could change the values in diagenetically altered bone and would then increase the perceived temperature change. Thus, the Zanazzi et al. (2009) estimate of temperature change is questionable and needs to be verified with other proxies.

When changes in $\delta^{18}O$ values in marine benthic foraminifera are considered, there is a synchronous increase in $\delta^{18}O$ values across the ocean basins, implying a decrease in temperature (Zachos et al., 1996; Zachos et al., 2001; Coxall et al., 2005; Ivany et al., 2006; Palike et al., 2006; Pearson et al., 2008; Cramer et al., 2009). There is evidence that glaciers began to grow in Antarctica at this time, but the magnitude of glacier growth adds an element of uncertainty to temperature estimates from $\delta^{18}O$ values, since more of the lighter ^{16}O is preferentially trapped in ice, altering the composition of the oceans (Zachos, et al., 2001; Ivany et al., 2006). As a result, the extent of how much cooling occurred is still controversial (Zachos et al., 2001; Coxall et al., 2005; Katz et al., 2008; Wade et al., 2012; Śliwińska et al., 2019). Coxall et al. (2005) suggested that glaciation lagged slightly behind the Eocene-Oligocene boundary, so ice sheet expansion could not account for all of the shift in $\delta^{18}O$ across the boundary.

Alternatively, mean $\delta^{18}O$ values from aragonite in marine fish otoliths across the E-O boundary did not support cooling average temperature, but microsamples of the layers from these

same otoliths revealed that the winters became 4 °C colder in the Oligocene as seasonal variation increased instead (Ivany et al., 2000).

Petersen et al. (2015) used clumped isotopes from benthic foraminifera to estimate temperature changes in the Southern Ocean. They found that cooling of 0.4 ± 1.1°C began between 0-1.5 Myr before the Oi-1 oxygen isotope event (33.70–34.15 Ma) and continued 1-2 Myr after it. The Oi-1 is the second and larger shift in $\delta^{18}O$ reported by Galeotti et al. (fig. 2, 2016) (Figure 2-3). Clumped isotopes are not impacted by the $\delta^{18}O$ of the water in which they mineralized and are therefore not affected by glacial growth shifting $\delta^{18}O$ values in the ocean water (Eagle et al., 2013).

Although temperature change in the continental interior of North America is not well resolved, several studies have shown evidence for increased aridity in the early Oligocene. Paleosol proxies from White River exposures show a ~300 mm decrease in mean annual precipitation in the early Oligocene and indicate that climate was semiarid by 30 Ma (Terry; 2001; Sheldon and Retallack, 2004; Retallack, 2007; Sheldon, 2009). Carbon and oxygen stable isotopes from several White River mammalian genera show an overall shift towards drier and more open environments in the early Oligocene. Although there were still dry areas in the Eocene and wet areas in the Oligocene, the wet areas became more restricted in the Oligocene (Boardman and Secord, 2013). Carbon isotope values in Eocene mammals living in drier environments remained relatively stable in the Oligocene, while those that had lived in wetter environments in the Eocene either died out (*Megacerops* and *Trigonias*) or shifted to drier environments in the Oligocene. Sheldon and Retallack (2004) suggested that the aridity increase may have resulted from the development of a rain shadow in western North America due to the rising Cascade Range. This would support the findings of Terry (2001), who suggested that

drying occurred from west to east. If drying was caused by the development of a rain shadow, it would not be related to climate change at the EOCT and should not result in abrupt changes in the geologic record.

Further supporting a cooling and drying climate, Evanoff et al. (1992) documented an extinction of terrestrial gastropods at or slightly above the Eocene-Oligocene boundary in the interior of North America. Correspondingly, there was a sudden decline in the generic diversity of large-bodied reptiles (Hutchison, 1982, 1992). The floral record is poor for the early Oligocene in the mid-continent but in the Pacific Northwest, evergreen broad-leaved forest was replaced with temperate broad-leaved forest (Wolfe, 1978; Myers, 2003).

Root traces and soil structure suggest that the region shifted from being forested in the late Eocene to a combination of wooded and open terrain in the Oligocene (Retallack 1983, 1992; Terry, 2001), but phytoliths from the late Eocene and Oligocene of Nebraska suggest the area was dominated by forest, with only ~5-7% grasslands appearing in the Oligocene. However, at least one unit of rock, the brown siltstone member, contained enough grassland phytoliths to suggest as much as ~12% (Strömberg, 2004).

Stable Carbon and Oxygen Isotopes

Previous studies have shown that *Merycoidodon*, the taxon used here for tracking changes in $\delta^{13}C$ values in atmospheric CO_2, consumed exclusively C_3 vegetation (Boardman and Secord, 2013; Zanazzi and Kohn, 2008). Carbon used for building plant tissues originates from atmospheric CO_2 fixed during photosynthesis, and in this way plants track atmospheric CO_2

values; however, carbon values in C_3 vegetation can also be influenced by other factors (O'Leary, 1988; Farquhar et al., 1989; Van der Merwe and Medina, 1991; Ehleringer and Monson, 1993; Koch, 1998; Heaton, 1999). C_3 plants are most strongly influenced by water availability, which is strongly correlated with precipitation (Kohn, 2010; Diefendorf et al., 2010). Accordingly, $\delta^{13}C$ values in broad-leafed plants generally increase with increasing aridity or higher amounts of solar radiation (Ehleringer et al., 1986; Stewart et al., 1995). Carbon isotope values are also influenced by vegetation density as a function of water availability (more humid conditions under a canopy) and light levels affecting photosynthetic rates (O'Leary, 1988; Koch, 1998; Van der Merwe and Medina, 1991). Closed areas have lower $\delta^{13}C$ values than open areas where water stress increases $\delta^{13}C$ values (Farquhar et al., 1989; Stewart et al., 1995). Thus, changes in precipitation or "openness" across the EOCT are both factors that could influence $\delta^{13}C$ values in plants, although water availability is expected to be the primary control.

Herbivores fractionate carbon from the food they ingest. The diet-to-enamel enrichment factor for large, modern ruminant ungulates is ~14.1±0.5‰ (Cerling and Harris, 1999; Passey et al., 2005). Although the exact enrichment factor for *Merycoidodon* is not known, it should be effectively invariant since all species of *Merycoidodon* sampled in this study were presumably closely related. Thus, *Merycoidodon* should faithfully track changes in plant and atmospheric $\delta^{13}C$ values.

Mammals can also potentially be used to track changes in $\delta^{18}O$ values in local meteoric water or changes in precipitation (Levin et al., 2006); however, $\delta^{18}O$ values are influenced by a variety of factors, including local atmospheric temperature, and the source and transport history of water vapor. To reduce seasonal variability, I sampled only third molars. Most artiodactyls living in temperate regions have seasonal breeding cycles and thus form their teeth seasonally

(e.g., Hillson, 1986). The low-crowned teeth in *Merycoidodon* probably formed in only a few months, based on the teeth of analogous ungulates (e.g., Hillson, 1986). Thus, by sampling only a single tooth position $\delta^{18}O_E$ values should reflect only a single season, reducing $\delta^{18}O_E$ variability. Cooling across the EOCT might be expected to result in a negative shift in $\delta^{18}O_E$ values (e.g., Boardman and Secord, 2013), while drying should result in a positive shift in $\delta^{18}O_E$ values, if other factors remain constant.

Oxygen isotopes in mammals are influenced by a variety of other factors as well. Oxygen isotopes in mammals that consume leaves are strongly influenced by water availability in plants. In drier conditions, lighter ^{16}O will preferentially be lost through evapotranspiration in leaves and through evaporation in closed bodies of water like ponds and lakes. Any animal that eats these plants or drinks this water will have a higher ^{18}O level in their bodies compared to the animals living in wetter conditions (Bohme, 2003). In this way, fossil mammals can indirectly track environmental changes such as humidity and precipitation (Bryant and Froelich, 1995; Kohn, 1996; Kohn et al., 1996; Levin et al., 2006; Secord et al., 2008, 2010, 2012; Zanazzi and Kohn, 2008; Tütken and Vennemann, 2009). Generally, mammals that get a significant part of their water from leaves, as opposed to drinking, are better for tracking changes in humidity or rainfall (Bryant and Froelich, 1995; Kohn, 1996; Levin et al., 2006), than changes in meteoric water values.

Merycoidodon had brachy-selenodont dentition and intermediate to high variability in $\delta^{18}O$ consistent with artiodactyls that consume browse with a high portion of leaves (Stevens and Stevens, 2007; Zanazzi and Kohn, 2008; Boardman and Secord, 2013). Thus, *Merycoidodon* is probably not a good candidate for tracking meteoric water values but potentially could provide information about changes in precipitation.

Stable isotopes in teeth can be diagenetically altered after a fossil is buried (Koch, 1997; Kohn and Cerling, 2002; Jacques et al., 2008), making it important to consider the possibility of alteration when making interpretations. However, $\delta^{13}C$ and $\delta^{18}O$ values in enamel have been shown to be highly resistant to diagenesis. Previous studies of White River ungulates have found consistent separation among taxa (Zanazzi and Kohn, 2008; Boardman and Secord, 2013). For example, the oreodont *Agriochoerus* and horse *Mesohippus* both maintain the same position in $\delta^{13}C$-$\delta^{18}O$ isotopic space, relative to the rest of the fauna, in both the late Eocene and the early Oligocene (fig. 4, Boardman and Secord, 2013). This can only be explained by the preservation of a strong primary isotope signal in these taxa. This does not necessarily mean that no alteration has occurred, but rather that any alteration was minor enough to not affect the relative positions of these taxa.

MATERIALS AND METHODS

Specimens Used for Abundance Calculations

All 4,894 specimens used in this study are curated at UNSM in Lincoln, Nebraska. Data were collected on fossils from twenty genera from fourteen mammalian families: Agriochoeridae (*Agriocheorus*), Anthracotheriidae (*Aepinacodon*), Brontotheriidae (*Megacerops*), Camelidae (*Paratylopus* and *Poebrotherium*), Entelodontidae (*Archaeotherium*), Equidae (*Mesohippus*), Hyracodontidae (*Hyracodon*), Leptomerycidae (*Leptomeryx*), Merycoidodontidae (*Merycoidodon* and *Miniochoerus*), Nimravidae (*Nimravus* and *Hoplophoneus*), Oromerycidae (*Eotylopus*), Rhinocerotidae (*Subhyracodon*, *Penetrigonias*, and *Trigonias*), Tapiridae (*Colodon*), and Tayassuidae (*Perchoerus*). These fourteen mammalian families come from the

orders of Artiodactyla, Perissodactyla, and Carnivora. With the exceptions of Leptomerycidae and Brontotheriidae, these specimens are all around the same body size range to avoid a preservation bias towards size. All taxa except the Nimravids (predators) and Entelodonts (omnivores) are considered to be browsers or mixed feeders (Joeckel, 1990; Wall and Collins, 1998; Zanazzi and Kohn, 2007; Clifford, 2010). Rodentia, Lagomorpha, Creodonta, much of Carnivora, and insectivores and marsupials were not included in this work. Most specimens consist of associated material from single individuals. In those cases where it appeared that more than one individual was present under a single number, the minimum number of individuals possible was calculated. An example of this would be a box containing isolated teeth that could potentially belong to several individuals, but a minimum of two individuals is indicated by the presence of two right rami.

Sample Collection for Isotope Analysis

Specimens were cleaned thoroughly with water and dental picks before sampling. Five-minute epoxy was used to strengthen teeth and bone to withstand the pressure and vibration of sampling. Enamel was tested for hardness using a carbide pick and any decalcified enamel was removed. Samples were drilled from teeth using a variable speed rotary dental drill with a 1 mm diamond burr mounted under a binocular microscope. 3-4 mg of powder were collected from each tooth. Samples were pretreated following the procedure of Koch et al. (1997) except for lyophilization, which was substituted by drying in an oven 60 °C. 2-3% sodium hypochlorite (NaOHCL) was added to sample to remove organic matter and allowed to react overnight. Samples were then centrifuged, rinsed five times with deionized water, and dried. Samples were

next reacted with 1 M acetic acid buffered solution overnight to remove unwanted carbonates, followed by five rinses and drying.

Isotope ratios were determined at the University of Michigan Stable Isotope Laboratory (UMSIL). Samples were reacted with phosphoric acid for 17 minutes at 77±1.0 ºC in a Finnigan MAT Kiel IV preparation device. This produced gaseous CO_2 with an isotopic ratio that could be measured using a Finnigan MAT 253 triple collector isotope ratio mass spectrometer.

The results of isotopic analysis are written in standard δ-notation using the formula below:

$$X = \left(\frac{R_{sample}}{R_{std}} - 1\right) * 1000$$

where X is the $\delta^{13}C$ or $\delta^{18}O$ value and R is the heavy/light isotope ratio for the sample and international standard (std). Standards are the Vienna PeeDee Belemnite (VPDB) for $\delta^{13}C$ and Vienna Standard Mean Ocean Water (VSMOW) for $\delta^{18}O$. All error on mean values in this paper is reported with 95% confidence of the mean (1.96*standard error) unless otherwise stated. An intra-lab enamel standard (MES-1), made from fossil mammoth enamel, was also used to monitor sample variance.

Moving Averages

Stratigraphic levels for *Merycoidodon* specimens were recorded to the nearest foot in the original field books. Because of potential uncertainty in measurements, specimens were grouped into two-foot intervals and a three-point weighted average was calculated using the formula: $([n_A*A]+[n_B*B]+[n_c*C])/(n_A+n_B+n_C)$ where n=number of samples from that level, A=average isotope value of specimens at the highest stratigraphic level, B=average value of specimens at

the middle stratigraphic level, C=average value of specimens at the lowest stratigraphic level. This smoothed the data to better recognize trends and decreasing the influence of outliers.

Binning Models

When measuring changes in abundance through the WRG sequence, I used several different sets of stratigraphic bins. This was done because of uncertainty in the stratigraphic position of the two main pulses of climate change at Toadstool Geologic Park described by Galeotti et al. (2016). The position of these pulses relative to bin size and position can affect the outcomes of the abundance analyses. The first set of bins used were the zones of Schultz and Stout (S&S zones) (Figs. 4 and 5). The second and third set of bins were made based on the average sediment accumulation rates of Sahy et al. (2015). This allowed me to estimate an age (Table 1) for each of the *Merycoidodon* isotope values relative to the Galeotti et al. (2016) $\delta^{18}O$ values. The average sediment accumulation rate varied, so the Galeotti et al. (2016) isotope data were stretched or compressed relative to the Toadstool stratigraphy. Each of the bins was designed to cover a roughly equal amount of time, but a varying amount of sediment. In both cases Bin 0 was the bin that contained the UPW (0 m on the stratigraphic column).The bin size was based on the amount of time between the first pulse of climate change and the second shift in climate reported in the Galeotti et al. (2016) data.

Because it is unclear how the Sahy et al. (2015) average sediment accumulation rates were calculated, I used a cubic spline curve to determine the ages of the specimens for the fourth and fifth set of bins instead, and removed the second and third bin series from the results section.

The fourth set of bins (Bins -2 through 3) were created using a cubic spline curve calibrated with $^{206}Pb/^{238}U$ zircon ash dates (Sahy et al., 2015) to estimate the ages of samples and stratigraphic levels between calibration points in the Toadstool stratigraphy. Using this age

model, the marine stable isotope data of Galeotti et al. (2016) were correlated to the Toadstool section. This method does not utilize the *Merycoidodon* isotope curve. Although it should be possible to also use magnetochrons reversal to calibrate the spline curve, I found that there was great inconsistency in results, presumably due to the Sahy et al. (2015) ash dates being more accurate than the less constrained dates based on marine magnetochrons (Ogg, 2012). Additionally, there appears to be uncertainty up to several meters as to where the magnetochrons are placed precisely in the stratigraphy (D. Terry written communication. Using the current stratigraphic positions for the chron reversals (Sahy et al., 2015) results in a disjunction of ages relative to the cubic spline curve age estimates. As such, a grey box of uncertainty was placed on the C13r-C13n boundary (Fig. 3), and this boundary is correlated between the marine and terrestrial realms within the upper limit of this uncertainty to better fit the cubic spline results until more accurate placement of the magnetochrons are published (D. Terry written communication). The newly calibrated spline dates resulted in bins defined as follows: Bin -2 (34.64-35.04 Ma) 21.6-29.6 m below UPW, Bin -1 (34.24-34.64 Ma) 12.2-21.6 m below UPW, Bin 0 (33.84-34.24 Ma) 4.9 m above UPW-12.2 m below UPW, Bin 1 (33.44-33.84 Ma) 21.9-4.9 m above UPW, Bin 2 (33.04-33.44 Ma) 39-21.9 m above UPW, Bin 3 (32.64-33.04 Ma) 59.1-39 m above UPW.

The fifth bin series terrestrial stratigraphic ages were also based on the same cubic spline curve, but like the second bin series it shifted the marine data stratigraphically to correlate with the peaks and troughs in the *Merycoidodon* $\delta^{13}C$ results. This results in the onset of the EOCT climate shift being placed ~10 m lower than in the fourth bin series. Each of the six bins here represented approximately 0.34 million years. Like the proceeding bin series, they are based on the distance between the two largest pulses of climate shift as the boundaries of Bin 0 They are

defined as follows: Bin 3 (32.7-33.04 Ma) 39 to 55 m above UPW, Bin 2 (33.04-33.38 Ma) 24 to 39 m above UPW, Bin 1 (33.38-33.72 Ma) 10 to 24 m above UPW, Bin 0 (33.72-34.06 Ma) 10 m above UPW to 5 m below UPW, Bin -1 (34.06-34.4 Ma) 5 to 17 m below UPW, and Bin -2 (34.4-34.74 Ma) 17 to 25 m below UPW.

The sixth bin series was based on the same cubic spline as the fourth and fifth bin series, with the bins being of equal size in the length of time they represented stratigraphically. Instead of a bin being placed between the first and second shifts of the EOCT as is the case in the second, third, fourth, and fifth bin series, the bin boundaries began around the E-O boundary similarly to the S&S zones. The sixth series bins represent the same amount of time as the fourth and fifth series bins (approximately 0.34 million years) Figure 1). They are defined as follows: Bin 2 (33.339-33.039 Ma) 26.1 to 38.7 m above UPW, Bin 1 (33.639-33.339 Ma) 13.4-26.1 m above UPW, UPW lower boundary of Bin 0 (33.939-33.639 Ma) 0 to 13.4 m above UPW, Bin -1 (33.939-34.239 Ma) 0.1 to 13.3 m below UPW, and Bin -2 (34.239-34.539 Ma) 13.3 to 21.3 m below UPW.

For each bin series, other than the S&S zones, the bins are of equal length in time, but of varying length stratigraphically. This results in small sample sizes for the lowest Chadron bins, which increases the resulting variance in percent change.

Analysis of Abundance Data

For each of these bin series, two datasets were made, one with the very small primitive ruminant *Leptomeryx* included, and one without. Results showed that because of the great abundance of *Leptomeryx* in some zones, and its low abundance in others, this taxon accounted for a large percentage of the overall fossils, greatly affecting the percentage changes in other taxa

among zones. To avoid abundance changes driven largely by *Leptomeryx*, datasets without *Leptomeryx* were also complied. Datasets with *Leptomeryx* included can be seen in Appendix C.

Percent relative abundance was calculated to measure changes in the proportions of taxa through time. This was calculated as the total number of individuals of that taxon divided by the total number of individuals in a bin multiplied by 100. To determine significance, 95% confidence intervals were derived from the formula

$$p \pm 1.96 * [(p * q)/(n-1)]^{\frac{1}{2}}$$

where p is the relative abundance of the taxon being analyzed; q is equal to 1-p, and n is the number of specimens in the sample (Buzas, 1990; Hayek & Buzas, 1997; Bobe et al., 2002). Differences in abundance ratios were considered significant with 95% confidence when confidence intervals did not overlap.

To compare whole fossil assemblages from one-time interval to the next, I used chord distance (CRD). CRD is a measure of dissimilarity for relative abundance (Ludwig & Reynolds, 1988). CRD between j and k as an example is calculated by:

$$CRD_{jk} = [2(1 - ccos_{jk})]^{\frac{1}{2}}$$

$$with\ ccos_{jk} = \sum^{S} (Xij * Xik)/[\sum^{S} X^2\, ij \sum^{S} X^2\, ik]^{\frac{1}{2}}$$

where Xij represents the abundance of the ith taxon in the jth assemblage, Xik represents the abundance of the ith taxon in the kth assemblage, and S is the total number of taxa in the two assemblages. Chord distance values range from zero (assemblages with identical taxonomic abundances and composition) to the square root of 2 (1.41) (assemblages that have nothing in common).

As an additional measure, the bins before and after the EOCT were combined in each of the bin series where they are essentially NALMA for the S&S zones. In each second through sixth bin series, the bin that is bounded by the two largest pulses of climate shift was not combined with any of the other bins so that changes in relative abundance across the two large climate shifts could be measured separately.

Simpson-D and Shannon H indices were used to measure ‘evenness’ and diversity. The Simpson index (1-dominance) measures dominance as D=sum((ni/n)2) where ni is the number of individuals of taxon n within i. This index measures 'evenness' of the community from 0 (one taxon dominates the zone entirely) to 1 (all taxa equally present). The Shannon H index is calculated as H=-sum((ni/n)ln(ni/n)) where ni is the number of individuals of taxon i. This index measures diversity considering the number of individuals as well as number of taxa. Diversity indices were run in Past 3.23 on each of the bin series.

Principal Components Analysis (PCA) was performed on each series of bins with, and without, *Leptomeryx* included in the dataset to determine where most of the variation in relative abundance originated. The results these analyses are presented in Appendix J.

Where sample size allowed, the natural log of average tooth area was calculated from up to three specimens per taxa from the width length measurements of the m1. This is displayed in a histogram for each S&S zone or bin (Figs. 6 and 7; Table 2). This was done to test if there was a taphonomic bias related to the size of the fossils being preserved or a collection bias.

Percent change in relative abundance vs. carbon and oxygen isotope data values taken from Boardman and Secord (2013) was also compared in linear regressions. This was measured before and after the climate shift using the NALMA and combined bins of the fourth series (Figs.

C4-C6; E1-E4). This was done to test the hypothesis that water dependence was a significant factor contributing to success of some taxa. If there were a significant, positive correlation between the $\delta^{18}O$ mean values of the taxa in Boardman and Secord (2013) and relative abundance, for example, it would suggest that water dependence was a factor driving abundance change.

RESULTS

Taxa with less than 60 specimens were excluded from the final analyses of results since their increases or decreases in relative abundance were very sensitive to small changes in sample size, sometimes resulting in huge percent changes. Taxa that go extinct at the Eocene-Oligocene boundary were also removed from the relative abundance datasets so as not to create an artifact on the relative abundance increases or decreases of the other taxa. Removing these taxa, however, did not change any of the general patterns. Thus, *Agriochoerus, Aepinacodon, Megacerops, Leptomeryx, Dinictis, Hoplophoneus, Eotylopus, Amphicaenopus, Penetrigonias, Subhyracodon, Trigonias, Colodon,* and *Perchoerus* were removed from the analysis. Analyses with these taxa included in the dataset can be found in Appendix C. However, they were all included in the diversity and chord distance analyses for a better picture of as much of the fauna as possible.

Throughout each bin series, the same taxa increase or decrease in relative abundance through time in separate bin series. *Mesohippus* and *Archaeotherium* decrease in relative abundance through time in every bin series for example. This is true of many of these long-term

through-time patterns, but placement of bin boundaries can slightly alter the results of bin-to-bin changes in relative abundance. Despite this small degree of variation in relative abundance changes, most taxa display similar increase and decreases between largely contemporaneous bins (Fig. 4-5; 12-13; 17-18).

After it was apparent that the results of all the bin series were found to be largely consistent and the fourth bin series matched the placement of the Galeotti et al. (2016) climate curve well, the fifth bin series was also removed from the results.

Uncertainty in Magnetic Polarity Zones

Figure 7 shows the difference in cubic spline curves obtained using different sets of calibration points for the Toadstool Geologic Park section. Both curves that use single sets of calibration points, namely either new $^{206}Pb/^{238}U$ ash dates from Sahy et al. (2015) or ages from the latest geomagnetic polarity time scale (Ogg, 2012), produce relatively smooth curves. However, when the data from both sources are combined, dramatic changes appear in the curve. This implies that the two datasets are not in accordance. Ages for polarity reversals have been calibrated by interpolating between radiometric dates from the marine record with a cubic spline function based on estimated seafloor spreading rates (e.g., Bergman et al., 1995; Ogg and Smith, 2004; Ogg et al., 2008). This has more recently been refined using orbital tunings (Ogg, 2012). Nevertheless, the often-large temporal distances between radioisotopic calibration points in the marine record ultimately results in some uncertainty for the ages of chron reversals. Thus, the new ash dates from the Toadstool Geologic Park sequence should provide a stronger

geochronologic framework for calibrating the section than dates from the polarity reversals from the marine record. The Orellan-Chadronian boundary is placed at 33.9 Ma which is synchronous with the UPW at 33.939 ±0.033 Ma (Sahy et al., 2015), and near the Eocene-Oligocene boundary at 34.09 ± 0.08 Ma (Sahy et al., 2017). The accuracy of these dates is vital to correlating the terrestrial and marine climate records. Many studies suggest the EOCT occurred over a relatively short time period starting around 34.0-33.8 Ma in the earliest Oligocene (Zachos et al., 2008; Liu et al., 2009; Miller et al., 2009; Petersen, 2015; Galeotti et al., 2016;). Many more studies have documented evidence of climate change starting slightly earlier across the Eocene-Oligocene Boundary (MacGinitie, 1953; Shackleton and Kennett, 1975; Wolfe 1978, 1992, and 1994; Ivany et al., 2000; Zachos et al., 2001; Terry, 2001; Sheldon and Retallack, 2004; Ivany et al., 2006; Zanazzi et al., 2007; Retallack, 2007; Katz et al., 2008; Sheldon, 2009; Zanazzi et al., 2009; Sheldon, 2009; Bohaty et al., 2012; Wade et al., 2012; Boardman and Secord, 2013), implying that it is the boundary that marks major climate change. The chord distance results presented here also consistently show a greater chord distance between bins of any series in the Eocene to bins in the Oligocene (Tables 3, 4, and5).

Stable Isotope Results from *Merycoidodon* Teeth

Results for the *Merycoidodon* isotope stratigraphy are plotted in Figures 2 and 8 (data in Table 1). The sampling range was originally planned based on the polarity chron reversals of Prothero and Swisher (1992), but revised geochronology in Sahy et al. (2015) and research in review (pers. com. Dennis Terry, 2019) resulted in the samples covering a smaller range of time than originally planned. *Merycoidodon* samples do not appear to extend high enough in the

Toadstool Geologic Park section to capture the second large positive shift in carbon isotope values seen in the Galeotti et al. (2016) record but may capture the lower positive shift. Both shifts in marine $\delta^{13}C$ values closely covary with shifts in marine $\delta^{18}O$ values, purportedly indicating pulses of cooling. The *Merycoidodon* $\delta^{13}C$ values positively increase through the sampled section until they start to decrease just above ~4m (Fig. 2). Suggested correlation of the *Merycoidodon* $\delta^{13}C$ record to the Galeotti et al. (2016) marine record is shown in Fig. 3 and is based off two peaks and two troughs in both the marine and the continental record. The *Merycoidodon* $\delta^{18}O$ values show high variation over short intervals of time and are difficult to confidently interpret (Fig. 3).

Schultz and Stout (1955) Zones

Changes in relative abundance of the well-sampled taxa using the S&S zones are shown in Figure 4 (data in Tables 6-9). Tables report number of specimens in each zone (Table 6), relative abundance of each genus for each zone (Table 7), and 95% confidence intervals (Table 8).

In the S&S zones, the onset of the EOCT begins gradually within the lower Chadron C before two pulses of climate change occur within Orella A and Orella B respectively (Zanazzi et al., 2009; Bohaty et al., 2012; Galeotti et al., 2016). Many papers (e.g. Zachos et al., 2001; Terry, 2001; Sheldon and Retallack, 2004; Ivany et al., 2006; Zanazzi et al., 2007; Retallack, 2007; Katz et al., 2008; Sheldon, 2009; Zanazzi et al., 2009; Sheldon, 2009; Bohaty et al., 2012; Wade et al., 2012; Boardman and Secord, 2013; Galeotti et al., 2016) examine changes between the Eocene and Oligocene and suggest the EOCT to occur around the E-O boundary. As such, the

largest changes in relative abundance should be expected to be between Chadron C and Orella A as Orella A contains the first large pulse of climate change near its lower boundary.

Mesohippus and *Archaeotherium* decrease ~20% and ~13% respectively in relative abundance from the combined Chadron B&C through time to Orella C. *Merycoidodon* stays stable but varies by ~7% in relative abundance through time when the Chadron zones are combined. The cursorial rhinocerotoid *Hyracodon* also remains stable in abundance but varies ~5% in relative abundance from Chadron B&C through to Orella C. The small oreodont *Miniochoerus,* and the gracile camelids *Poebrotherium,* and *Paratylopus* all increase in relative abundance through time by ~15%, ~10%, and ~4% respectively from the combined Chadron B&C to Orella C.

Percent changes in relative abundance are shown in Fig. 5. (data in Table 9). Of the taxa considered, only *Poebrotherium* has its largest abundance change across the E-O boundary (Chadron C to Orella A). When the Chadron zones are not combined due to small sample size, both of the most abundant taxa, *Mesohippus* and *Merycoidodon,* have their largest percent change in relative abundance from Chadron B to Chadron C. *Merycoidodon* increases by ~905% from Chadron B to Chadron C while *Mesohippus* decreases ~49% at the same time (Table 9). This is slightly before the onset of the EOCT. Taken together, there are no large coordinated changes in relative abundance during the EOCT.

There was no significant change in diversity or evenness across the S&S zones, although there are insignificant peaks in diversity and evenness in Chadron C (Figs. 10 and 11; Table 10).

Zones after the EOCT are closer in chord distance than they were to those before it, indicating that there is greater similarity between the zones after the EOCT and the other Orellan zones than to the Chadronian zone (Table 3). As chord distance measures the entire fauna in each

zone, this suggests that the largest shift in mammalian faunal composition is between the Chadronian and Orellan NALMAs.

Histograms of the natural log of average tooth area (Fig 6.) show that the largest changes in tooth area across the S&S zones occur in *Poebrotherium* (ln[tooth area])=4.5mm^2) and *Merycoidodon* (ln[tooth area]=5.1mm^2) , but the distribution of body size remains fairly constant (mean ln[tooth area] ranges from 4.3-4.8; median ln[tooth area] ranges from 4.3-4.7).

Fourth Bin Series

The fourth bin series is shown in Figure 1 and partly in Figure 3. Figure 3 also shows a suggested correlation with the Galeotti et al. (2016) oxygen record using the newly calibrated Toadstool Geologic Park section and inflection points in the *Merycoidodon* δ^{13}C moving average. This correlation places the gradual onset of the EOCT within Bin 0, with the first pulse of the climate shift between Bin 0 and 1, and the second (Oi-1) between Bin 1 and Bin 2.

The lithology changes from the Chadron Formation to the Brule Formation near where the second climate shift would take place based on the correlation between the *Merycoidodon* δ^{13}C and the Galeotti et al. (2016) δ^{13}C record (Fig. 3). This lithology change occurs near the largest increases in relative abundance seen in *Paratylopus* and *Miniochoerus* between Bin 1 and Bin 2. The larger increases in relative abundance of *Poebrotherium* is lower in the section near the first pulse of climate shift of the EOCT between Bin 0 and Bin 1, which is also before the lithology shift.

Just as in the S&S zones, *Mesohippus* decreases in relative abundance through time in the fourth bin series from Bin -2 to Bin 3 (~30%) (Fig. 12). Again, similarly to the S&S zones,

Archaeotherium also decreases in relative abundance through time (~15%) while *Merycoidodon* increases almost 25% through time, peaking in relative abundance within Bin 0. This increase in *Merycoidodon* is hidden when the Chadron zones or bins are combined, which is why it appears much more stable in relative abundance in the S&S zones (Fig. 4) than it does here. *Hyracodon* remains relatively stable in abundance through time, though it varies by ~3% (Table 11). *Miniochoerus* and *Poebrotherium* increase in relative abundance through time at ~15% and ~21% respectively (Table 11).

Like the S&S zones, when the first pulse of climate shift is placed near the E-O boundary, as the correlation for the fourth bin series suggests, only *Poebrotherium* exhibits its biggest change in relative abundance across the first climate shift of the EOCT (Fig. 13). Unlike the S&S zones, in this bin series *Paratylopus* and *Miniochoerus* have their largest shifts in relative abundance across the second climate shift of the EOCT (Bin 1 to 2, Fig. 12; Table 11). The largest percent changes in relative abundance for the most common taxa (~61% decrease in *Mesohippus* and ~275% increase in *Merycoidodon*) are again between Chadron B and C (Bins -1 and 0), which occurs slightly before with the gradual onset of the EOCT. Those taxa that showed increasing trends in the S&S zones also show increasing trends in this bin series (*Paratylopus*, *Poebrotherium*, *Merycoidodon*, and *Miniochoerus*). Similarly, *Hyracodon* remains stable through time and *Archaeotherium* and *Mesohippus* decline in relative abundance through time as they did in the S&S zones (Fig. 12; Tables 4; 11-15).

Bins after the EOCT are closer in chord distance than they were to those before it. Similarly, Bins before the EOCT are closer in chord distance to each other than they are to the Orellan zones after it (Table 4). This pattern between bin distances implies greater similarity among taxa in the same NALMA than between NALMAs.

Again, evenness and diversity do not significantly change, but there is an insignificant peak in evenness before the EOCT (Figs. 13-15; Table 15).

Sixth Bin Series

The sixth bin series utilizes the same cubic spline as the fourth bin series, but the bins are based around the E-O boundary instead. This results in the same pulses in climate being in different bins than in the fourth series. In the sixth bin series the gradual onset of the EOCT begins in Bin -1, the first pulse of climate shift occurs in Bin 0, and the second pulse of climate shift (Oi-1) occurs within the upper limits of Bin 1. The E-O boundary is also the boundary between Bin -1 and Bin 0. As both the E-O boundary and the first pulse of climate shift occur near the base of Bin 0, this is where the greatest changes in relative abundance would be expected to occur.

Changes in relative abundance of the well sampled taxa using the sixth bin series are shown in Figure 16 (data in Tables 16-18). *Mesohippus* and *Archaeotherium* decrease ~30% and ~12% respectively in relative abundance from the combined Chadron B&C to Orella C, which is similar to the decrease seen in the other bin series, though it is larger for *Mesohippus* here. *Merycoidodon* increases almost 20% in relative abundance through time, with a period of stability from Bin 1 onward. *Hyracodon* also remains stable in abundance but varies ~5% in relative abundance from through time. *Miniochoerus*, *Poebrotherium,* and *Paratylopus* all increase in relative abundance through time by ~15%, ~10%, and ~4% respectively through time.

Percent changes in relative abundance are shown in Fig. 17. (data in Table 19). Of the taxa considered, only *Poebrotherium* has its largest abundance change across the E-O boundary

(Chadron C to Orella A). When the Chadron bins are not combined, both of the most abundant taxa, *Mesohippus* and *Merycoidodon*, have their largest percent change in relative abundance from Bin -1 to Bin 0. This is again similar to the largest percent changes seen in the S&S zones from Chadron B to Chadron C. This larger percent change is slightly before the onset of the EOCT in this bin series as well. Three taxa, *Miniochoerus*, *Paratylopus*, and *Poebrotherium*, exhibit trends in increasing relative abundance through the two subsequent zones. *Hyracodon* and *Merycoidodon* remain stable in relative abundance. Two taxa, *Mesohippus* and *Archaeotherium* exhibit trends in declining relative abundance through the section. Taken together, there are no large coordinated changes in relative abundance during the EOCT.

There was no significant change in diversity or evenness across the sixth series bins, although there is an insignificant peak in diversity or evenness in Chadron C (Figs. 18 and 19; Tables 20).

Zones after the EOCT are closer in chord distance than they were to those before it, indicating that there is greater similarity between the zones after the EOCT and the other Orellan zones than to the Chadronian zone (Table 5). As chord distance measures the entire fauna in each zone, suggesting that the largest shift in mammalian faunal composition is between the Chadronian and Orellan NALMAs.

Histograms of the natural log of average tooth area (Fig 20.) show that the largest changes in tooth area across the sixth bin series occur in *Poebrotherium* (ln[tooth area])=4.5mm^2) and *Merycoidodon* (ln[tooth area]=5.1mm^2) , but the distribution of body size remains fairly constant (mean ln[tooth area] ranges from 4.3-4.8; median ln[tooth area] ranges from 4.3-4.7).

DISCUSSION

Most studies suggest that the first pulse of climate shift from the EOCT occurs near the E-O boundary (MacGinitie, 1953; Shackleton and Kennett, 1975; Wolfe 1978, 1992, and 1994; Ivany et al., 2000; Zachos et al., 2001; Terry, 2001; Sheldon and Retallack, 2004; Ivany et al., 2006; Zanazzi et al., 2007; Retallack, 2007; Katz et al., 2008; Sheldon, 2009; Zanazzi et al., 2009; Sheldon, 2009; Bohaty et al., 2012; Wade et al., 2012; Boardman and Secord, 2013). Accordingly, those bin series (S&S zones and sixth bin series) that have a bin boundary near the E-O boundary (UPW) should be the most reliable. Since the bin boundary is right on the E-O boundary and near the climate shift, it is less likely to include faunas from before and after the climate shift in the same bin. Combining faunas from before and after a change in climate would thus mute the perceived change in the relative abundance.

Within these bin series, changes in the most abundant taxa are most meaningful as they control much of the overall variation in relative abundance in the fauna. A significant change in a taxon represented by a large number of specimens is also more meaningful since it is more difficult to shift the abundance percentage, relative to poorly sampled taxa. Thus, the significant decrease in *Mesohippus* and increase in *Merycoidodon* in the fourth (Fig. 12) and sixth (Fig. 16) bin series are important single changes in the overall fauna. These changes occur between Chadron B and Chadron C, near the onset of the EOCT, but still slightly before it. These changes cannot be seen in the S&S zone abundance chart (Fig. 5) because the Chadron zones were combined due to small sample size in Chardon B but they can be seen if the zones are treated separately (Fig. B1). The change in relative abundance between Chadron B and C appears to predate the large pulses of climate change seen in the marine record (Coxall et al., 2005; Zanazzi

et al., 2007; Zachos et al., 2008; Liu et al., 2009; Miller et al., 2009; Petersen, 2015; Galeotti et al., 2016). Furthermore, *Merycoidodon* does not continue to increase in relative abundance after Chadron C and the decrease in *Mesohippus* does not get faster at the two pulses of climate change higher in the section. The two genera do appear to have become permanently subequal in abundance after this change as their abundance ratios never return to the levels seen in Chadron B. Therefore, the EOCT does not appear to be responsible for these changes in relative abundance because these changes predate it.

Previous work suggests that the significant change in climate that began at the E-O boundary persisted through much of the Oligocene (Evanoff et al., 1992; Hutchison, 1982 and 1992; Wolfe, 1978; Myers, 2003; Retallack, 1983 and 1992; Terry, 2001; Palike et al., 2006; Pearson et al., 2008; Zachos et al., 1996; Zachos et al., 2001; Coxall et al., 2005; Katz et al., 2008; Wade et al., 2012; Śliwińska et al., 2019). In particular, terrestrial studies suggest drier, and possibly cooler conditions in the early Oligocene (Evanoff et al., 1992; Hutchison, 1982, 1992; Wolfe, 1978; Myers, 2003; Boardman and Secord, 2013). Thus, even if the correlation of the EOCT used here is imprecise, any lasting change in relative abundance should still be detected. This is because imprecise placement of bins, relative to EOCT climate change, could result in intervals of relative abundance change being divided between bins. For example, this could be the case with the fourth bin series, for which the base of Bin 1 falls within Orella A, dividing the zone (Fig. 1). Chord analysis indicates that Orella A is more similar to the other Orellan zones above it, than to any of the Chadron zones, suggesting important faunal differences between Chadron C and Orella A. Thus, this placement would result in the smoothing of the percent change from Chadron C to Orella A. Nevertheless, I would have

expected one of the six bin series to have captured EOCT climate change and any abundance change that might have corresponded with it.

With chord distance, the bins, or zones, after the E-O boundary (Orellan) are more similar to one another than they are to the bins, or zones, that came before it (Chadron) in all cases. In other words, chord distances consistently show that the Chadronian bins are more similar to each another than they are to any of the Orellan bins (Tables 3, 4, B4, B10, B15, B21, D4, and E4). Similarly, the Orellan bins are closer in chord distance to each other than they are to the Chadronian bins. This suggests an important change in the fauna between the Chadronian and Orellan, despite the lack of a pulse of change in relative abundance or evenness at the E-O boundary. The chord distances were measured with all taxa and seem to be sensitive to the loss or decrease in relative abundance of late Eocene taxa like *Eotylopus* and *Megacerops,* decreasing in relative abundance as some taxa become more dominant in the Orellan, such as *Merycoidodon*. Removing these Eocene taxa removes the increased change in chord distance across the E-O boundary in all bin series.

When percent changes in relative abundance were calculated for each zone or bin (Figs. 13 and 17, Fig. B4; Tables 9, 11, and 19), all the binning schemes had their largest changes in relative abundance before the EOCT. This consistency in results across the bin series suggests that the increased change in relative abundance from Chadron B to C is real and is not an artifact of the analysis. The large changes in abundance of the most common taxa, *Merycoidodon* and *Mesohippus,* suggest that there was major change in the underlying ecosystem at this time. Although a variety of causes are possible, the close stratigraphic proximity of this faunal change to known climate change during the EOCT suggests that it may have been climatically driven. If

this change was climatically driven, this study implies that climate change in the interior of North America preceded the large pulse of cooling implied by the marine oxygen isotope record. As noted above, numerous studies of terrestrial climate change across the EOCT have yielded mixed results, some finding little evidence for change (e.g. MacGinitie, 1953; Prothero and Heaton, 1996; Strömberg, 2004; Petersen et al., 2015) and others finding strong evidence (e.g. Wolfe, 1978, 1992, and 1994; Zachos et al., 1996; Zachos et al., 2001; Coxall et al., 2005; Ivany et al., 2006; Palike et al., 2006; Pearson et al., 2008; Cramer et al., 2009; Zanazzi et al., 2009). A recent global study of vegetation and terrestrial temperature change across the EOCT found a heterogeneous response in vegetation with cooling being well before the EOCT and being most prevalent in coastal areas (Pound and Salzmann). Another study using stomatal indices in fossil leaves recently found a decrease in CO_2 levels, and implied cooling, beginning 1 to 2 million years before the EOCT (Steinthorsdottir et al., 2016). Thus, climate change preceding the EOCT is not unreasonable, and is a potential cause for the abundance changes reported here. More work needs to be done to test this hypothesis.

Poebrotherium is the only taxon that has its highest percent change across the Eocene-Oligocene boundary. This is shown in both the S&S zones, the fourth bin series, and the sixth bin series, with its largest percent change in relative abundance being from Chadron C to Orella A (269% increase in S&S zones, 182% increase in fourth bin series into Bin 1; 110% increase in the sixth bin series into Bin 0) (Figs. 4, 12, and 20). In the fourth bin series it is joined by *Paratylopus* (129% increase) and *Miniochoerus* (111% increase) which have their largest percent change in relative abundance across the second, larger climate shift of the EOCT if correctly correlated, but lithology change between Orella A and B cannot be ruled out here as a driver of this change. In the sixth bin series *Poebrotherium* (110% increase) is joined by only

Miniochoerus (100% increase) having its largest change in relative abundance across the E-O boundary. These taxa are not as abundant as *Mesohippus* and *Merycoidodon*, so the increased change in relative abundance equates to less change in the fauna overall. Furthermore, it is unclear if this is being caused by changing climate or something else as it predates the onset and greater pulses of climate change seen in the EOCT. The lack of a coordinated pulse in relative abundance in taxa other than *Poebrotherium* also does not support a greater climate shift near the E-O boundary. Additionally, the possibility that abundance changes were influenced by taphonomic biases or collecting biases in the UNSM collections needs to be considered.

Assessment of Taphonomic and Collecting Biases

Samples sizes in the Chadron Formation are small, relative to the Brule Formation, and there appears to be a taphonomic bias against smaller taxa. Many Chadron localities contain only medium or large taxa and microsites are rare (Ross Secord, University of Nebraska-Lincoln, pers. com.). Microtaxa, such as insectivores and rodents, are more common in the Orellan. A large increase in the abundance of fossils occurs in the upper part of the Chadron Formation, in Orella A. This is illustrated by number of *Leptomeryx* specimens (Tables A1 and A2).

There are huge differences in the raw abundance of *Leptomeryx* among the bins (786 specimens in Orella A vs 23 in the entire Chadronian), which do not seem to be related to absolute sample size (Tables B1, B2, C1, and C5). Although it is possible that changes in the abundance of *Leptomeryx* reflect actual underlying populational changes, it seems more likely that this is either a collecting bias or a taphonomic bias. *Leptomeryx* is the most abundant small artiodactyl at Toadstool Geologic Park and it is possible that some collectors did not collect all specimens present. However, the UNSM collections include an extensive collection of

lagomorphs and rodents, consisting of thousands of specimens. This suggests that smaller specimens were not commonly ignored. Taxa larger than *Leptomeryx* do not seem to have been impacted by taphonomic or collecting biases based on the overall distribution of tooth sizes, which remains fairly stable (Figs.6 and 9; Table 2). The mean or median tooth area for each bin also does not change significantly throughout the section, suggesting that samples for medium and large taxa were not significantly impacted by a size bias in preservation.

Lithologic differences between the Chadron and Brule formations could potentially impact fossil preservation. The Brule formation starts at the base of Orella B (Terry, 1998, 2001; LaGarry, 1998). Both the Chadron and Brule formations are composed of fine-grained sedimentary rocks. Siltstones and claystones in the Brule and Chadron appear to have formed in similar fluvial depositional environments with comparable amounts of transport and deposition energy (Terry, 1998, 2001; LaGarry, 1998). The Brule Formation, however, is also interbedded with nodule layers and sheet sandstones (Terry, 1998, 2001; LaGarry, 1998). The higher hydraulic energy associated with sandstone deposits could suggest a taphonomic bias against preservation of smaller fossils but there are actually more microfossils within the Brule Formation than lower in the stratigraphy. Additionally, eolian ash deposits increase up section throughout the White River Group (Retallack, 1983). However, if taphonomic changes were the driving force of changes in relative abundance I would expect the greatest changes in relative abundance, percent change, chord distance, and evenness to be between Orella A and Orella B where the lithology changes. However, this only occurs in the fourth bin series where the upper boundary of Bin 1 falls near within Orella B (Fig. 1), resulting in the second climate shift being near the lithology shift. This means that the largest shifts of *Paratylopus* and *Miniochoerus* could potentially have been influenced by this change in lithology, even if the rest of the fauna does not

have any larger percent change. Meanwhile, the percent change in relative abundance in *Poebrotherium* lower in the stratigraphy near the E-O boundary are not near this lithology change and cannot be explained by it. The larger percent change seen in *Merycoidodon* and *Mesohippus* is even further removed from this lithology change as well and must therefore be driven by something else. Evenness does not change significantly between Orella A and Orella B, and the largest change in evenness is between Chadron C and Orella A (Figs 10-11, 14-15; Tables 10, 15). Percent change is consistently larger in the lower bins of the Chadron Formation, but when these are combined, the percent change is no larger from the Chadron to Orella A than in later percent changes (Figs 4 and 12). In taxa that were increasing or decreasing in relative abundance the rates of increase or decrease do not change into Orella B, suggesting that lithology change is not a significant source of change in the relative abundance results. Finally, chord distance between the Orellan S&S zones is much smaller than it is from the Chadron S&S zones to Orella A. This change is below the lithology change (Tables 3, 9, B4, B10, B15, B21, D4, and E4). This increased chord distance is repeated in every bin series. Additionally, histograms of average tooth area also do not show any significant change in mean or median tooth area from Orella A to Orella B, nor does the distribution of tooth sizes change (Figs. 3 and 14). These observations suggest that lithology changes between the Chadron and Brule formations are not a significant source of variation in the relative abundance results.

Finally, Moore and Norman (2007) found that whole bone bulk density was the most important taphonomic bias in fossils from the Brule formation. Moore and Norman (2007) calculated whole bone bulk density based on average measurements from Behrensmeyer (1975) who in turn, calculated whole bone bulk density based on volume (water displacement)/weight. In those fossils with dentition, density of the teeth enamel was used for the whole specimen as it

was most likely to preserve and often represented most of the fossil (Moore and Norman, 2007). All of the specimens in this dataset contain at least a partial tooth. This removes density as a factor from the taphonomic preservation bias as all the teeth have very dense enamel layers. The second and third largest taphonomic biases described by Moore and Norman (2007) were for shape and size of the fossilized elements. However, the consistent distribution of tooth area sizes in the histograms related to sample size through time suggests that this also is not greatly impacting my dataset. These observations suggest that lithology changes and potential changes in taphonomic preservation are not a significant source of variation in the relative abundance results of the genera included in this study.

Interpretation of Changes in Relative Abundance

A drying climate might be expected to favor taxa that had developed drought-tolerant physiologies. Studies by Zanazzi and Kohn (2009), and Boardman and Secord (2013) found that the oreodont *Agriochoerus* and the camelid *Poebrotherium* had the highest $\delta^{18}O$ values relative to the rest of the White River fauna, strongly suggesting water-independence. In agreement with expectations for drier conditions, *Poebrotherium* shows a relative increase in abundance in the EOCT and it continues to increase in subsequent bins (Figs 5 and 13, Tables 6-8, 12-14). Samples of *Agriochoerus* are too small to adequately test. Notably, another camelid, *Paratylopus*, also exhibits increases in abundance from the Chadronian to the Orellan. Given that *Paratylopus* and *Poebrotherium* were closely related, they may have had similar physiologies for water independence. However, stable isotope data are needed to test this hypothesis. Also, *Paratylopus* comprises a small percentage of the overall fauna, so it is more sensitive to small changes in numbers than taxa represented by larger samples. The only other taxon with $\delta^{18}O$

values high enough to suggest water independence is the rhinoceros *Hyracodon*. It shows no clear abundance trend, however, and appears to be relatively stable.

Similarly, it might be expected that those taxa that have lower $\delta^{18}O$ values, and are therefore more water-dependent, should decrease in relative abundance as the climate dried. Of the well-sampled taxa, the entelodont *Archaeotherium* is the strongest candidate for water dependence. It consistently has the lowest $\delta^{18}O$ values (Boardman and Secord, 2013) of any of the well-sampled taxa considered here. Moreover, studies of entelodont teeth and jaw mechanisms indicate that it had an omnivorous diet probably containing a significant portion of carrion, as well as crushing bone for the marrow (Joeckel, 1990). Modern carnivores are obligate drinkers and are thought to be ideal water-dependent mammals (Iacumin and Longinelli, 2002). For similar physiological reasons, omnivores that do not consume much leaf water should also be water-dependent. Notably, *Archaeotherium* shows a significant decline in abundance in the EOCT using all binning schemes, followed by continued decline in subsequent zones. This is consistent with expectations for drier conditions.

In addition to differences in water dependence, there are presumed differences between how White River ungulates digested food that would be impacted by a drying climate. Many perissodactyls are presumptively hindgut-fermenting taxa, or animals that have simple, single-chambered stomachs that ferment food in their cecum to aid digestion. Presumptive hindgut-fermenters include *Mesohippus, Trigonias,* and *Megacerops*, which decrease in abundance or go extinct across the EOCT. Two other putative hindgut-fermenters, *Hyracodon* and *Subhyracodon* (Zanazzi and Kohn, 2008), remain stable in relative abundance across the EOCT. Foregut fermentation involves fermenting food in a specialized chamber in the stomach and is a more

efficient way to process nutrient-poor foods (Alexander, 1993). Therefore, it confers an advantage in drier, open, environments characterized by widespread grasses and other nutrient-poor plants (Jiao et al., 2016; Gong et al., 2017). However, widespread grasses were probably not present at this time (Stromberg, 2004). It is uncertain whether the Merycoidodontidae were fore-gut fermenters. Phylogenetic analyses indicate that they are only distantly related to ruminants (Stevens and Stevens, 2007) and they have no living descendants. *Poebrotherium*, a putative foregut fermenter (Zanazzi and Kohn, 2008), does increase in abundance through time. However, these physiological differences do not explain all of the changes in relative abundance that occur across the EOCT, as not all hind-gut fermenting taxa decrease in relative abundance across the EOCT. Furthermore, groups like equids successfully spread and became abundant in an even drier Miocene later in time, so differences in digestion do not explain the decreasing abundance of hind-gut fermenters like *Mesohippus* (e.g. Cerling et al., 1997).

Similarly, differences in dentition do not seem to be a selection factor for the relative abundance of White River taxa. Though all the taxa sampled here with bilophodont, buno-selenodont, and bunodont molars did decrease in relative abundance, taxa with brachy-lophodont molars like *Mesohippus* and *Trigonias* also decrease in abundance while *Hyracodon* and *Subhyracodon* remain stable (Fig C1-4; Tables 7, 13, B2, B8, B13, B19, C2, C6, D2, and E2). Brachy-selenodont dentition was also not a guarantee of increasing abundance across the EOCT as *Megacerops* goes extinct before Orella A and the rare taxon *Aepinacodon* decreases in abundance through the Chadron Formation while *Merycoidodon* increases. A drying environment would be expected to decrease nutrients in plants (Gon et al., 2017) and change the composition of the flora, but unfortunately the White River flora of this time is not preserved as macrofossils to accurately measure this. Phytoliths and root traces provide conflicting levels of

change to more open conditions as well (Retallack 1983, 1992; Terry, 2001; Strömberg, 2004). This makes it difficult to predict what dentitions could be advantageous in the White River fauna and further interpret changes in relative abundance with respect to dentition.

Locomotor adaptations also do not seem to be an important factor in the success of taxa across the EOCT. A drier environment would presumably be more open, especially if precipitation dropped below the threshold necessary to sustain a forest (e.g., fig. 2.1, Allen-Diaz et al., 1995). Cursorial mammals that are adapted for feeding in open areas should have an advantage for outrunning predators. Taxa that show cursorial adaptations are *Mesohippus, Hyracodon,* and *Poebrotherium* (Webb, 1972; Thomason, 1984; Prothero, 1998). However, these taxa show no consistent pattern of abundance change (*Mesohippus* decreases, *Hyracodon* remains stable, and *Poebrotherium* steadily increases in abundance through time). Thus, cursoriality does not appear to explain changes in relative abundance across the EOCT.

CONCLUSIONS

There is a consistent pulse of coordinated relative abundance change in the most common taxa, *Mesohippus* and *Merycoidodon,* between Chadron B and Chadron C before the onset of EOCT, in all of the binning schemes used here. However, it does not appear this larger percent change in relative abundance is being driven by climate change, as it predates the pulses of greater climate shift in the EOCT. Alternatively, the close proximity of this change to the EOCT raises the possibility that climate change in the continental interior of North America began earlier than indicated by the marine oxygen isotope record, which is subject to the influence of

ice sheet growth in Antarctica. Additionally, there was neither significant nor marked change in diversity indices in or near the EOCT, though there is an insignificant peak in evenness in Chadron C. A change in chord distance did, however, occur across the EOCT, indicating greater similarity among zones within the Chadron or Orellan, than between the zones within these NALMAs. Diversity changes and the loss or the near loss of Chadron taxa like *Megacerops* and *Eotylopus* appear to be responsible for the greater chord distance before and after the EOCT. Chord distance analyses of only taxa that cross the EOCT do not show this pattern. In addition to the pulse of relative abundance change across the EOCT in the most abundant taxa, several taxa exhibited longer term increases or decreases in relative abundance. For the only two taxa that could be classified as water-dependent or water-independent with confidence, the patterns of changing relative abundance agreed with the expectations of a shift to drier conditions starting in the EOCT. Water-independent *Poebrotherium* progressively increased in relative abundance through the Orellan, while water-dependent *Archaeotherium* showed a progressive decrease. Trends in other taxa cannot, as yet, be confidently explained by dietary or locomotor patterns.

ACKNOWLEDGEMENTS

Special thanks to my advisor, Dr. Ross Secord for his continued patience, knowledge, guidance, interest, and for allowing me the incredible experience of going into the field to collect fossils for the first time. I would also like to thank Dr. David Watkins for his teaching of statistics that were vital to this work, his advice, and for convincing me to finally leave the country for the first time in his Schram Course. Thanks also to Dr. Matt Joeckel for his help, the doughnuts, and for making geomorphology even more fascinating to me than it had been before. Thank you to Gail Littrell, Carrie Herbel, and R. George Corner for their kindness, humor, and help around the Museum's fossils and systems. I would also like to acknowledge Shane Tucker for his help giving me access to many identification papers I had not been able to get hold of. I am also very thankful for the University of Nebraska-Lincoln Department of Earth and Atmospheric Sciences for funding my time as a master's student and allowing me to do this research. Additionally, I would like to thank the Nebraska Geological Society and the Geological Society of America for funding the stable isotope sampling of enamel from the *Merycoidodon* specimens. Finally, I would like to give thanks to my wife and family for their love, support, and patience.

LITERATURE CITED

.

Alexander, R.M., 1993, The relative merits of foregut and hindgut fermentation: Journal of Zoology, v. 231, p. 391–401, doi: 10.1111/j.1469-7998.1993.tb01927.x.

Allen-Diaz, B., Chapin, F. S., Diaz, S., Howden, M., Puigdefábregas, J., Smith, M. S., Benning, T., Bryant, F., Campbell, B., J. duToit, Z., Galvin, K., Holland, E., Joyce, L., Knapp, A. K., Matson, P., Miller, R., Ojima, D., Polley, W., Seastedt, T., Suarez, A., Svejcar, T., and Wessman, C., 1995, Rangelands in a changing climate: impacts, adaptations and mitigation, in Watson, R. T., Zinyowera, M. C., and Moss, R. H., eds., Impacts, adaptations and mitigation of climate change: scientific-technical analyses, Volume SAR 2, Ingergovernmental Panel on Climate Change, p. 131-158..

Allen, B., Kon, M., and Bar-Yam, Y., 2009, A New Phylogenetic Diversity Measure Generalizing the Shannon Index and Its Application to Phyllostomid Bats: The American Naturalist, v. 174, p. 236–243, doi: 10.1086/600101.

Alroy, J., 2000, New methods for quantifying macroevolutionary patterns and processes: Paleobiology, v. 26, p. 707–733, doi: 10.1666/0094-8373(2000)026<0707:nmfqmp>2.0.co;2.

Alroy, J., Koch, P.L., and Zachos, J.C., 2000, Global climate change and North American mammalian evolution: Paleobiology, v. 26, p. 259–288, doi: 10.1017/s0094837300026968.

Barrett, P. Z., 2016. Taxonomic and systematic revisions to the North American Nimravidae (Mammalia, Carnivora) PeerJ 4:e1658 https://doi.org/10.7717/peerj.1658

Behrensmeyer, A.K., 1975, The taphonomy and paleoecology of Plio-Pleistocene vertebrate assemblages east of Lake Rudolf, Kenya: Bulletin of the Museum of Comparative Zoology, Harvard University, v. 146, no. 10, p. 473–578.

Benton, R. C., Evanoff, E., Herbel, C. L., and Terry, Jr., D. O., 2001, Baseline mapping of fossil bone beds at Badlands National Park; p.85–94 in V. L. Santucci and L. McClelland (eds.), Proceedings of the 6th Fossil Resource Conference: National Park Service Geological Resources Division Technical Report NPS/NRGRD/ GRDTR-01/01

Berggren, W.A., Kent, D.V., Swisher, C.C., and Aubry, M.-P., 1995, A Revised Cenozoic Geochronology and Chronostratigraphy: Geochronology, Time Scales, and Global Stratigraphic Correlation, p. 129–212, doi: 10.2110/pec.95.04.0129.

Boardman, G.S., and Secord, R., 2013, Stable isotope paleoecology of White River ungulates during the Eocene–Oligocene climate transition in northwestern Nebraska: Palaeogeography, Palaeoclimatology, Palaeoecology, v. 375, p. 38–49, doi: 10.1016/j.palaeo.2013.02.010.

Bobe, R., Behrensmeyer, A.K., and Chapman, R.E., 2002, Faunal change, environmental variability and late Pliocene hominin evolution: Journal of Human Evolution, v. 42, p. 475–497, doi: 10.1006/jhev.2001.0535.

Bohaty, S. M; Zachos, J. C; Delaney, M. L., 2012, Foraminiferal Mg/Ca and Mn/Ca ratios across the Eocene-Oligocene transition: Pangaea, https://doi.org/10.1594/PANGAEA.783839, Supplement to: Bohaty, SM et al. (2012): Foraminiferal Mg/Ca evidence for Southern Ocean cooling across the Eocene-Oligocene transition. Earth and Planetary Science Letters, 317-318, p. 251-261, https://doi.org/10.1016/j.epsl.2011.11.037

Bump, J.D., 1956, Geographic names for members of the Brule Formation of the Big Badlands of South Dakota: American Journal of Science, v. 254, p. 429–432, doi: 10.2475/ajs.254.7.429.

Cerling, T.E., Harris, J.M., Macfadden, B.J., Leakey, M.G., Quade, J., Eisenmann, V., and Ehleringer, J.R., 1997, Global vegetation change through the Miocene/Pliocene boundary: Nature, v. 389, p. 153–158, doi: 10.1038/38229.

Clark, J., J. R. Beerbower, and K.K. Kietzke., 1967a, General geology; p. 9–15 in E. G. Nash and P. M. Williams (eds.), Oligocene Sedimentation, Stratigraphy, Paleoecology, and Paleoclimatology in the Big Badlands of South Dakota. Fieldiana: Geology Memoirs, v. 5.

Clark, J., J. R. Beerbower, and K.K. Kietzke., 1967b, The Slim Buttes Formation; p. 16–20 in E. G. Nash and P. M. Williams (eds.), Oligocene Sedimentation, Stratigraphy, Paleoecology, and Paleoclimatology in the Big Badlands of South Dakota. Fieldiana: Geology Memoirs, v. 5.

Colbert, M. W., 1999, Patterns of evolution and variation in the Tapiroidea (Mammalia: Perissodactyla). [Ph.D. dissertation], The University of Texas at Austin, Austin, Texas, p. 464.

Colbert, M. W. 2005. The facial skeleton of the early Oligocene *Colodon* (Perissodactyla, Tapiroidea). Palaeontologia Electronica v. 8:27 p. 600 kB; http://palaeo-electronica.org/paleo/2005_1/colbert1/issue1_05.htm.

Coxall, H.K., Wilson, P.A., Pälike, H., Lear, C.H., and Backman, J., 2005, Rapid stepwise onset of Antarctic glaciation and deeper calcite compensation in the Pacific Ocean: Nature, v. 433, p. 53–57, doi: 10.1038/nature03135.

Cramer, B.S., Toggweiler, J.R., Wright, J.D., Katz, M.E., and Miller, K.G., 2009, Ocean overturning since the Late Cretaceous: Inferences from a new benthic foraminiferal isotope compilation: Paleoceanography, v. 24, doi: 10.1029/2008pa001683.

Dansgaard, W., 1964, Stable isotopes in precipitation: Tellus, v. 16, p. 436–468, doi: 10.3402/tellusa.v16i4.8993.

Desantis, L.G., 2011, Stable Isotope Ecology of Extant Tapirs from the Americas: Biotropica, v. 43, p. 746–754, doi: 10.1111/j.1744-7429.2011.00761.x.

Diefendorf, A.F., Mueller, K.E., Wing, S.L., Koch, P.L., and Freeman, K.H., 2010, Global patterns in leaf 13C discrimination and implications for studies of past and future climate: Proceedings of the National Academy of Sciences, v. 107, p. 5738–5743, doi: 10.1073/pnas.0910513107.

Dockery, D. T., Louzet, P., 2003. Molluscan faunas across the Eocene/Oligocene boundary in the North American Gulf Coastal Plain, with comparisons to those of the Eocene and Oligocene of France, in: Prothero, D.R., Ivany, L.C., Nesbitt, E.A. (Eds.), From greenhouse to icehouse: the marine Eocene-Oligocene transition. Columbia University Press, New York, p. 303-340.

Dupont-Nivet, G., Krijgsman, W., Langereis, C.G., Abels, H.A., Dai, S., and Fang, X., 2007, Tibetan plateau aridification linked to global cooling at the Eocene–Oligocene transition: Nature, v. 445, p. 635–638, doi: 10.1038/nature05516.

Eagle, R.A., Eiler, J.M., Tripati, A.K., Ries, J.B., Freitas, P.S., Hiebenthal, C., Jr., A.D.W., Taviani, M., Elliot, M., Marenssi, S., Nakamura, K., Ramirez, P., and Roy, K., 2013, The influence of temperature and seawater carbonate saturation state on 13C-18O bond ordering in bivalve mollusks: Biogeosciences Discussions, v. 10, p. 157–194, doi: 10.5194/bgd-10-157-2013.

Emry, R.J., Bjork, P.R., Russell, L.S., 1987, The Chadronian, Orellan, and Whitneyan land mammal ages. In: Woodburne, M.O. (Ed.), Cenozoic Mammals of North America: Geochronology and Biostratigraphy. University of California Press, Berkeley, p. 118–152.

Emry, R.J., and Korth, W.W., 2012, Early Chadronian (late Eocene) rodents from the Flagstaff Rim area, central Wyoming: Journal of Vertebrate Paleontology, v. 32, p. 419–432, doi: 10.1080/02724634.2012.649329.

Evanoff, E., Prothero, D.R., Lander, R.H., 1992, Eocene-Oligocene climatic change in North America: the White River Formation near Douglas, east-central Wyoming, in: Prothero, D.R., Berggren, W.A. (Eds.), Eocene-Oligocene Climatic and Biotic Evolution. Princeton University Press, Princeton, p. 116-130.

Foss, S.E., 2007, "Family Entelodontidae." The Evolution of the Artiodactyls, p. 120-129

Galeotti, S., DeConto, R. and Naish, T., Stocchi, P. and Fabio, F., Pagani, M., Barrett, P., Bohaty, S., Lanci, L., Pollard, D., Sandroni, S., Talarico, F., Zachos, J. C., 2016, Antarctic Ice Sheet variability across the Eocene-Oligocene boundary climate transition. Science. p. 352.

Gat, J.R., 1996, Oxygen and Hydrogen Isotopes in The Hydrologic Cycle: Annual Review of Earth and Planetary Sciences, v. 24, p. 225–262, doi: 10.1146/annurev.earth.24.1.225.

Gong, Y., Lv, G., Guo, Z., Chen, Y., and Cao, J., 2017, Influence of aridity and salinity on plant nutrients scales up from species to community level in a desert ecosystem: Scientific Reports, v. 7, doi: 10.1038/s41598-017-07240-6.

Gong, Y., Lv, G., Guo, Z., Chen, Y., and Cao, J., 2017, Influence of aridity and salinity on plant nutrients scales up from species to community level in a desert ecosystem: Scientific Reports, v. 7, doi: 10.1038/s41598-017-07240-6.

Hillson, S., 1986, Teeth, Cambridge, Cambridge University Press, p. 376.

Holbrook, T., 1999, The Phylogeny and Classification of Tapiromorph Perissodactyls (Mammalia) (project): MorphoBank datasets, doi: 10.7934/p849.

Hooker, J., Grimes, S., Mattey, D., Collinson, M., and Sheldon, N., 2009, Refined correlation of the UK Late Eocene–Early Oligocene Solent Group and timing of its climate history: The Late Eocene Earth—Hothouse, Icehouse, and Impacts, doi: 10.1130/2009.2452(12).

Hutchison, J., 1982, Turtle, crocodilian, and champsosaur diversity changes in the Cenozoic of the north-central region of western United States: Palaeogeography, Palaeoclimatology, Palaeoecology, v. 37, p. 149–164, doi: 10.1016/0031-0182(82)90037-2.

Hutchison, J.H., 1992, Western North America reptile and amphibian record across the Eocene/Oligocene boundary and its climatic implications, in: Prothero, D.R., Berggren, W.A. (Eds.), Eocene-Oligocene Climatic and Biotic Evolution. Princeton University Press, Princeton, p. 451-463.

Iacumin, P., and Longinelli, A., 2002, Relationship between $\delta^{18}O$ values for skeletal apatite from reindeer and foxes and yearly mean $\delta^{18}O$ values of environmental water: Earth and Planetary Science Letters, v. 201, p. 213-219.

Ivany, L.C., Simaeys, S.V., Domack, E.W., and Samson, S.D., 2006, Evidence for an earliest Oligocene ice sheet on the Antarctic Peninsula: Geology, v. 34, p. 377, doi: 10.1130/g22383.1.

Jacques, L., Ogle, N., Moussa, I., Kalin, R., Vignaud, P., Brunet, M., and Bocherens, H., 2008, Implications of diagenesis for the isotopic analysis of Upper Miocene large mammalian herbivore tooth enamel from Chad: Palaeogeography, Palaeoclimatology, and Palaeoecology, v. 266, p. 200-210.

Janis, C.M., Constable, E., 1993, Can ungulate craniodental features determine digestive physiology? Journal of Vertebrate Paleontology. V. 13, p. 43A.

Jiménez-Hidalgo, E., & Guerrero-Arenas, R., 2018, The oldest camel footprints from Mexico. Boletín de la Sociedad Geológica Mexicana, v. 70(2), p. 351-359.

Jiao, F., Shi, X. R., Han, F. P., & Yuan, Z. Y., 2016, Increasing aridity, temperature and soil pH induce soil CNP imbalance in grasslands. Scientific reports, 6, p. 19601.

Joeckel, R.M., 1990, A functional interpretation of the masticatory system and paleoecology of entelodonts: Paleobiology, v. 16, p. 459–482, doi: 10.1017/s0094837300010198.

Kohn, M. J., and Cerling, T. E., 2002, Stable isotope compositions of biological apatite, in Kohn, M. J., Rakovan, J., and Hughes, J. M., eds., Reviews in mineralogy and geochemistry: Washington, D. C., Mineralogical Society of America 48, p. 455-488.

Korth, William., 1989, Lagomorphs (Mammalia) from the Oligocene (Orellan and Whitneyan) Brule Formation, Nebraska. Journal of Vertebrate Paleontology – J Vertebrate Paleontology. v. 9 p. 400-414. 10.1080/02724634.1989.10011773.

Kowalski, E.A., and Dilcher, D.L., 2002, Warmer paleotemperatures for terrestrial ecosystems: Proceedings of the National Academy of Sciences, v. 100, p. 167–170, doi: 10.1073/pnas.232693599.

Kowalski, E. A., & Dilcher, D. L., 2003, Warmer paleotemperatures for terrestrial ecosystems. Proceedings of the National academy of Sciences, 100(1) p. 167-170.

Kron, D.G., Manning, E., 1998, Anthracotheriidae. In: Janis, C.M., Scott, K.M., Jacobs, L.L. (Eds.), Evolution of Tertiary Mammals of North America, Volume 1: Terrestrial Carnivores, Ungulates, and Ungulate-like Mammals. Cambridge University Press, Cambridge (UK), p. 381-388.

Labrecque, J.L., Kent, D.V., and Cande, S.C., 1977, Revised magnetic polarity time scale for Late Cretaceous and Cenozoic time: Geology, v. 5, p. 330, doi: 10.1130/0091-7613(1977)5<330:rmptsf>2.0.co;2.

LaGarry, H. E., 1997, Geology of the Toadstool Park region of northwestern Nebraska, with the lithostratigraphic revision and redescription of the Brule Formation and remarks on Oligocene bone processing. [Ph.D. Thesis]: Lincoln, University of Nebraska.

Lee-Thorp, J., Van Der Merwe, N.J., 1987, Carbon isotope analysis of fossil bone apatite, South African Journal of Science 83 (11), p. 712-715.

Leidy, J. 1848, On a new fossil genus and species of ruminantoid Pachydermata; *Merycoidodon culbertsonii*: Proceedings of the Academy of Natural Sciences of Philadelphia, 1848, p. 47-50.

Levin, N.E., Cerling, T.E., Passey, B.H., Harris, J.M., and Ehleringer, J.R., 2006, A stable isotope aridity index for terrestrial environments: Proceedings of the National Academy of Sciences, v. 103, p. 11201–11205, doi: 10.1073/pnas.0604719103.

Liu, Z.-H., Pagani, M., Zinniker, D., DeConto, R., Huber, M., Brinkhuis, H., Shah, S.R., Leckie, R.M., Pearson, A., 2009, Global Cooling During the Eocene-Oligocene Climate Transition. Science 323, p. 1187-1190.

Ludtke J. A., 2008, Systematic review of Agriochoerids, In the Evolution of Artiodactyls (eds Prothero DR, Foss SE). John Hopkins Press; p. 151-156

Macdonald, J. R., 1956, The North American anthracotheres. Journal of Paleontology, 30 p. 615–645.

MacGinitie, H. D., 1953, Fossil Plants of the Florissant Beds, Colorado. Carnegie Inst. Washington publ. p. 599.

Martin, J. E., 1987, The White River Badlands of South Dakota; p. 233–236 in S. S. Beus (ed.) Centennial Field Guide volume 2, Geological Society of America, Inc., Boulder, Colorado.

Masciale, D., 2010, An analysis of anchitherine equids across the eocene–oligocene boundary in the white river group of the western great plains. [Master's Thesis]: Lincoln, University of Nebraska

Mead, A.J., Wall, W.P., 1998a, Paleoecological implications of the craniodental and premaxilla morphologies of two rhinocerotoids (Perissodactyla) from Badlands National Park, South Dakota. National Park Service Paleontological Research 3, p. 23-28.

Meek, F. B. and F. V. Hayden., 1857, Explorations under the War Department: Description of new Cretaceous and Tertiary fossils collected by Dr. F. V. Hayden in Nebraska, under the supervision of Lieut. G. K. Warren, U. S. Top. Engineer, with some remarks on the

geology of the Upper Missouri country. Proceedings of the Academy of Natural Sciences of Philadelphia 9, p. 117–148.

Mendoza, M., Janis, C.M., and Palmqvist, P., 2006, Estimating the body mass of extinct ungulates: a study on the use of multiple regression: Journal of Zoology, doi: 10.1111/j.1469-7998.2006.00094.x.

Mihlbachler, M., Lucas, S., Emry, R., 2004. The holotype specimen of Menodus giganteus , and the "insoluble" problem of Chadronian brontothere taxonomy. New Mexico Museum of Natural History and Science Bulletin v. 26.

Miller, K.G., Wright, J.D., Katz, M.E., Wade, B.S., Browning, J.V., Cramer, B.S., and Rosenthal, Y., 2009, Climate threshold at the Eocene-Oligocene transition: Antarctic ice sheet influence on ocean circulation: The Late Eocene Earth—Hothouse, Icehouse, and Impacts, doi: 10.1130/2009.2452(11).

Moore, J.R., and Norman, D.B., 2009, Quantitatively evaluating the sources of taphonomic biasing of skeletal element abundances in fossil assemblages: Palaios, v. 24, p. 591–602, doi: 10.2110/palo.2008.p08-135r.

Myers, J.A., 2003, Terrestrial Eocene-Oligocene vegetation and climate in the Pacific Northwest, in: Prothero, D.R., Ivany, L.C., Nesbitt, E.A. (Eds.), From greenhouse to icehouse: the marine Eocene-Oligocene transition. Columbia University Press, New York, p. 171-185.

Nesbitt, E.A., 2003, Changes in shallow-marine faunas from the northeastern Pacific margin across the Eocene/Oligocene boundary, in: Prothero, D.R., Ivany, L.C., Nesbitt, E.A. (Eds.), From greenhouse to icehouse: the marine Eocene-Oligocene transition. Columbia University Press, New York, p. 57-70.

O'Leary, M.H., 1988, Carbon isotopes in photosynthesis. Bioscience v. 38, p. 328-336.

Ogg, J. G. and A.G. Smith., 2004, The geomagnetic polarity time scale; p. 63–86 in F. Gradstein, J. Ogg., and A. G. Smith (eds.), A Gelogic Time Scale. Cambridge University Press, Cambridge, U. K.

Ogg, J. G., Ogg, G., and Gradstein, F. M., 2008, The concise geologic time scale, Cambridge, Cambridge University Press, 177 p.

Ogg, J. G., Gradstein, F. M., Schmitz, M., & Ogg, G. (Eds.), 2012, The geologic time scale 2012. elsevier.

Owen, R., 1848, Description of teeth and portion of the jaws of two extinct anthracotheroid quadrupeds (Hyopotamys vectianus and Hyopop. Bovinus) discovered by the Marchioness of Hastings in the Eocene deposits on the N. W. coast of the Isle of Wight: with an attempt to develop Cuvier's idea of the classification of pachyderms by the number of their toes. Quarterly Journal of the Geological Society of London v. 4 p.103–141.

Owen, D. D., 1850, Notice of fossil remains from the "Mauvais Terres" or badlands of White River [South Dakota]. Proceedings of the Academy of Natural Sciences of Philadelphia v. 5 p.66-67.

Pälike, H., Norris, R. D., Herrle, J. O, Wilson, P. A., Coxall, H., Lear, C. H., Shackleton, N. J., Tripati, A. K., Wade, B. S., 2006, Age models and stable isotope analysis on sediment core Site 199-1218 from the equatorial Pacific. Pangaea, https://doi.org/10.1594/PANGAEA.547942, Supplement to: Pälike, H et al., 2006, The Heartbeat of the Oligocene Climate System. Science, v. 314, p. 1894-1898, https://doi.org/10.1126/science.1133822

Passey, B.H., Cerling, T.E., Perkins, M.E., Voorhies, M.R., Harris, J.M., Tucker, S.T., 2002, Environmental change in the Great Plains: an isotopic record from fossil horses. Journal of Geology 110, p. 123-140.

Passey, B.H., Robinson, T.F., Ayliffe, L.K., Cerling, T.E., Sponheimer, M., Dearing, M.D., Roeder, B.L., and Ehleringer, J.R., 2005, Carbon isotope fractionation between diet, breath CO2, and bioapatite in different mammals: Journal of Archaeological Science, v. 32, p. 1459–1470, doi: 10.1016/j.jas.2005.03.015.

Pearson, P.N., McMillan, I.K., Wade, B.S., Jones, T.D., Coxall, H.K., Bown, P.R., H. Lear, C.H., 2008, Extinction and environmental change across the Eocene -Oligocene boundary in Tanzania. Geology 36, p. 179-182.

Petersen, S.V., and Schrag, D.P., 2015, Antarctic ice growth before and after the Eocene-Oligocene transition: New estimates from clumped isotope paleothermometry: Paleoceanography, v. 30, p. 1305–1317, doi: 10.1002/2014pa002769.

Pound, M. J., and Salzmann, U., 2017, Heterogeneity in global vegetation and terrestrial climate change during the late Eocene to early Oligocene transition: Scientific Reports, v. 7, no. 43386, doi: 10.1038/srep43386

Prothero D. R., and C. C. Swisher, III, 1992, Magnetostratigraphy and geochronology of the terrestrial Eocene–Oligocene Transition in North America; p. 46–73 in D. R. Prothero and W. A. Berggren (eds.), Eocene–Oligocene Climatic and Biotic Evolution. Princeton University Press, Princeton, New Jersey. 17:449–505.

Prothero, D. R., 1994, The late Eocene–Oligocene extinctions. Annual Review of Earth Science 22, p.145–165.

Prothero, D.R., Heaton, T.H., 1996, Faunal stability during the early Oligocene climatic crash. Palaeogeography, Palaeoclimatology, Palaeoecology 127, p. 239-256.

Prothero, D. R., and R. J. Emery., 1996a, Summary; p. 646–664 in D. R. Prothero and R. J. Emery (eds.), The Terrestrial Eocene–Oligocene Transition in North America. Cambridge University Press, Cambridge, U. K.

Prothero, D. R., and R. J. Emery., 1996b, Magnetostratigraphy of the Eocene–Oligocene transition in Trans–Pecos Texas; p. 189–198 in D. R. Prothero and R. J. Emery (eds.), The Terrestrial Eocene–Oligocene Transition in North America. Cambridge University Press, Cambridge, U. K.

Prothero, D. R., and K. E. Whittlesey., 1998, Magnetic stratigraphy and biostratigraphy of the Orellan and Whitneyan land mammal “ages” in the White River Group; p. 39–62 in D. O. Terry, Jr., H. E. LeGarry, and R. M. Hunt, Jr. (eds.), Depositional Environments,

Lithostratigraphy, and Biostratigraphy of the White River and Arikaree Groups (Late Eocene to Early Miocene, North America): Geological Society of America Special Paper 325. Geological Society of America, Inc., Boulder, Colorado.

Prothero, D. R., 1998, Hyracodontidae. In: Janis, C.M., Scott, K.M., Jacobs, L.L. (Eds.), Evolution of Tertiary Mammals of North America. Volume 1: Terrestrial Carnivores, Ungulates, and Ungulate-like Mammals. Cambridge University Press, Cambridge (UK), p. 381-388.

Prothero, D.R., 1999, Does climatic change drive mammalian evolution? GSA Today 9, p. 1-5.

Prothero, D.R., Emry, R.J., 2004, The Chadronian, Orellan, and Whitneyan North American land mammal ages, in: Woodburne, M.O. (Ed.), Late Cretaceous and Cenozoic Mammals of North America: biostratigraphy and geochronology. Columbia University Press, New York, p. 156-168.Retallack, G. J. (ed.)., 1983. Late Eocene and Oligocene Paleosols from Badlands National Park: Geological Society of America Special Paper 325. Geological Society of America, Inc., Boulder, Colorado, p. 82.

Retallack, G. J., 1992, Paleosols and changes in climate and vegetation across the Eocene/Oligocene boundary; p. 382–398 in D. R. Prothero and W. A. Berggren (eds.), Eocene–Oligocene Climatic and Biotic Evolution. Princeton University Press, Princeton, New Jersey.

Retallack, G.J., 2007, Cenozoic paleoclimate on land in North America. Journal of Geology 115, p. 271-294.

Quade, J., Cerling, T.E., Andrews, P., Alpagut, B., 1995, Paleodietary reconstruction of Miocene faunas from Pasalar, Turkey using stable carbon and oxygen isotopes of fossil tooth enamel. Journal of Human Evolution 28, p. 373-384.

Sahy, D., Condon, D.J., Terry, D.O., Fischer, A.U., and Kuiper, K.F., 2015, Synchronizing terrestrial and marine records of environmental change across the Eocene–Oligocene transition: Earth and Planetary Science Letters, v. 427, p. 171–182, doi: 10.1016/j.epsl.2015.06.057.

Sahy, D., Condon, D.J., Hilgen, F.J., and Kuiper, K.F., 2017, Reducing Disparity in Radio-Isotopic and Astrochronology-Based Time Scales of the Late Eocene and Oligocene: Paleoceanography, v. 32, p. 1018–1035, doi: 10.1002/2017pa003197.

Schultz, C. B. and T. M. Stout., 1955, Classification of Oligocene sediments in Nebraska: A guide for the stratigraphic collecting of fossil mammals. Bulletin of the University of Nebraska State Museum 4, p. 17–52.

Schultz, B.C., and Falkenbach, C.H., 1969, The Phylogeny of the Oreodonts. Part I and 2.: The Quarterly Review of Biology, v. 44, p. 297–297, doi: 10.1086/406151.

Schultz, W. A., 2006, Body Size Evolution in Leptomeryx And Rhinocerotinae (Subhyracodon And Trigonias) Across the Eocene – Oligocene (Chadronian – Orellan) Boundary. [Master's Thesis]: Lincoln, University Nebraska.

Secord, R., Wing, S.L., Chew, A., 2008, Stable isotopes in early Eocene mammals as indicators of forest canopy structure and resource partitioning. Paleobiology 34, p. 282-300.

Shannon, C. E., 1948, A mathematical theory of communication. Bell system technical journal, 27(3), p. 379-423.

Sheldon, N.D., and Retallack, G.J., 2004, Regional Paleoprecipitation Records from the Late Eocene and Oligocene of North America: The Journal of Geology, v. 112, p. 487–494, doi: 10.1086/421076.

Sheldon, N. D., 2009, Nonmarine records of climatic change across the Eocene– Oligocene transition; p. 241–248 in C. Koeberl and A. Montanari (eds.), The Late Eocene Earth—Hothouse, Icehouse, and Impacts: GSA Special Paper 452. Geological Society of America, Inc., Boulder, Colorado.

Sijp, W.P., England, M.H., 2005, On the role of the Drake Passage in controlling the stability of the ocean's thermohaline circulation. Journal of Climate 18, p. 1957 -1966.

Simpson, E. H., 1949, Measurement of diversity. nature, 163(4148), p. 688.

Śliwińska, K.K., Thomsen, E., Schouten, S., Schoon, P.L., and Heilmann-Clausen, C., 2019, Climate- and gateway-driven cooling of Late Eocene to earliest Oligocene sea surface temperatures in the North Sea Basin: Scientific Reports, v. 9, doi: 10.1038/s41598-019-41013-7.

Stehlin, H. G., 1909, Remarques sur les faunules de mammifères des couches Éocènes et Oligocènes du Bassin de Paris. Bulletin de la Société Géologique de France v. 9 p. 488–520.

Steinthorsdottir, M., Porter, A. S., Holohan, A., Kunzmann, L., Collinson, M., and McElwain, J. C., 2016, Fossil plant stomata indicate decreasing atmospheric CO2 prior to the Eocene–Oligocene boundary: Climate of the Past, v. 12, p. 439-454.

Stevens, M.S., Stevens, J.B., 1996, Merycoidodontidae and Miniochoerinae, in: Prothero, D.R. and Emry, R.J. (Eds.), The Terrestrial Eocene-Oligocene Transition in North America. Cambridge University Press, Cambridge (UK), p. 498-573.

Stewart, G., Turnbull, M., Schmidt, S., and Erskine, P., 1995, 13C Natural Abundance in Plant Communities Along a Rainfall Gradient: a Biological Integrator of Water Availability: Functional Plant Biology, v. 22, p. 51, doi: 10.1071/pp9950051.

Stromberg, C., 2004, Using phytolith assemblages to reconstruct the origin and spread of grass-dominated habitats in the great plains of North America during the late Eocene to early Miocene: Palaeogeography, Palaeoclimatology, Palaeoecology, v. 207, p. 239–275, doi: 10.1016/s0031-0182(04)00043-4.

Stromberg, C.A.E., 2005, Decoupled taxonomic radiation and ecological expansion of open-habitat grasses in the Cenozoic of North America: Proceedings of the National Academy of Sciences, v. 102, p. 11980–11984, doi: 10.1073/pnas.0505700102.

Swinehart, J. B., V. L. Souders, H. M. Degraw, and R. F. Diffendal., 1985, Cenozoic paleogeography of western Nebraska; p. 209–229 in R. M. Flores and S. Kaplan (eds.), Cenozoic Paleogeography of the West Central United States: Rocky Mountain Section, Society of Economic Paleontologists and Mineralogists, Rocky Mountain

Palaeogeography Symposium 3. Society of Economic Paleontologists and Mineralogists, Rocky Mountain Section, Denver, Colorado.

Taylor, B.E., and Webb, S.D., 1976, Miocene Leptomerycidae (Artiodactyla, Ruminantia) and their relationships: American Museum Novitates, v. 2596, p. 1-22

Terry, D. O., Jr., and J. E. Evans., 1994, Pedogenesis and paleoclimate implications of the Chamberlain Pass Formation, Basal White River Group, Badlands of South Dakota. Palaeogeography, Palaeoclimatology, Palaeoecology 110, p. 197–215.

Terry, D. O., Jr. and LaGarry, H. E., 1998, The Big Cottonwood Creek Member: A new member of the Chadron Formation in northwestern Nebraska; p. 117–142 in D. O. Terry, Jr., H. E. LeGarry, and R. M. Hunt, Jr. (eds.), Depositional Environments, Lithostratigraphy, and Biostratigraphy of the White River and Arikaree Groups (Late Eocene to Early Miocene, North America): Geological Society of America Special Paper 325. Geological Society of America, Inc., Boulder, Colorado.

Terry, D. O., Jr., 1998, Lithostratigraphic revision and correlation of the lower part of the White River Group: South Dakota to Nebraska; p. 15–38 in D. O. Terry, Jr., H. E. LeGarry, and R. M. Hunt, Jr. (eds.), Depositional Environments, Lithostratigraphy, and Biostratigraphy of the White River and Arikaree Groups (Late Eocene to Early Miocene, North America): Geological Society of America Special Paper 325. Geological Society of America, Inc., Boulder, Colorado.

Terry, D. O., Jr. 2001, Paleopedology of the Chadron Formation, northwestern Nebraska: Implications for paleoclimate in the North American mid-continent across the Eocene–Oligocene boundary. Palaeogeography, Palaeoclimatology, Palaeoecology 168, p. 1–39.

Thomas, E., 1992, Middle Eocene–late Oligocene bathyal benthic foraminifera (Weddell Sea): Faunal changes and implications for ocean circulation; p. 245–271 in D. R. Prothero and W. A. Berggren (eds.), Eocene–Oligocene Climatic and Biotic Evolution. Princeton University Press, Princeton, New Jersey.

Thomason, J. J. 1986, The functional morphology of the manus in the tridactyl equids Merychippus and Mesohippus: paleontological inferences from neontological models. Journal of Vertebrate Paleontology, 6(2), p. 143-161.

Tipple, B.J., Pagani, M., 2007, The early origins of terrestrial C_4 photosynthesis. Annual Review of Earth and Planetary Sciences 35, p. 435-461.

Toepelman, W. C., 1922, The paleontology of the [Badlands] area; p. 61–73 in F. Ward (ed.), The Geology of a Portion of the Badlands: South Dakota Geological and Natural History Survey Bulletin 11, p. 61–73.

Toggweiler, J.R., Bjornsson, H., 2000, Drake Passage and paleoclimate. Journal of Quaternary Science 15, p. 319-328.

Tütken, T., Vennemann, T., 2009, Stable isotope ecology of Miocene large mammals from Sandelzhausen, southern Germany. Paläeontologische Zeitschrift 83, p. 207 -226.

Van der Merwe, N.J., Medina, E., 1991, The canopy effect, carbon isotope ratios and foodwebs in Amazonia. Journal of Archaeological Science 18, p. 249-259.

Wall, W.P., Shikany, M.J., 1995, Comparison of feeding mechanisms in Oligocene Agriochoeridae and Merycoidodontidae from Badlands National Park. National Park Service Paleontological Research Volume 2, p. 27-33.

Wall, W. P., & Collins, C., 1998, A comparison of feeding adaptations in two primitive ruminants, Hypertragulus and Leptomeryx, from the Oligocene deposits of Badlands National Park. National Park Service Paleontological Research, 3, 13-17. Wall, W.P., Shikany, M.J., 1995. Comparison of feeding mechanisms in Oligocene Agriochoeridae and Merycoidodontidae from Badlands National Park. National Park Service Paleontological Research Volume 2, p. 27-33.

Wall, W. P.; Hauptman, J. A., 2001, "A craniodental interpretation of the dietary habits of Poebrotherium wilsoni (Camelidae) from the Oligocene of Badlands National Park, South Dakota". Proceedings of the 6th Fossil Resource Conference. (NPS/NRGRD/GRDTR-01/01) p. 76–82.

Wanless, H. R., 1922, Lithology of the White River sediments. American Philosophical Society Proceedings 62, p. 663–669.

Webb, S.D., 1972, Locomotor evolution in camels. Forma et Functio 5 p. 99-112.

Williams, D.G., Ehleringer, J.R., 1996, Carbon isotope discrimination in three semi-arid woodland species along a monsoon gradient. Oecologia 106, p. 455-460.

Wolfe, J. A., 1978, A paleobotanical interpretation of Tertiary climates in the Northern Hemisphere. American Scientist 66, p. 694–703.

Wolfe, J. A., 1992, Climatic, floristic, and vegetational changes near the Eocene– Oligocene boundary in North America; p. 421–436 in D. R. Prothero and W. A. Berggren (eds.), Eocene–Oligocene Climatic and Biotic Evolution. Princeton University Press, Princeton, New Jersey.

Wolfe, J.A., 1994, Tertiary climatic changes at middle latitudes of western North America: Palaeogeography, Palaeoclimatology, Palaeoecology, v. 108, p. 195–205, doi: 10.1016/0031-0182(94)90233-x.

Wood, H. E. II, R. W. Chaney, Jr., Clark, J. Colbert, E. H. , Jepsen, G. L., Reeside, J. B., and Stock, C., 1941, Nomenclature and correlation of the North American continental Tertiary: Geological Society of America Bulletin 52, p. 1–48.

Woodburne, M. O., 1987, Cenozoic mammals of North America, geochronology and biostratigraphy, Berkeley, University of California Press, Berkeley.

Wright, D.B., 1998, Tayassuidae, in: Janis, C.M., Scott, K.M., Jacobs, L.L. (Eds.), Evolution of Tertiary Mammals of North America, Volume 1: Terrestrial carnivores, ungulates, and ungulate-like mammals. Cambridge University Press, Cambridge (UK), p. 389-401.

Xiao, G., Abels, H.A., Yao, Z., Dupont-Nivet, G., Hilgen, F.J., 2010, Asian aridification linked to the first step of the Eocene–Oligocene climate Transition (EOT) in obliquity-dominated terrestrial records (Xining Basin, China). Climate Past 6, p. 627–657.

Yom-Tov, Y. and Geffen, E., 2006, Geographic variation in body size: the effects of ambient temperature and precipitation: Oecologia. 148, p. 213. https://doi.org/10.1007/s00442-006-0364-9

Zachos, J.C., Quinn, T.M., Salamy, K.A., 1996, High-resolution (10^4 years) deep-sea foraminiferal stable isotope records of the Eocene-Oligocene climate transition. Paleoceanography 11, p. 251-266.

Zachos, J., 2001, Trends, Rhythms, and Aberrations in Global Climate 65 Ma to Present: Science, v. 292, p. 686–693, doi: 10.1126/science.1059412.

Zachos, J.C., Dickens, G.R., Zeebe, R.E., 2008, An early Cenozoic perspective on greenhouse gas warming and carbon-cycle dynamics: Nature v. 451, p. 279–283.

Zanazzi, A., Kohn, M.J., Macfadden, B.J., and Terry, D.O., 2007, Large temperature drop across the Eocene–Oligocene transition in central North America: Nature, v. 445, p. 639–642, doi: 10.1038/nature05551.

Zanazzi, A., and Kohn, M.J., 2008, Ecology and physiology of White River mammals based on stable isotope ratios of teeth: Palaeogeography, Palaeoclimatology, Palaeoecology, v. 257, p. 22–37, doi: 10.1016/j.palaeo.2007.08.007.

Zanazzi, A., Kohn, M.J., Terry, D.O. Jr., 2009, Biostratigraphy and paleoclimatology of the Eocene-Oligocene boundary section at Toadstool Park, northwestern Nebraska, USA: Geological Society of America Special Paper v. 452, p. 197-214.

Zhang, C. and Guo, Z., 2014, Clay mineral changes across the Eocene–Oligocene transition in the sedimentary sequence at Xining occurred prior to global cooling: Palaeogeography, Palaeoclimatology, Palaeoecology, v. 411, p.18-29.

Zhang, X., Knorr, G., Lohmann, G., & Barker, S., 2017, Abrupt North Atlantic circulation changes in response to gradual CO 2 forcing in a glacial climate state: Nature Geoscience, v. 10, p. 518.

Appendix A: Biostratigraphy

The White River Group has a rich record of the mammalian faunas during the late Eocene and early Oligocene. These faunas were the original basis for the Chadronian and Orellan NALMAs (Wood et al., 1941; Woodburne 1987, 2004; Prothero and Emry, 2004). These NALMAs are informal as they are based only on the first occurrences of certain mammal species and have no formal chronostratigraphic sections. Currently, the age range for Eocene-Oligocene boundary ranges between 33.79 and 33.95 Ma (Brown et al., 2009; Hyland et al., 2009; Jovane et al., 2006; Pälike et al., 2006; Westerhold et al., 2014). The Eocene-Oligocene boundary lies close to the Chadronian-Orellan boundary (Zanazzi et al., 2009). As such, both the Eocene-Oligocene boundary and Chadronian-Orellan Boundary were placed at 33.84 ±0.10 Ma (Ogg and Smith, 2004) but are now placed at 34.09 ± 0.08 Ma (Sahy et al., 2017). *Mesohippus*

The Chadronian is also based on the Chadron Formation, with the type locality near its namesake: Chadron, Nebraska. Prothero and Emery (1996b), recommended that sections from Trans-Pecos, Texas; Douglas, Wyoming; and Flagstaff Rim, Wyoming be the chronostratigraphic standards of the Chadronian. These would be based on the first appearances of *Bathygenys, Brachyrhynchocyon dodgei, Merycoidodon dunagani,* and *Archaeotherium* with *Bathygenys* as the defining taxon.

Later in 1998, Prothero and Whittlesey redefined the boundary based on the first appearances of *Hypertragulus calcaratus*, *Leptomeryx evansi*, and *Poebrotherium wilsoni*, but suggested that it may be a diachronous event. Prothero and Emery (2004), then divided the Chadronian again into a series of interval biozones. The Chadronian and Orellan were both divided into four zones. These were numbered from lowest to highest in stratigraphy. Zanazzi et

al. (2009), correlated these zones to Toadstool Park. Chadronian 1 is the earliest Chadronian. Chadronian 2 is the late early Chadronian. Chadronian 3 is the middle Chadronian which ranges between 34 m and ~18 m below the UPW. Chadronian 4 is the late Chadronian which goes from the top of Chadronian 3 to ~2 m above the UPW. Orella 1 is the earliest Orellan and ranges 2 to 8 m above the UPW. Orella 2 is the late early Orellan and covers 8 m to 13 m above the UPW. Orella 3 is the early late Orellan and runs from 13 m above the UPW near the top of Orella C of Schultz and Stout (1955). Finally, Orella 4 is the latest Orellan and covers the remaining Orella C and Orella D as redefined by LaGarry, (1998).

In 1968 Schultz and Falkenbach proposed the Oreodont Faunal Zones for Nebraska. There were three Oreodon Zones: the Lower, the Middle, and the Upper Oreodon zones to better define rock above the Titanotherium Beds. These are often abbreviated to LOZ, MOZ, or UOZ in the UNSM collection catalogue cards and define what was then considered some of the Brule Formation. The upper boundary of the LOZ is the lower nodular layer (LNL), about 10 m or 33' above the UPW. The LOZ constitutes the 21 m or 70' below the LNL. The MOZ ranges from the LNL to the Upper Nodular Layer (UNL), roughly 14 m or 46'. Emery et al. (1987), reviewed the Oreodon Zones and found them inadequate definitions, but many of the fossils in the UNSM collections reference them still.

Korth (1989), presented a biostratigraphic scheme based on the mammals in the Brule Formation, but Prothero and Whittlesey (1998), proposed that the first appearance of *Leptomeryx evansi, Palaeolagus intermedius,* and *Hypertragulus calcaratus* should be used to recognize the start of the Orellan. They suggested *Hypertragulus calcaratus* as the defining taxon of the Orellan and divided Orella into a series of interval zones. These zones were defined by the first occurrences of different species.

Prothero and Emery (2004), and Zanazzi et al. (2009) have most recently redefined the biostratigraphy of the White River Group.

Appendix B: Datasets with *Leptomeryx* Included

Schultz and Stout Zones with *Leptomeryx*

With the two large peaks in *Leptomeryx* abundance, the relative abundances of other taxa like *Merycoidodon, Miniochoerus, Poebrotherium,* and *Paratylopus* are affected. Patterns before Orella A remain largely unchanged as *Leptomeryx* is much less abundant (Fig. B1). This is also true of the NALMA data where increases in the Orellan are dampened by *Leptomeryx* (Fig. E4; Tables shift in relative being across the EOCT.

Fourth Bin Series Results

Leptomeryx here has on one peak at Bin 1 at the start of the EOCT where it then remains stable. This largely removes the increasing relative abundance trends of all other taxa except Merycoidodontidae gen. indet. Patterns before Orella A remain largely unchanged as *Leptomeryx* is much less abundant (Fig. B7). These changes are also true of the combined bins for this series (Figs. B10; Tables B18-20).

With the two peaks in *Leptomeryx* abundance, the chord distance is very different for Bins after the EOCT, spiking in distance with its abundance (Table B21).

Diversity and evenness again drop when *Leptomeryx* peaks in abundance as it dominates the fauna and remains low from Bin 1 onward (Figs. B8-B9; B11-B12; Table B22).

Poebrotherium, Camelidae gen. indet., and *Archaeotherium* have the largest changes in abundance across the first climate shift of the EOCT. *Aepinacodon, Paratylopus, Leptomeryx, Miniochoerus, Dinictis,* Nimravidae gen. indet., *Eotylopus, Trigonias,* Rhinocerotineae gen. indet, and *Colodon* all have their largest abundance change across the second climate shift (Table B17).

Sixth Bin Series Results

Leptomeryx here has two large peaks. This largely removes the increasing relative abundance trends of all other taxa except Merycoidodontidae gen. indet. Patterns before Orella A remain largely unchanged as *Leptomeryx* is much less abundant (Fig. B13; Tables B24-26).

With the two peaks in *Leptomeryx* abundance, the chord distance is very different for Bins after the EOCT, spiking in distance with its abundance (Table B27).

Diversity and evenness again drop when *Leptomeryx* peaks in abundance as it dominates the fauna (Figs. B14-B15; B17-B18; Table B28).

Poebrotherium, Camelidae gen. indet., and *Archaeotherium* have the largest changes in abundance across the first climate shift of the EOCT. *Aepinacodon, Paratylopus, Leptomeryx, Miniochoerus, Dinictis,* Nimravidae gen. indet., *Eotylopus, Trigonias,* Rhinocerotineae gen. indet, and *Colodon* all have their largest abundance change across the second climate shift (Table B23).

Appendix C: All Taxa Plotted Together

In this appendix all figures display all the taxa in this study, plotted together in the same chart for a sense of the scale of the relative abundance patterns.

Appendix D: NALMA Abundance Figures

Taxa that increased relative abundance in Orella were *Merycoidodon, Miniochoerus, Poebrotherium, Paratylopus*. Meanwhile, taxa that decreased in relative abundance during the Orellan were *Megacerops* (went extinct), *Perchoerus*, *Eotylopus* (went extinct), *Aepinacodon, Archaeotherium, Trigonias* (went extinct) (Figs. D1-3). They are split into different groupings for greater legibility of changes in relative abundance (Figs. D2-3; Tables D1-D3).

Removing *Leptomeryx* seems to increase the distance between Chadron and Orellan bins (Table D4).

There is no significant change in evenness or diversity (Figs. D5-6; Table D5).

Appendix E: Combined Bins Before and After Climate Shift

Combined Fourth Bin Series

With *Leptomeryx* removed from the dataset, M*iniochoeru*s and *Poebrotherium* again increase in relative abundance, but *Merycoidodo*n and *Mesohippus* still decline. All those taxa that were declining into Bin 0 remain unchanged without *Leptomeryx* in the dataset (Fig. E7; Tables E11-E13).

Here the combined bins 1-3 are closer to bin 0 in chord distance than they are to the combined Bins -2—1 (Table E14).

Also, without Leptomeryx there is no significant change in evenness or diversity (Figs. F8-9; Tables E15).

Appendix F: Principle Components Analysis

In all cases, the largest source of variance was the most abundant taxon of that dataset (*Leptomeryx* when present, *Merycoidodon* when not). The second or third largest sources of variance change occasionally after that (Tables F1-4).

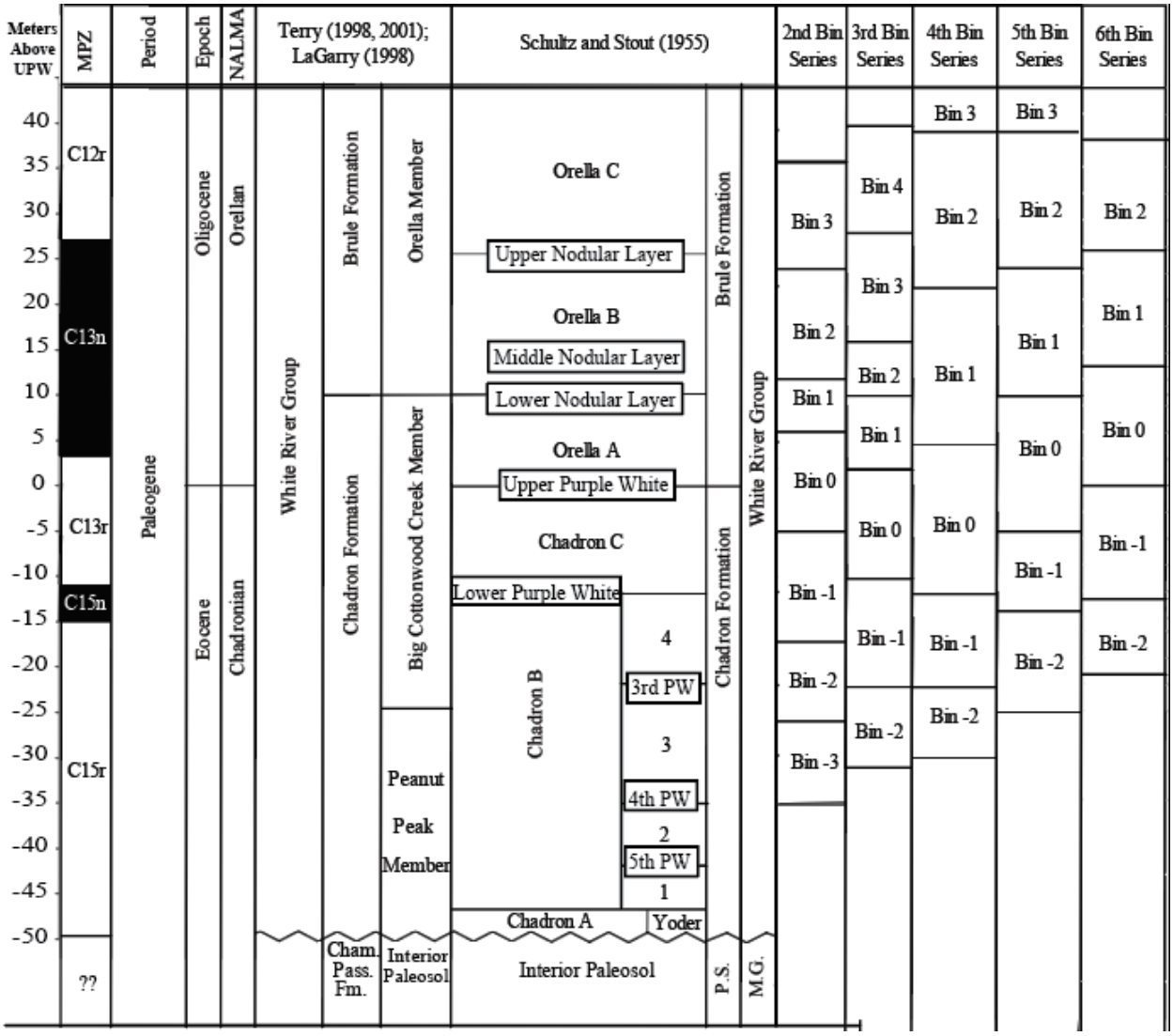

Figure 1. Various stratigraphic divisions of the White River Group depicting six bin series used in this work. Divisions shown are to stratigraphic scale. In all cases Bin 0 is the bin containing the UPW. Abbreviations: P.S., Pierre; Shale. M.G., Montana Group; MPZ, magnetochron polarity zones; Cham. Pass. Fm., Chamberlain Pass Formation. Unconformities are displayed as zig-zagging lines. Climate change is predicted to be within Bin 1 or between Chadron C and Orella A.

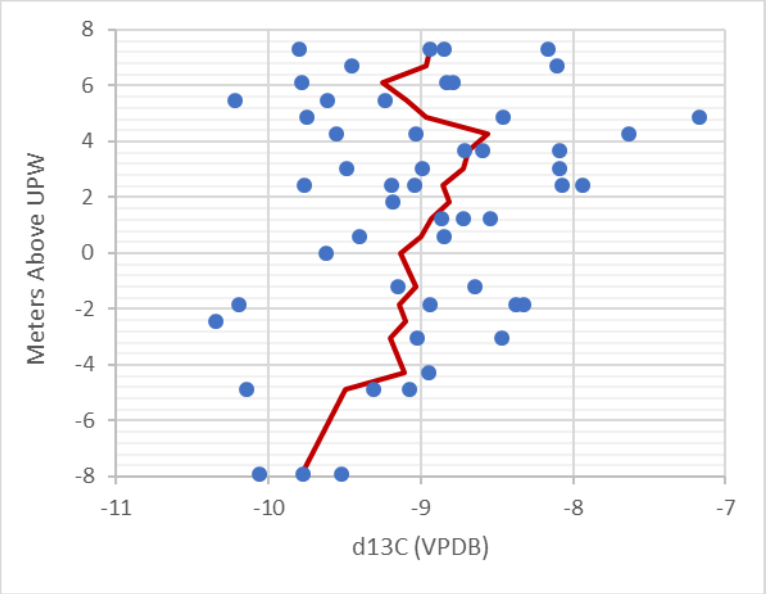

Figure 2. 66 *Merycoidodon* $\delta^{13}C$ enamel values plotted as meters from UPW. Blue circles represent one sample from one individual. Red trendline is a moving three-point moving average.

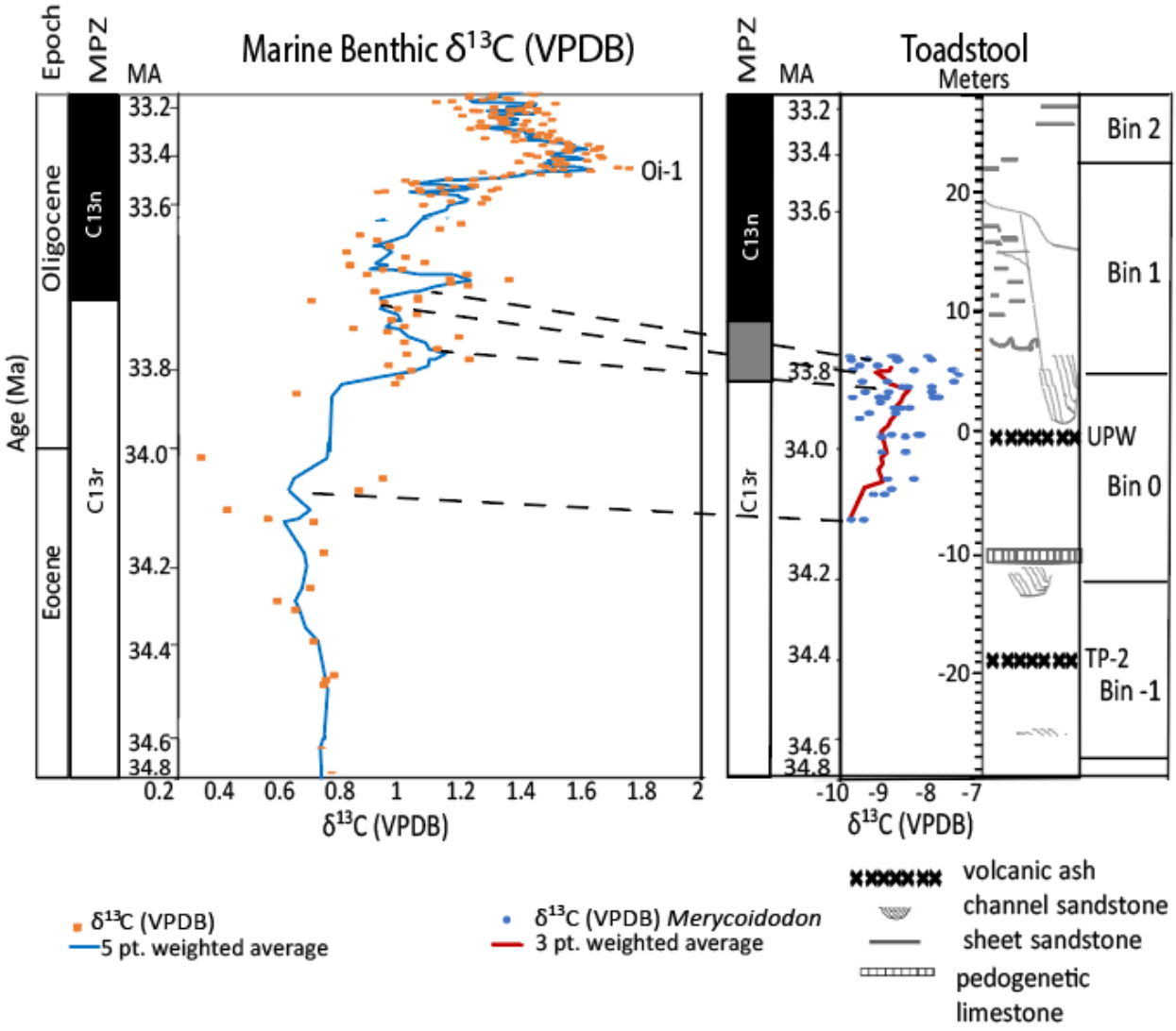

Figure 3. Fourth bin series. Modified in part from Galeotti et al. (2016) and Coxall and Pearson (2005) benthic foraminiferal $\delta^{13}C$ records of the latest Eocene and earliest Oligocene of the Southern Ocean Site 1218 correlated with *Merycoidodon* results-based on trends in $\delta^{13}C$ values. *Merycoidodon* $\delta^{13}C$ results from this study. Stratigraphy near the Upper Purple White (UPW) ash modified from Sahy et al. (2015). Magnetostratigraphy from Prothero and Swisher (1992), with grey box denoting several meters or uncertainty based on differing ages between the cubic spline curve and the chron boundary, as well as differing placement in different papers (D. Terry written communication; Boardman and Secord, 2013; Sahy et al., 2015). Starting at seven meters above the UPW, there is channel cut that incised ca. 20 m into the Brule and Chadronian formations, however the Chadronian–Orellan boundary interval is preserved outside the channel complex (Sahy et al., 2015). Bins created for this work are designed to be even in time but varying in stratigraphic thickness. Bin 1 is bounded above and below by the major shifts in the Galeotti et al., 2016 stable isotope data which was correlated by exact age. Note that Bin 3 and Bin -2 are not shown on this figure to allow the *Merycoidodon* stable isotope results to be more

legible. VPDB-Vienna PeeDee Belemnite. MA-Million years ago. MPZ-Magnetochron polarity zone.

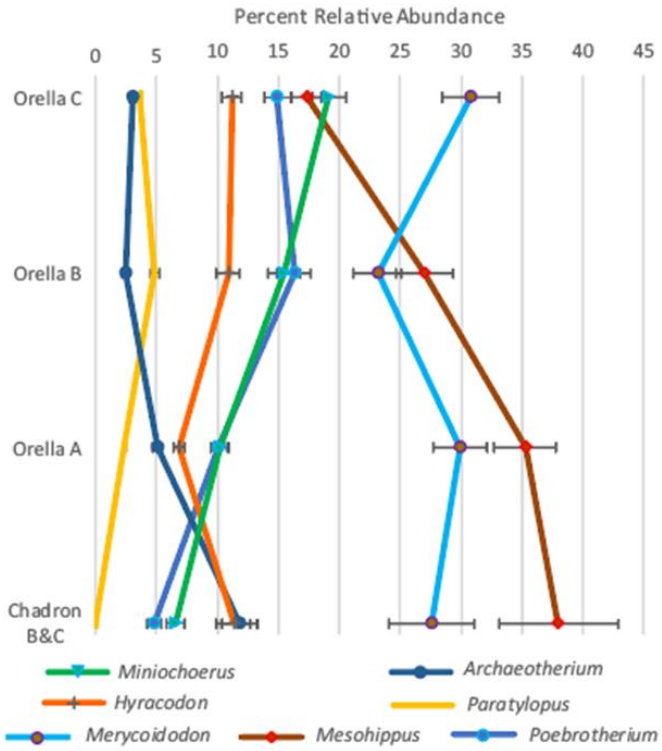

Figure 4. Relative abundance through S&S zones without *Leptomeryx*. Error bars show 95% confidence of mean.

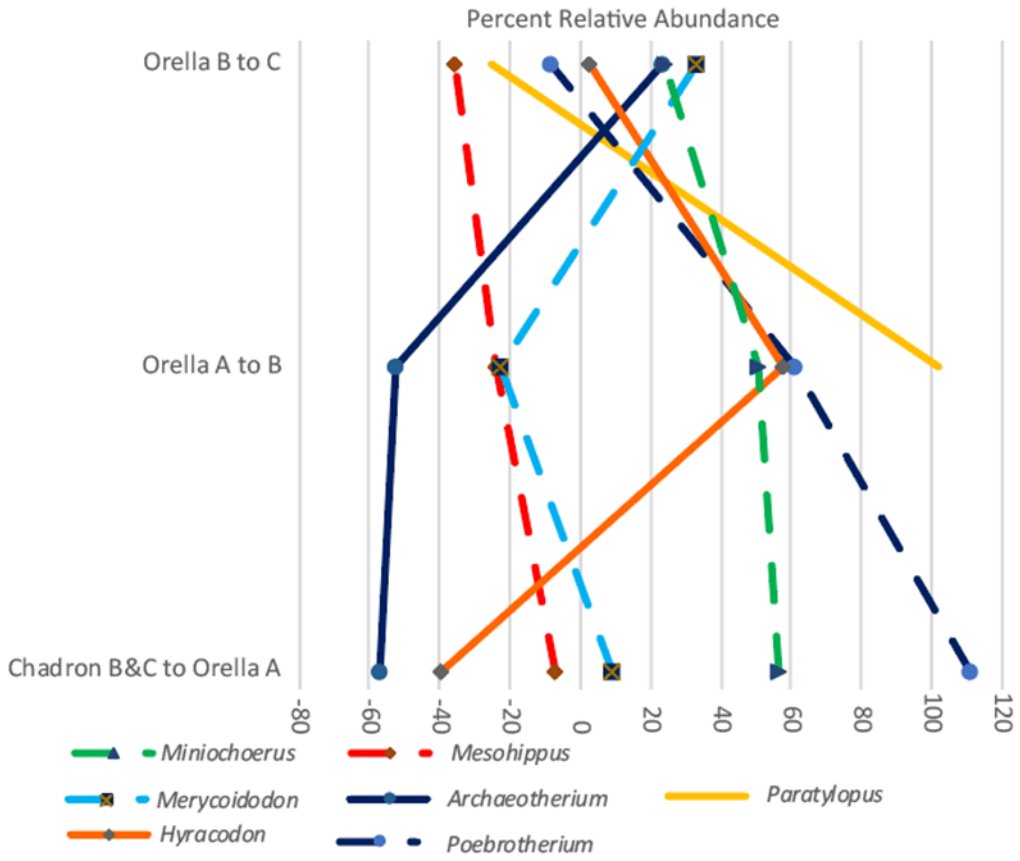

Figure 5. Percent change in relative abundance of well sampled taxa across S&S zones without *Leptomeryx*.

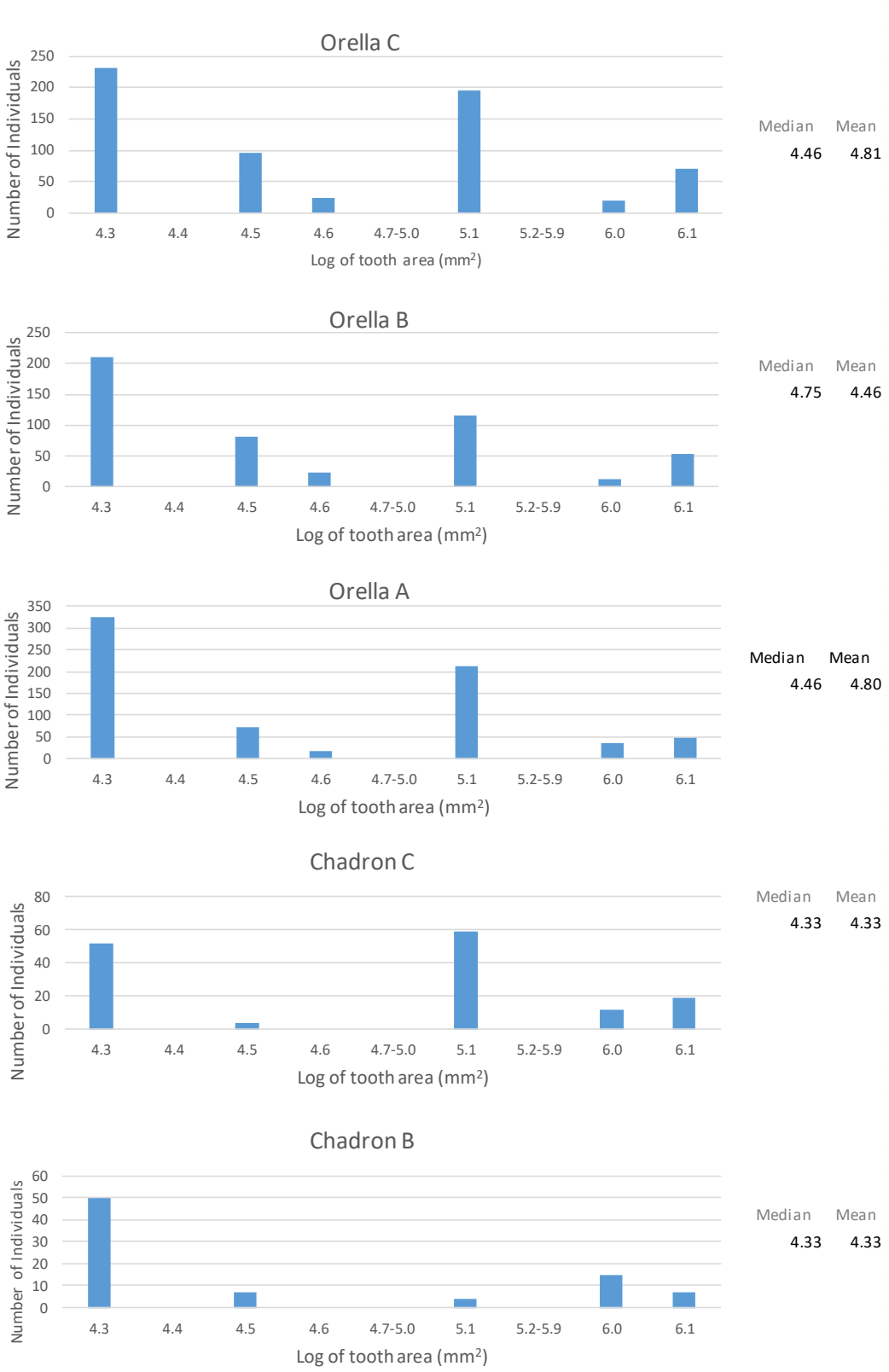

Figure 6. Histogram of the natural log of tooth area in each S&S zone. X-axis log of tooth area (mm^2) bins are mean values. Note that some natural log tooth areas (ln(4.7-5.0mm^2)and ln(5.2-5.9mm^2)) are combined for increased legibility of the other populated data.

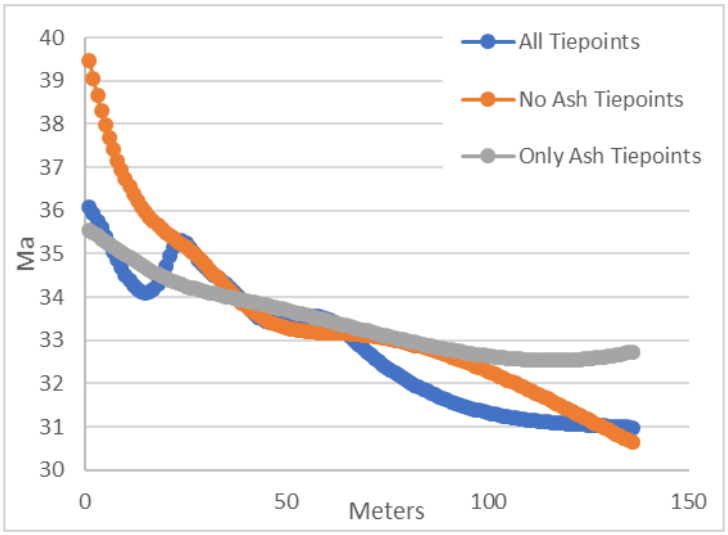

Figure 7. Different ages calculated by using different tie points for cubic spline curve. The All Tie Points line utilizes chron ages from Ogg (2012), and $^{206}Pb/^{238}U$ ash dates from Sahy et al. (2015) while the Ash Tie Points curves only use ash dates from Sahy et al., 2015. No Ash Tie Points is based only on the magnetochrons reversal ages from Ogg (2012).

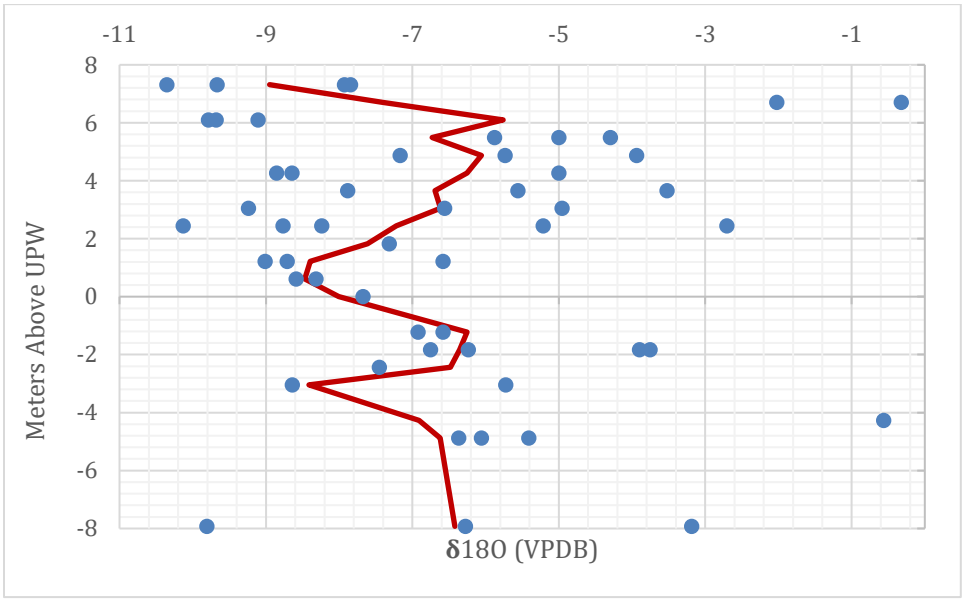

Figure 8. 66 *Merycoidodon* $\delta^{18}O$ enamel values plotted as meters from UPW. Blue circles represent one sample from one individual. Red trendline is a moving three-point moving average.

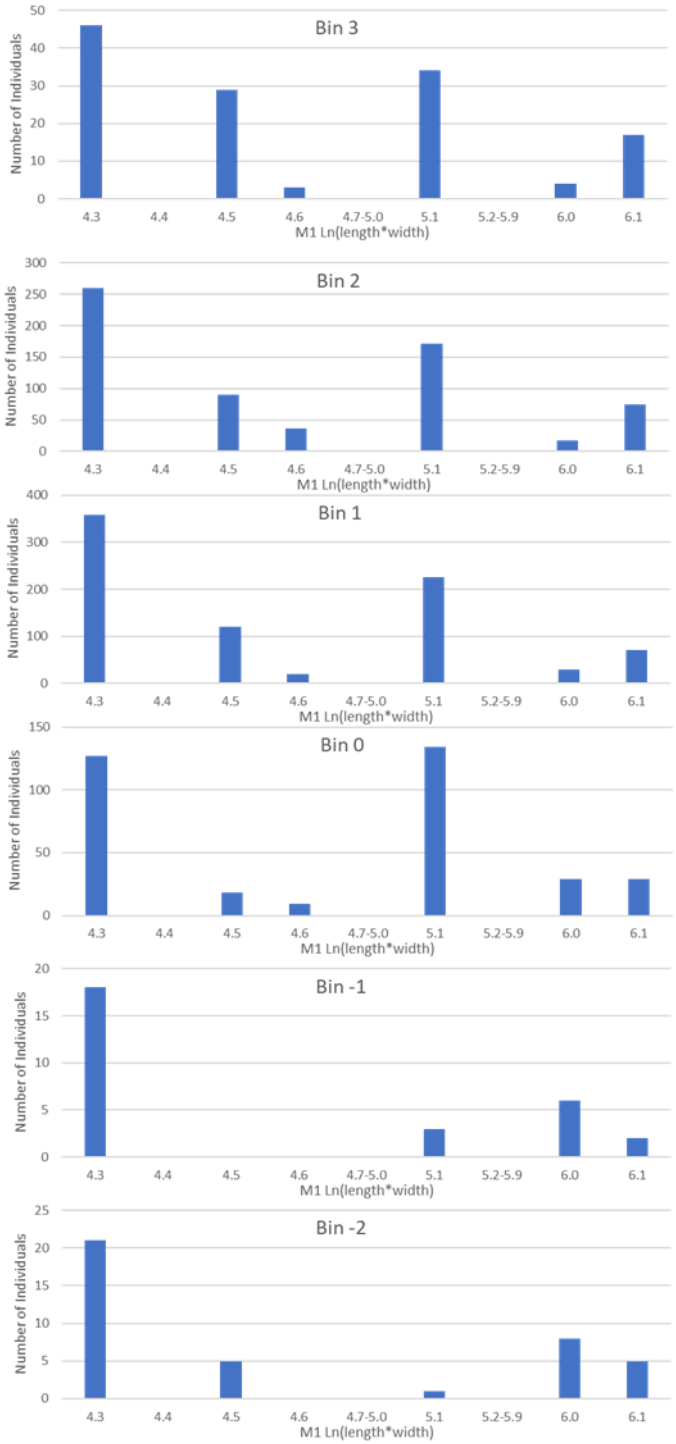

Figure 9. Histogram of the natural log of tooth area in each fourth series bin. X-axis log of tooth area (mm^2) bins are mean values. Note that some tooth areas (ln(4.7-5.0mm^2)and ln(5.2-5.9mm^2))are combined for increased legibility of the other populated data.

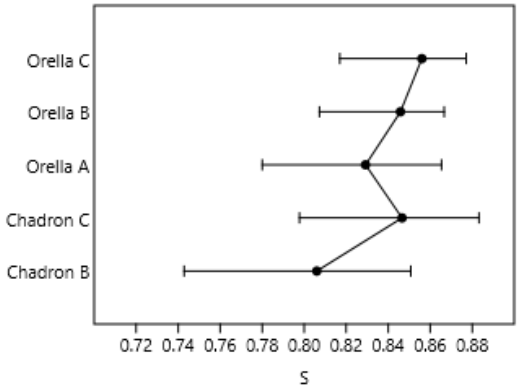

Figure 10. Measure of diversity using Simpson-D diversity index generated in Past 3.23 across the Schultz and Stout (1955) zones showing 95% confidence intervals. This index measures 'evenness' of community from 0 (one taxa dominates the zone entirely) to 1 (all taxa equally present).

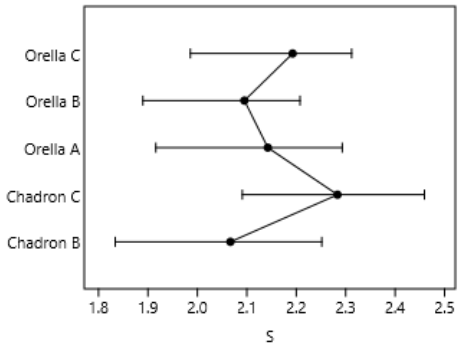

Figure 11. Measure of diversity using Shannon H index generated in Past 3.23 across the S&S zones showing 95% confidence intervals. This index measures diversity considering the number of individuals as well as number of taxa. This index varies from 0 for communities with just one taxon to high values for communities with many relatively rare taxa.

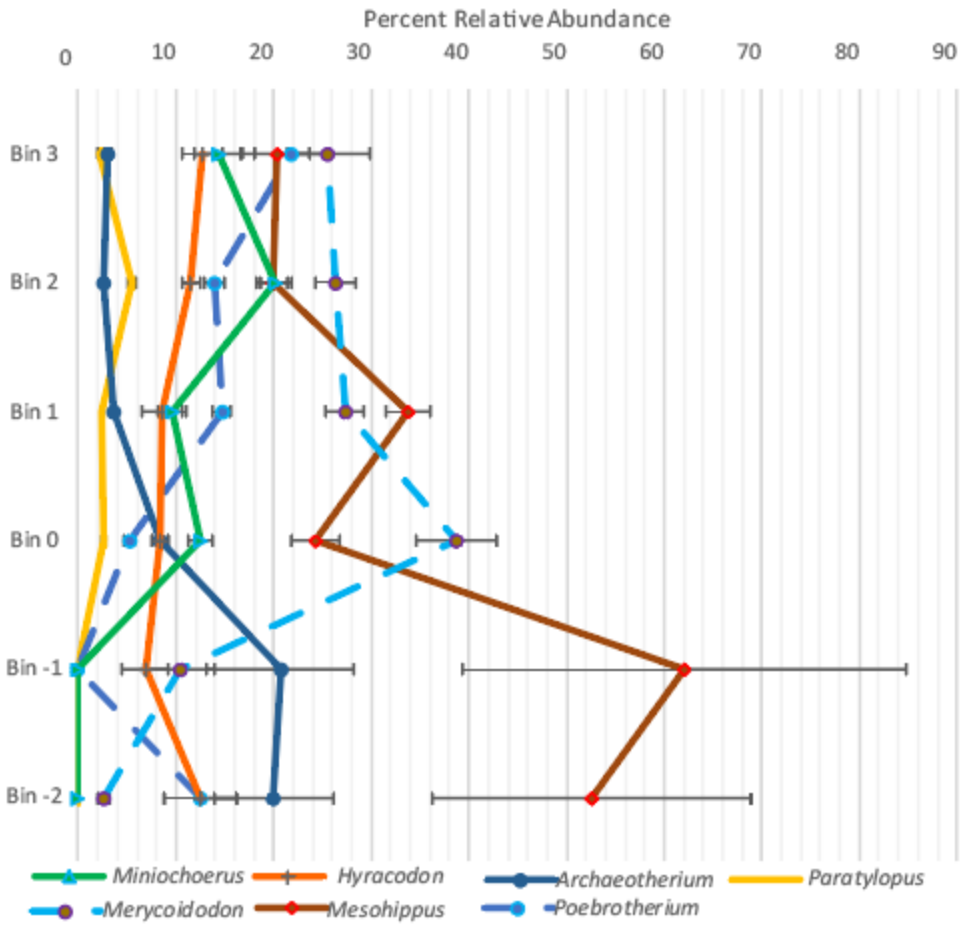

Figure 12. Fourth bin series relative abundance results with error bars showing 95% confidence intervals.

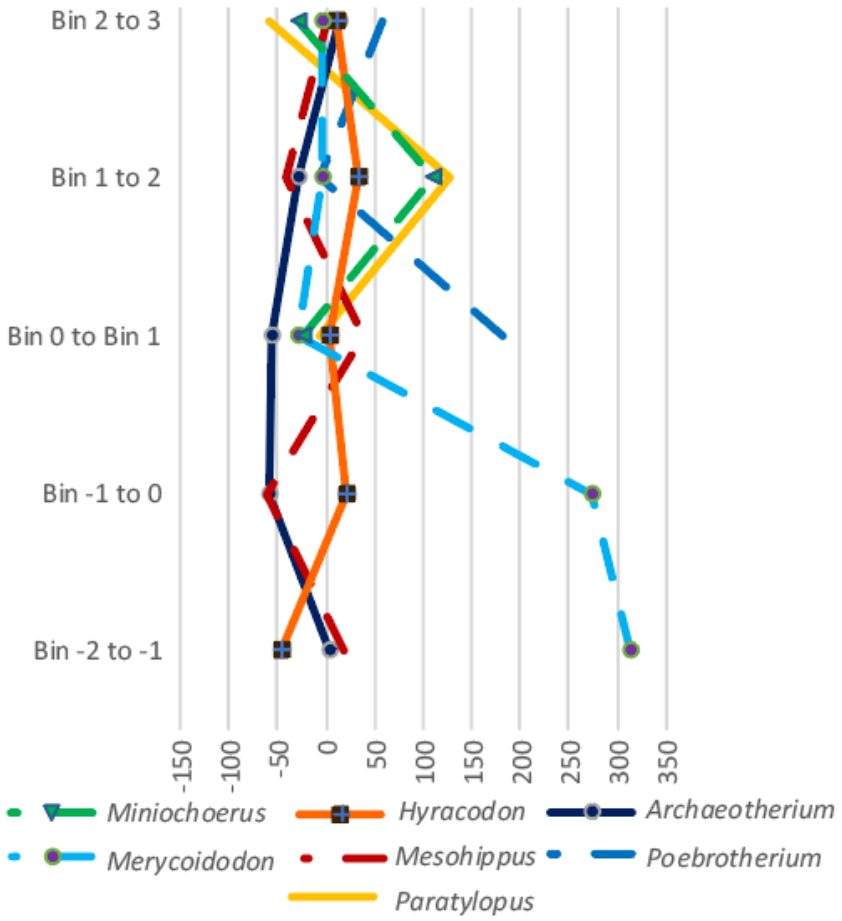

Figure 13. Percent change in relative abundance of well-sampled taxa across the fourth bin series. This dataset does not include *Leptomeryx.*

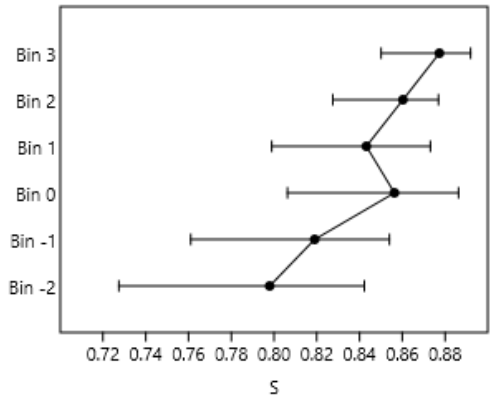

Figure 14. Measure of diversity using Simpson-D diversity index generated in Past 3.23 across the fourth series bins showing 95% confidence intervals. This index measures

'evenness' of the community from 0 (one taxa dominates the zone entirely) to 1 (all taxa equally present).

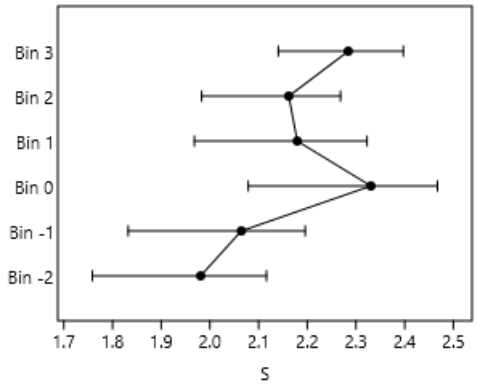

Figure 15. Measure of diversity using Shannon H index generated in Past 3.23 across the fourth series bins showing 95% confidence intervals. This index measures diversity considering the number of individuals as well as number of taxa. This index varies from 0 for communities with just one taxon to high values for communities with many relatively rare taxa.

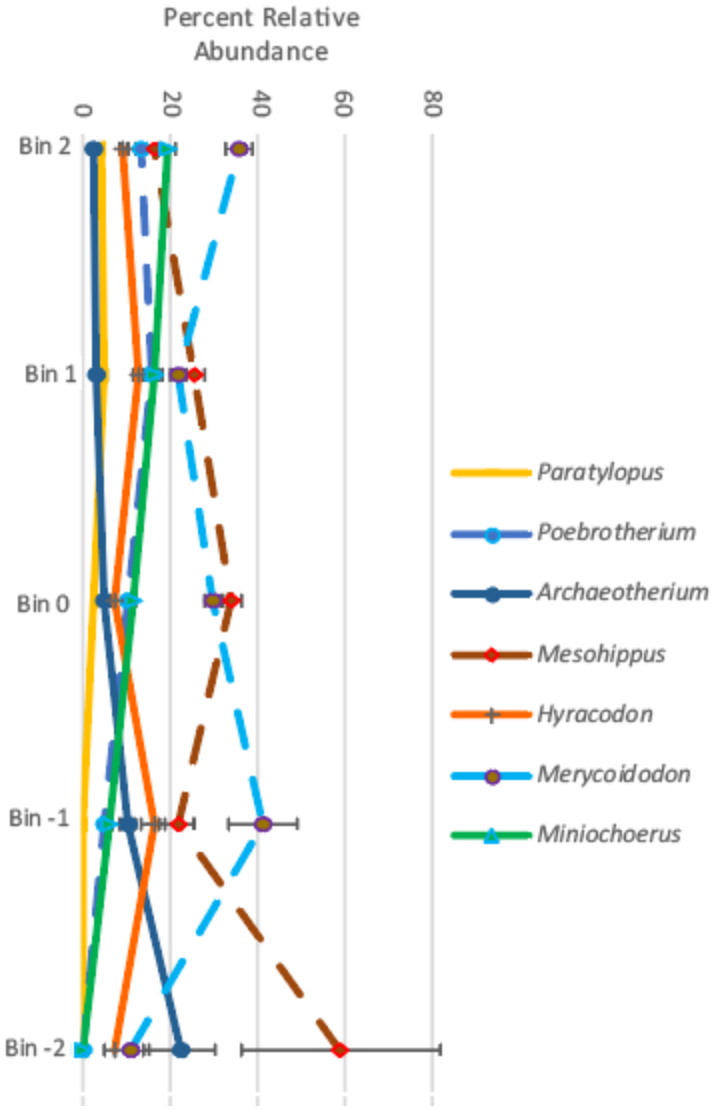

Figure 16. Sixth bin series relative abundance results with error bars showing 95% confidence intervals.

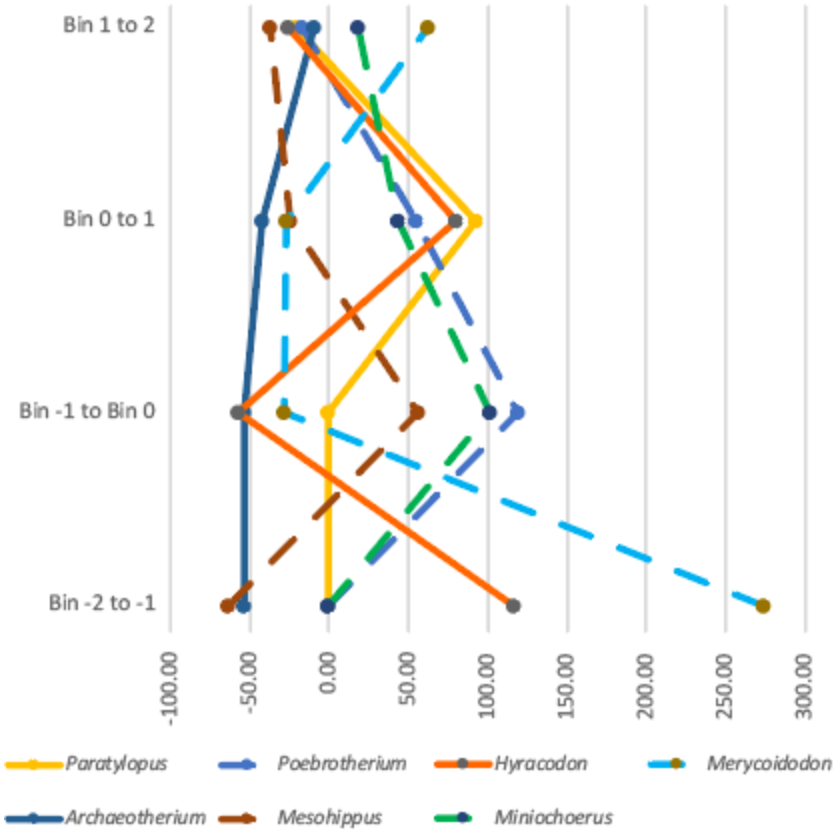

Figure 17. Percent change in relative abundance of well-sampled taxa across the sixth bin series. This dataset does not include *Leptomeryx*.

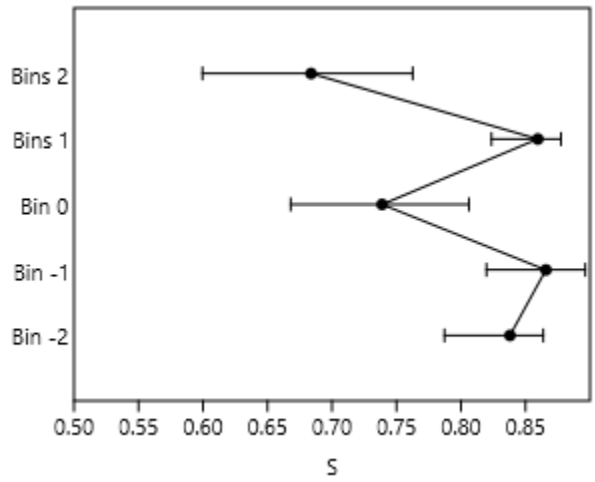

Figure 18. Measure of diversity using Simpson-D diversity index generated in Past 3.23 across the sixth series bins showing 95% confidence intervals. This index measures

'evenness' of the community from 0 (one taxa dominates the zone entirely) to 1 (all taxa equally present).

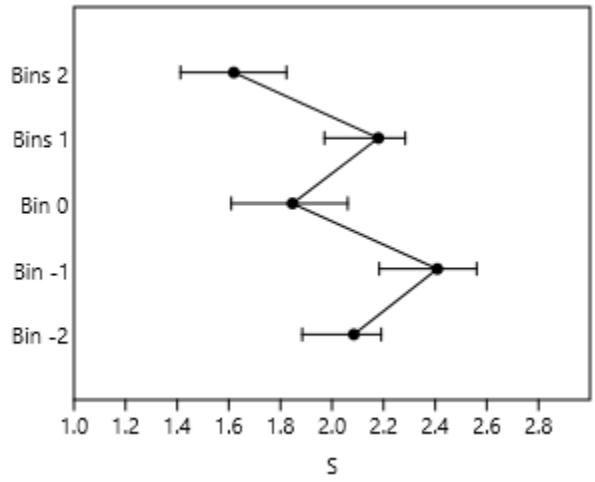

Figure 19. Measure of diversity using Shannon H index generated in Past 3.23 across the sixth series bins showing 95% confidence intervals. This index measures diversity considering the number of individuals as well as number of taxa. This index varies from 0 for communities with just one taxon to high values for communities with many relatively rare taxa.

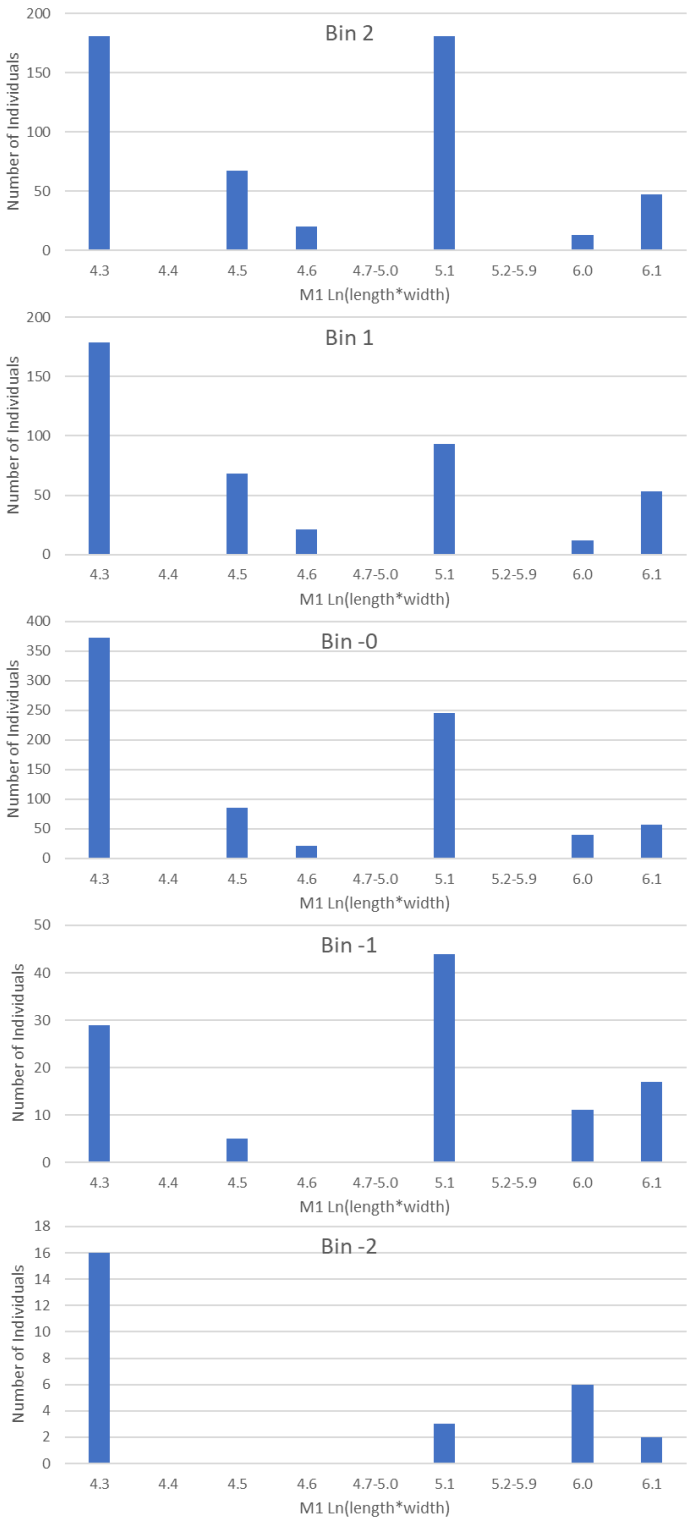

Figure 20. Histogram of the natural log of tooth area in each sixth series bin. X-axis log of tooth area (mm^2) bins are mean values. Note that some tooth areas (ln(4.7-5.0mm^2)and ln(5.2-5.9mm^2))are combined for increased legibility of the other populated data.

Appendix A: Biostratigraphy

Appendix B: Datasets with *Leptomeryx* Included

Schultz and Stout (1955) Zones

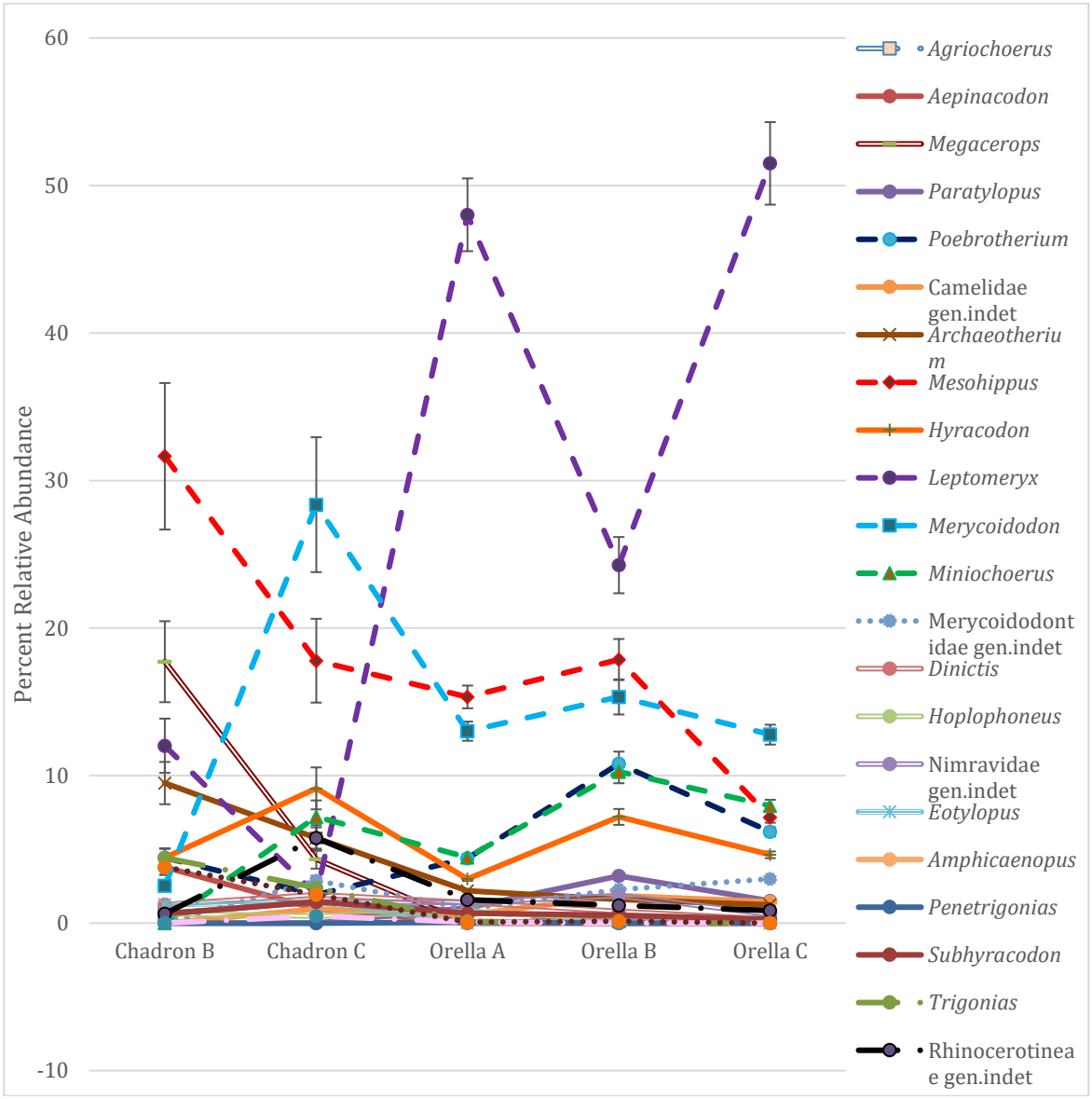

Figure B1. Percent Relative abundance through the S&S zones of well sampled taxa showing 95% confidence interval bars.

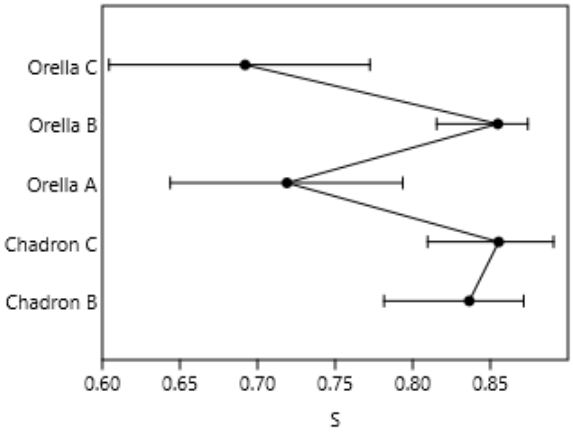

Figure B2. Measure of diversity using Simpson-D diversity index generated in Past 3.23 across the S&S zones showing 95% confidence intervals. This index measures 'evenness' of the community from 0 (one taxa dominates the zone entirely) to 1 (all taxa equally present).

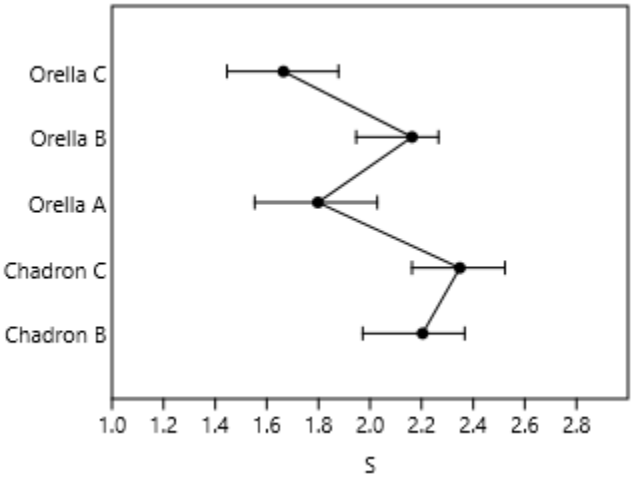

Figure B3. Measure of diversity using Shannon H index generated in Past 3.23 across the S&S zones showing 95% confidence intervals. This index varies from 0 for communities with just one taxon to high values for communities with many relatively rare taxa.

NALMA Combined Bin Series

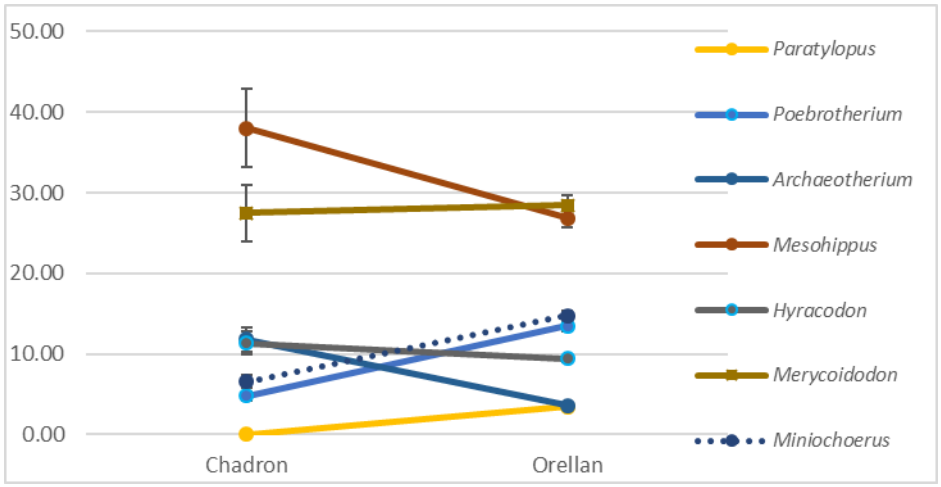

Figure B4. Relative abundance change in mammalian genera from the Chadronian NALMA to the Orellan NALMA as defined in Schultz and Stout (1955). Error bars are 95% confidence intervals.

.

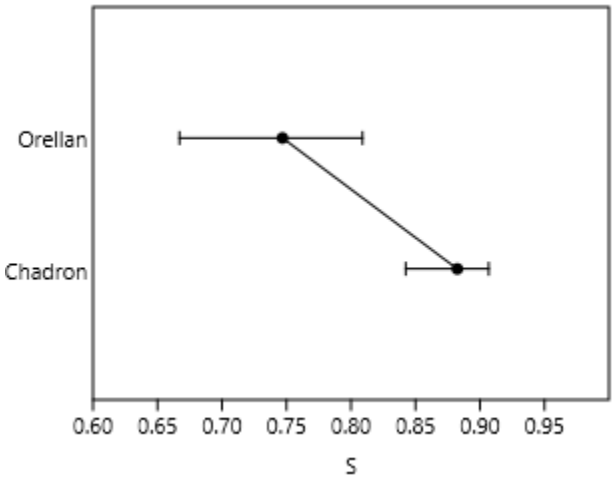

Figure B5. Measure of diversity using Simpson-D diversity index generated in Past 3.23 across the NALMAs showing 95% confidence intervals. This index measures 'evenness' of the community from 0 (one taxa dominates the zone entirely) to 1 (all taxa equally present).

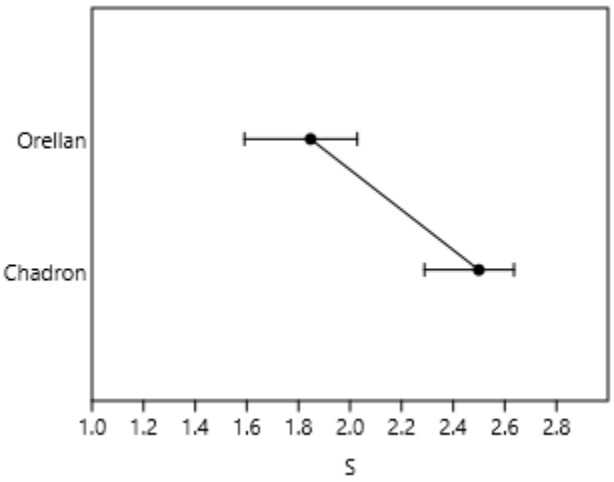

Figure B6. Measure of diversity using Shannon H index generated in Past 3.23 across the NALMAs showing 95% confidence intervals. This index varies from 0 for communities with just one taxon to high values for communities with many relatively rare taxa.

Fourth Bin Series Results

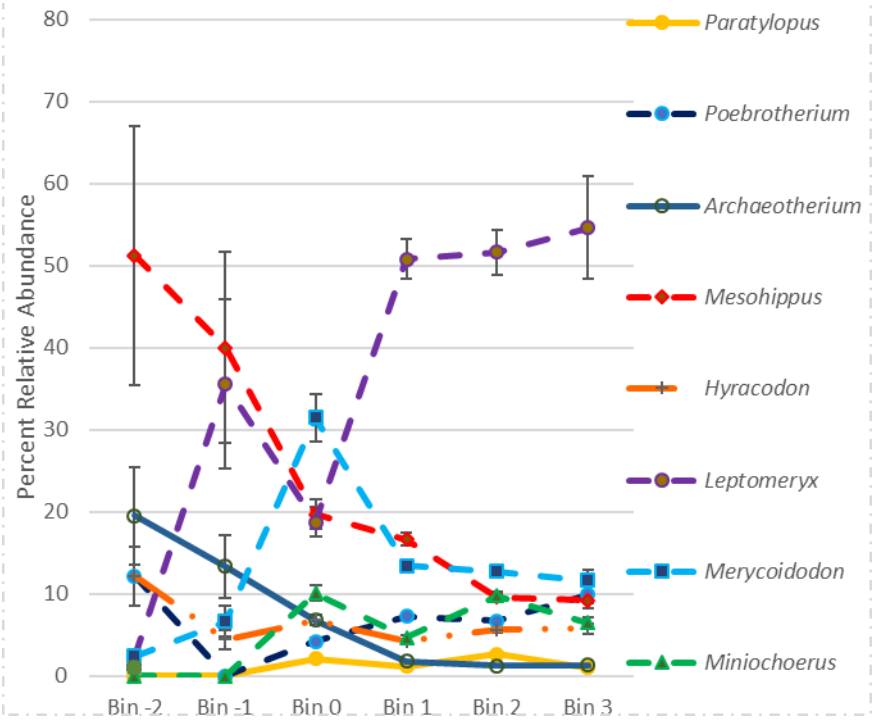

Figure B7. Fourth bin series showing *Leptomeryx* included in the dataset. Error bars are 95% confidence intervals

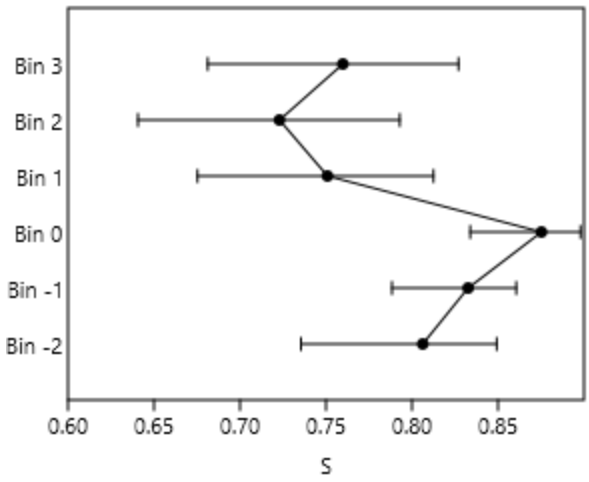

Figure B8. Measure of diversity using Simpson-D diversity index generated in Past 3.23 across the fourth series bins showing 95% confidence intervals. This index measures 'evenness' of the community from 0 (one taxa dominates the zone entirely) to 1 (all taxa equally present).

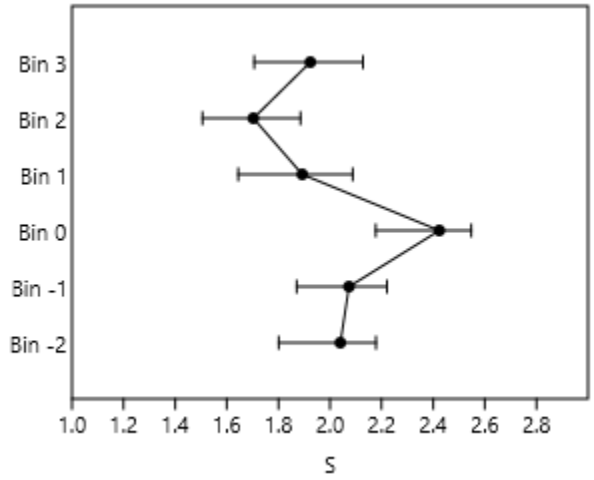

Figure B9. Measure of diversity using Shannon H index generated in Past 3.23 across the fourth series bins showing 95% confidence intervals. This index measures diversity considering the number of individuals as well as number of taxa. This index varies from 0 for communities with just one taxon to high values for communities with many relatively rare taxa.

Fourth Combined Bin Series

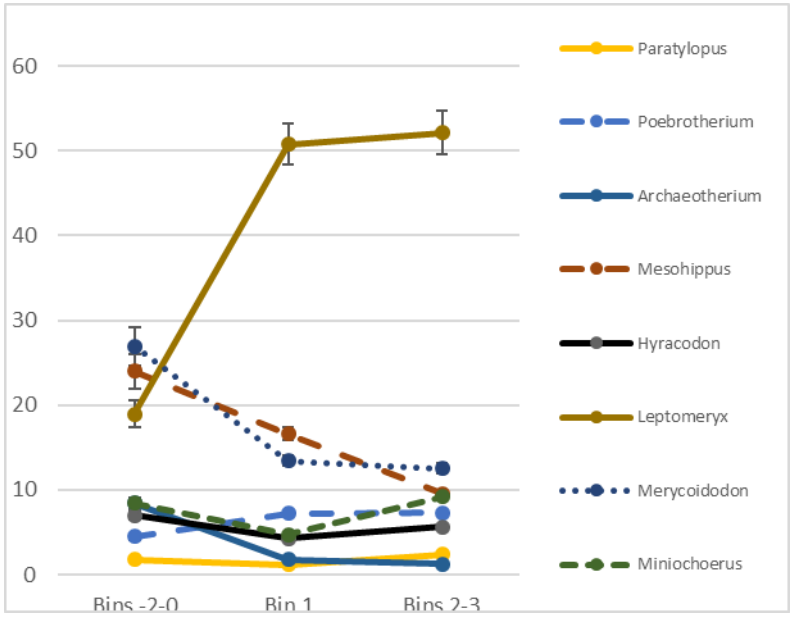

Figure B10. Combined fourth series bins before and after climate shift with *Leptomeryx* in the dataset. Error bars are 95% confidence intervals.

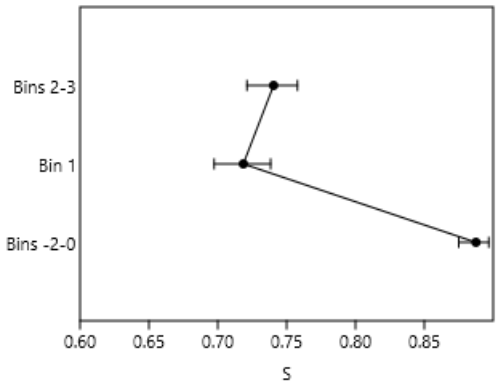

Figure B11. Measure of diversity using Simpson-D diversity index generated in Past 3.23 across the fourth series bins showing 95% confidence intervals. This index measures 'evenness' of the community from 0 (one taxa dominates the zone entirely) to 1 (all taxa equally present).

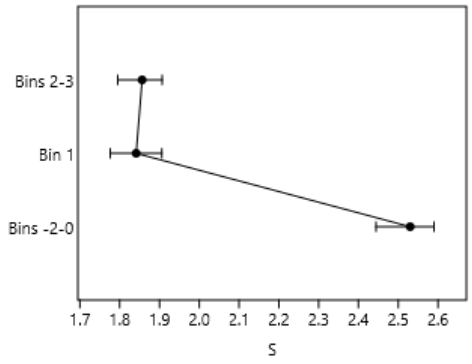

Figure B12. Measure of diversity using Shannon H index generated in Past 3.23 across the fourth bin series showing 95% confidence intervals. This index measures diversity considering the number of individuals as well as number of taxa. This index varies from 0 for communities with just one taxon to high values for communities with many relatively rare taxa.

Sixth Bin Series Results

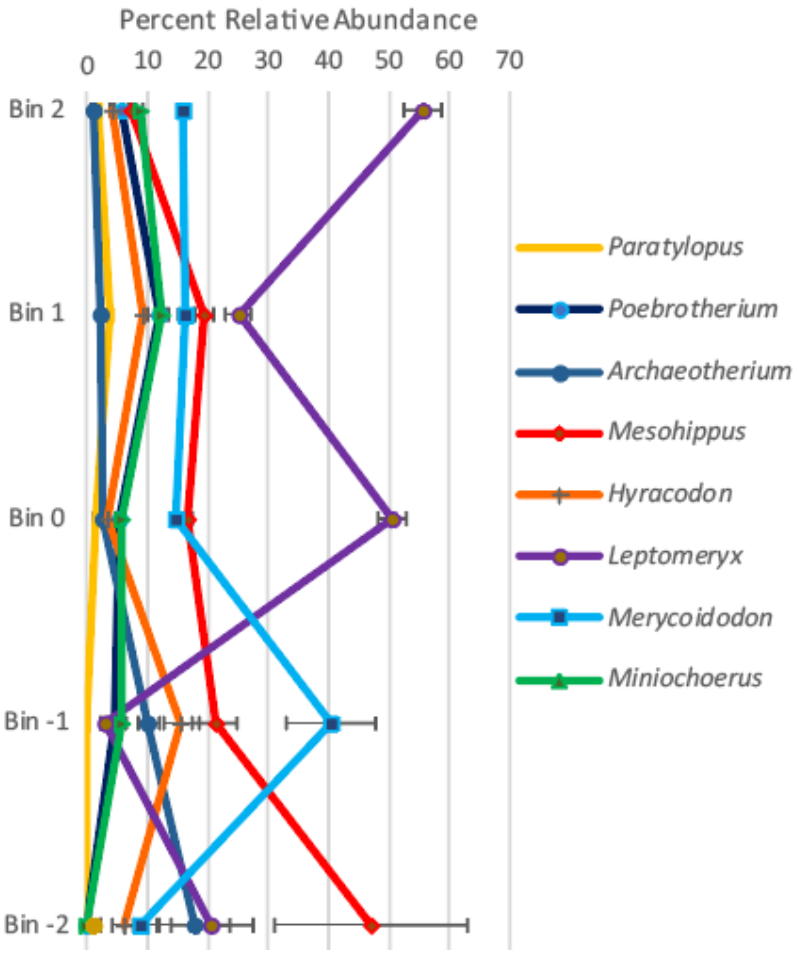

Figure B13. Sixth bin series with *Leptomeryx* included in the dataset. Error bars are 95% confidence intervals

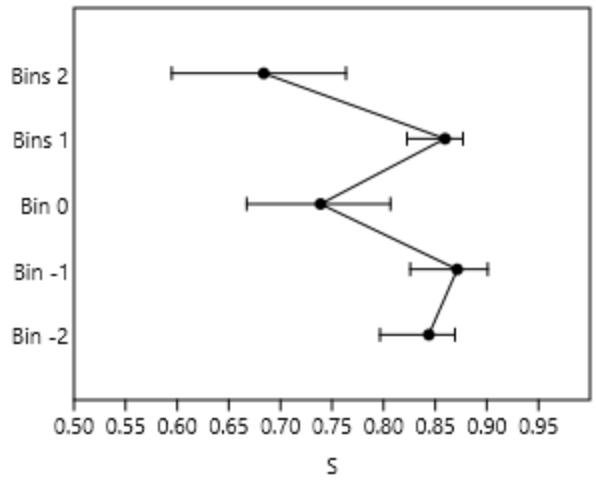

Figure B14. Measure of diversity using Simpson-D diversity index generated in Past 3.23 across the sixth series bins showing 95% confidence intervals. This index measures 'evenness' of the community from 0 (one taxa dominates the zone entirely) to 1 (all taxa equally present).

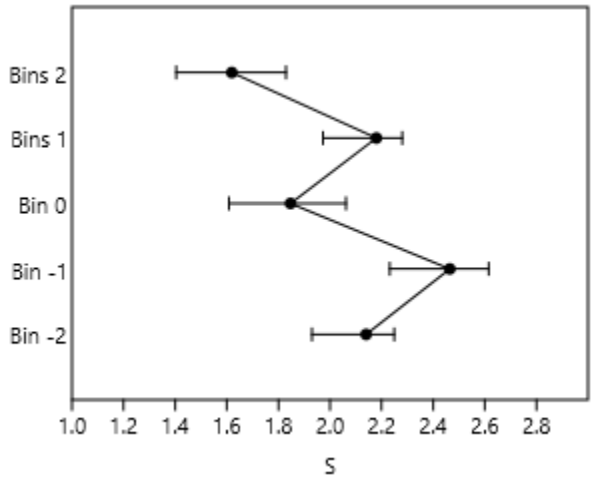

Figure B15. Measure of diversity using Shannon H index generated in Past 3.23 across the sixth series bins showing 95% confidence intervals. This index measures diversity considering the number of individuals as well as number of taxa. This index varies from 0 for communities with just one taxon to high values for communities with many relatively rare taxa.

Appendix C: All Taxa Plotted Together

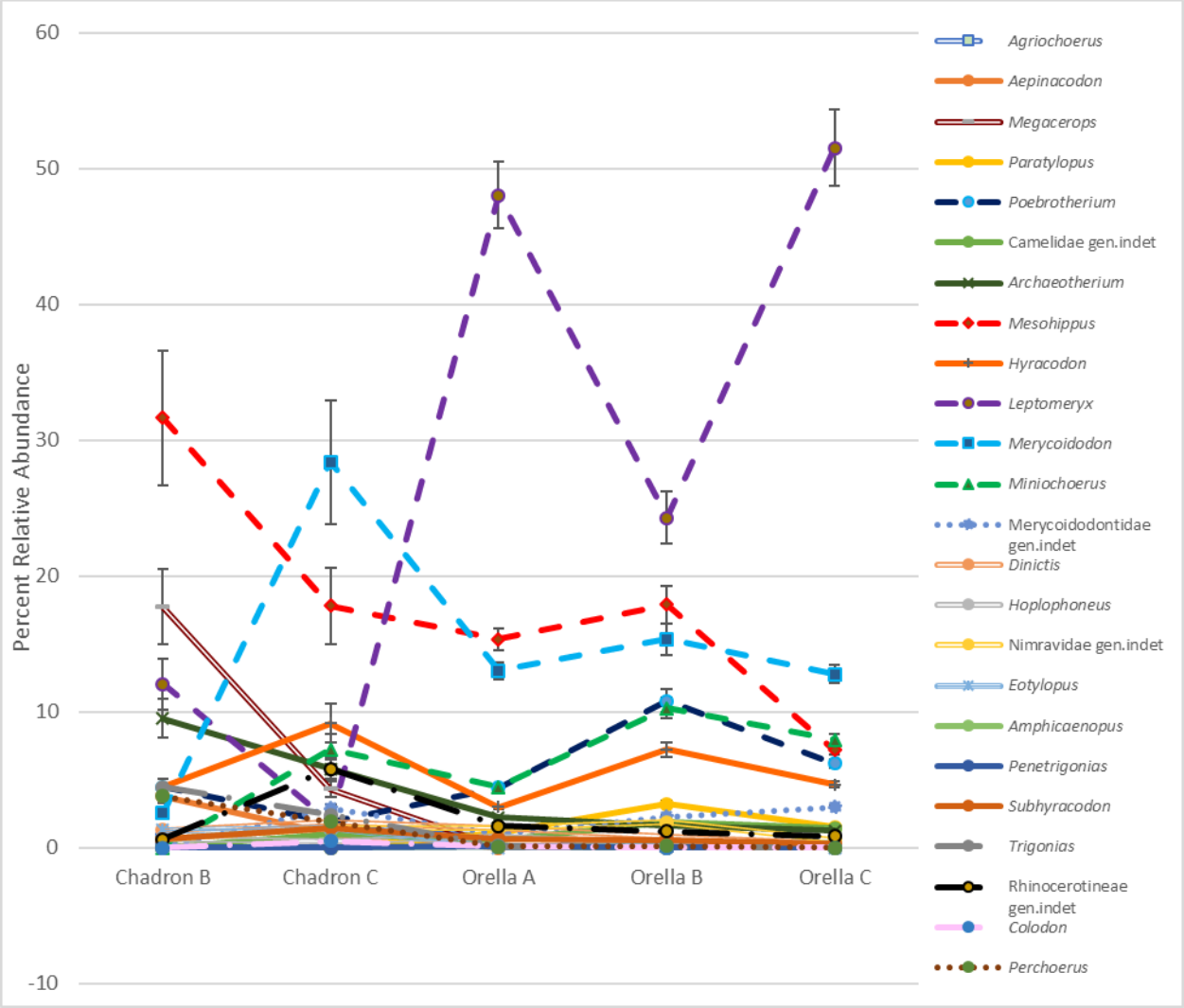

Figure C1. Percent Relative abundance through the Schultz and Stout(1955) zones showing 95% confidence interval bars.

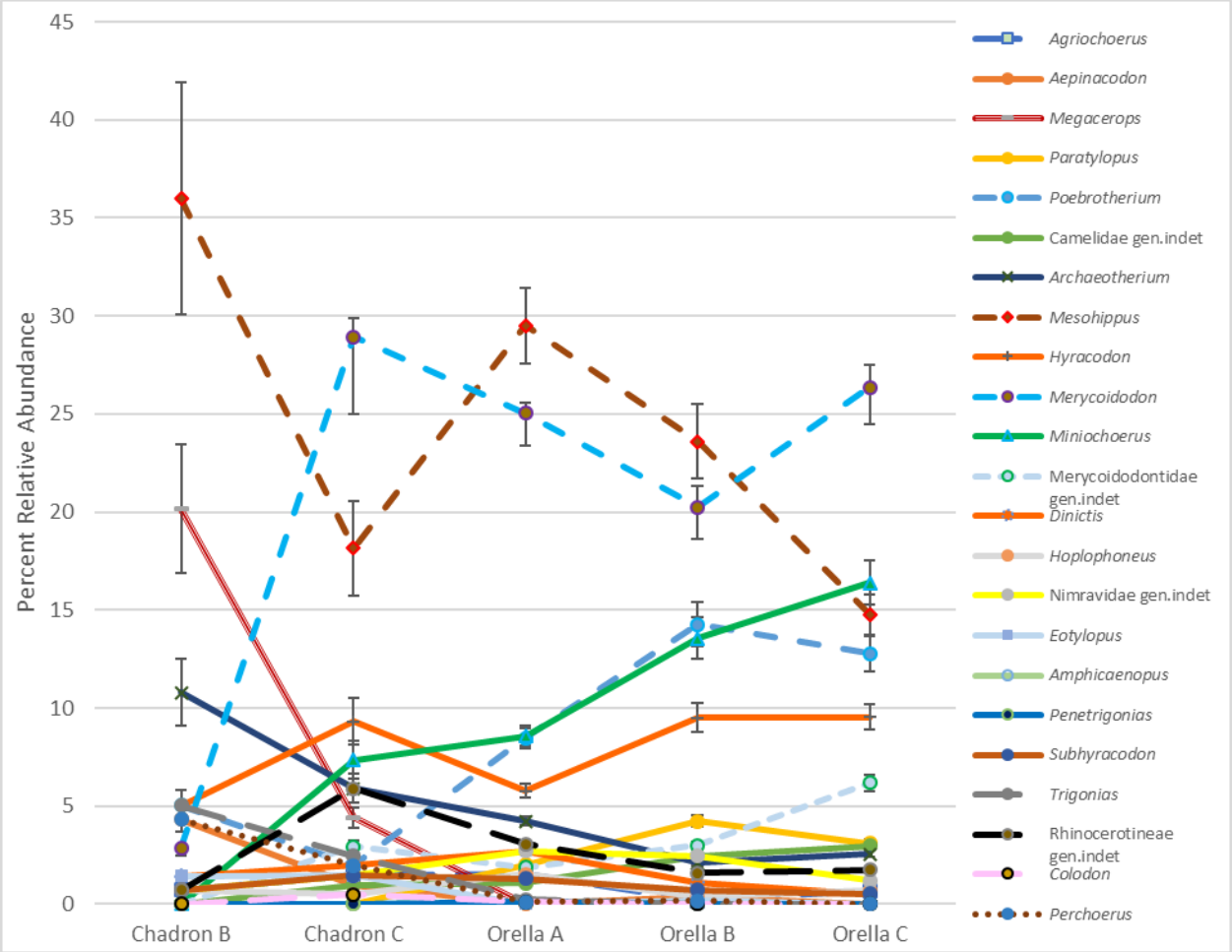

Figure C2. Percent Relative abundance without *Leptomeryx* through the Schultz and Stout(1955) zones showing 95% confidence interval bars.

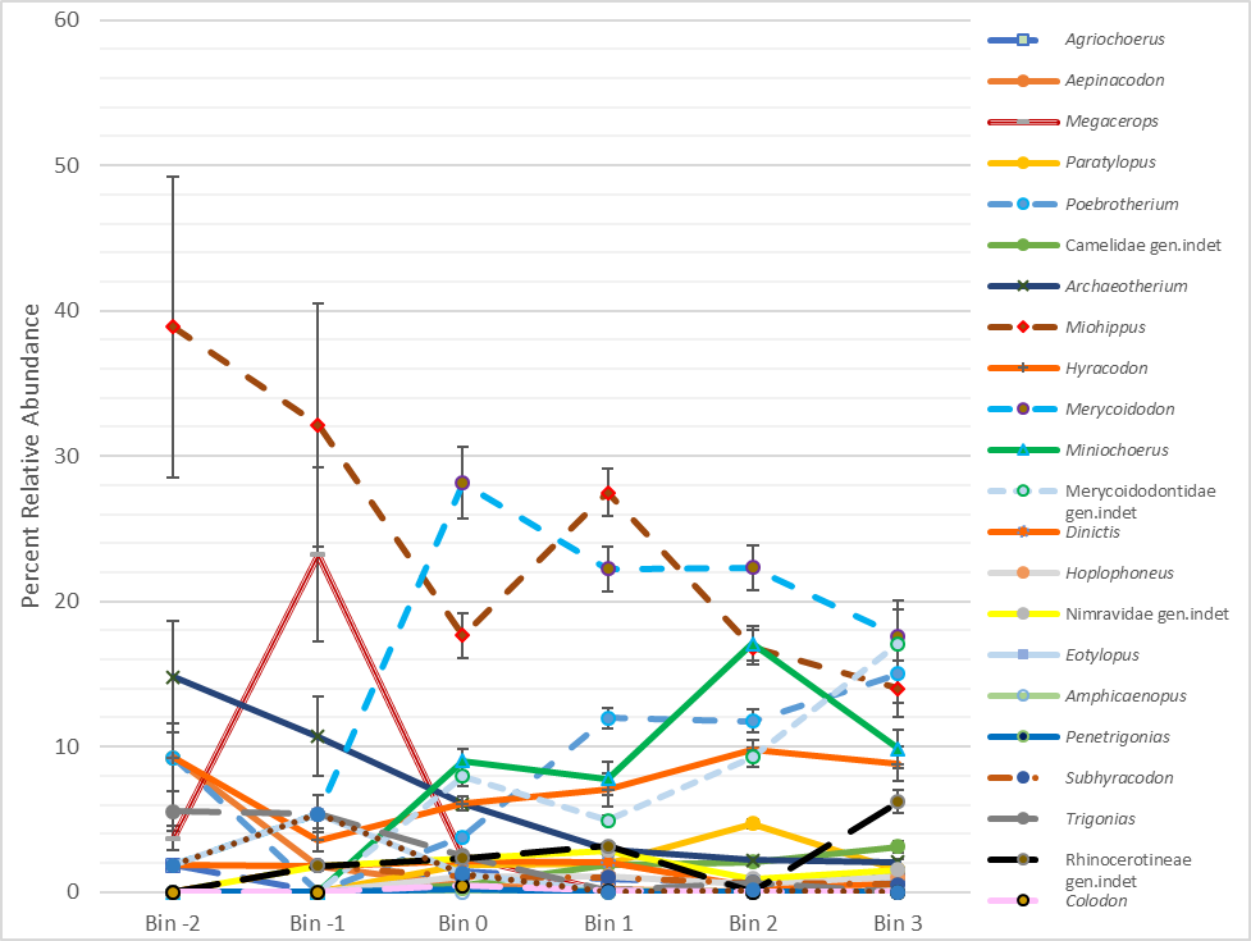

Figure C3. Fourth bin series relative abundance will all taxa included (except *Leptomeryx*) and 95% confidence interval bars.

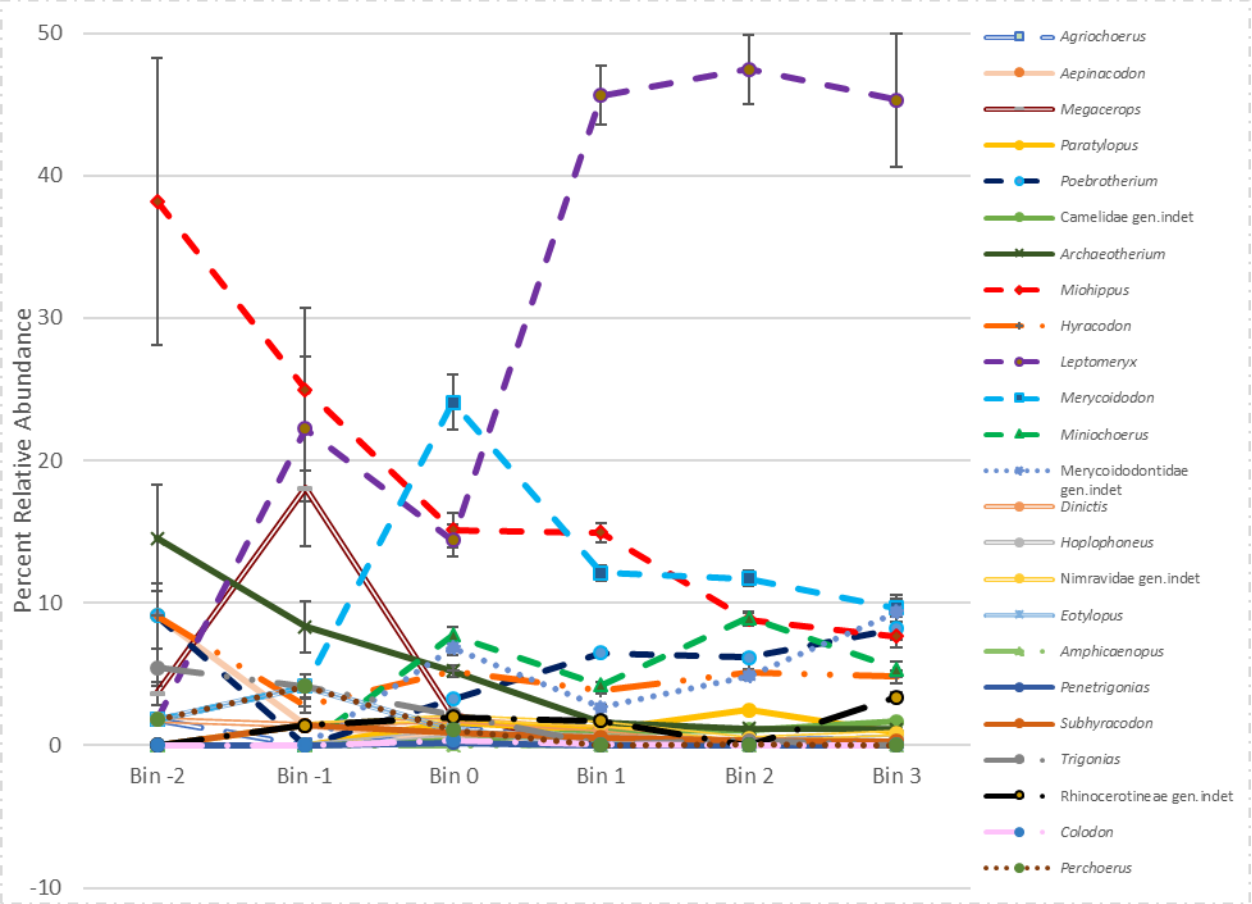

Figure C4. Fourth bin series relative abundance will all taxa included and 95% confidence interval bars.

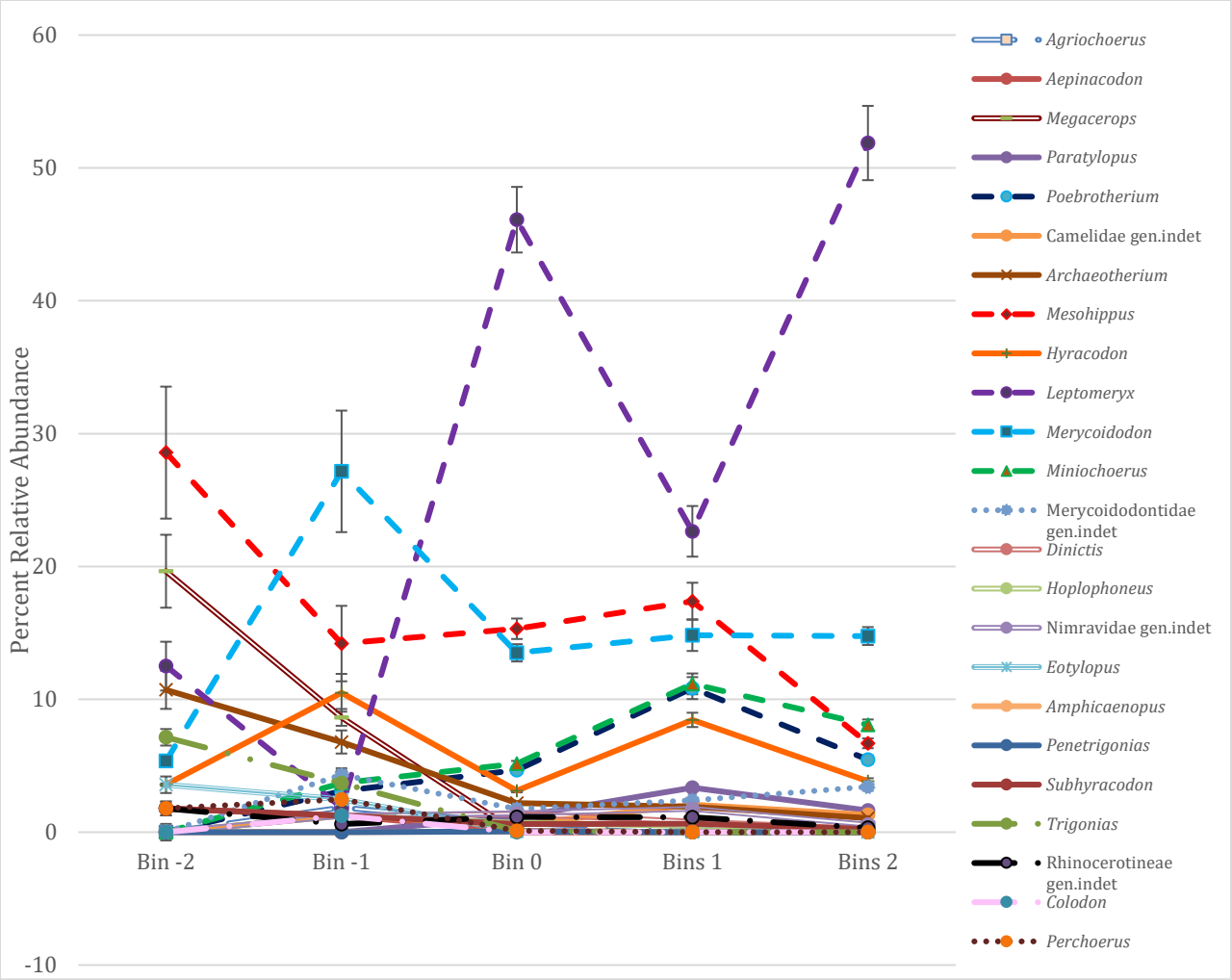

Figure C5. Sixth bin series relative abundance will all taxa included and 95% confidence interval bars.

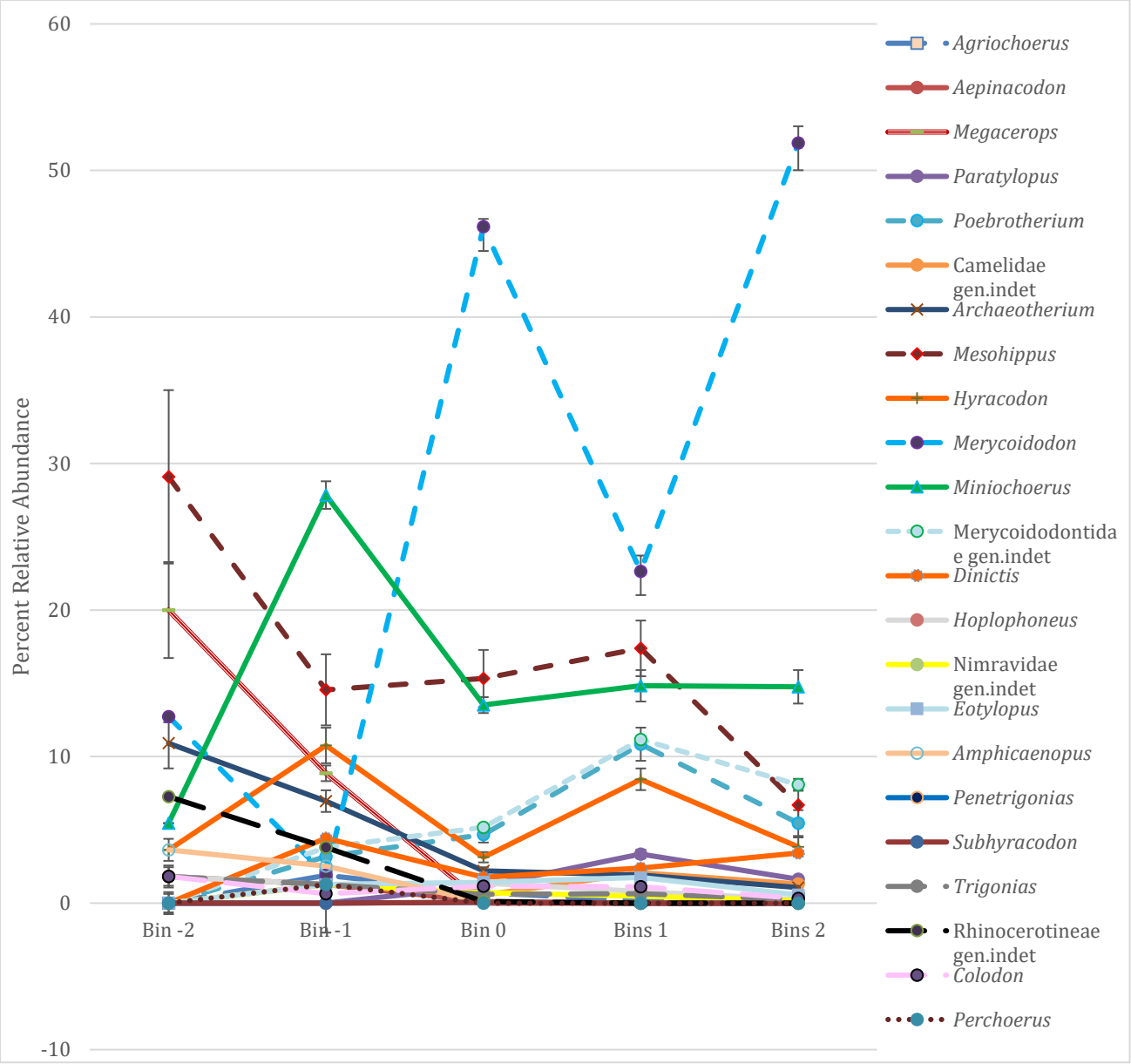

Figure C6. Sixth bin series relative abundance will all taxa included (except *Leptomeryx*) and 95% confidence interval bars.

Appendix D: NALMA Abundance Figures

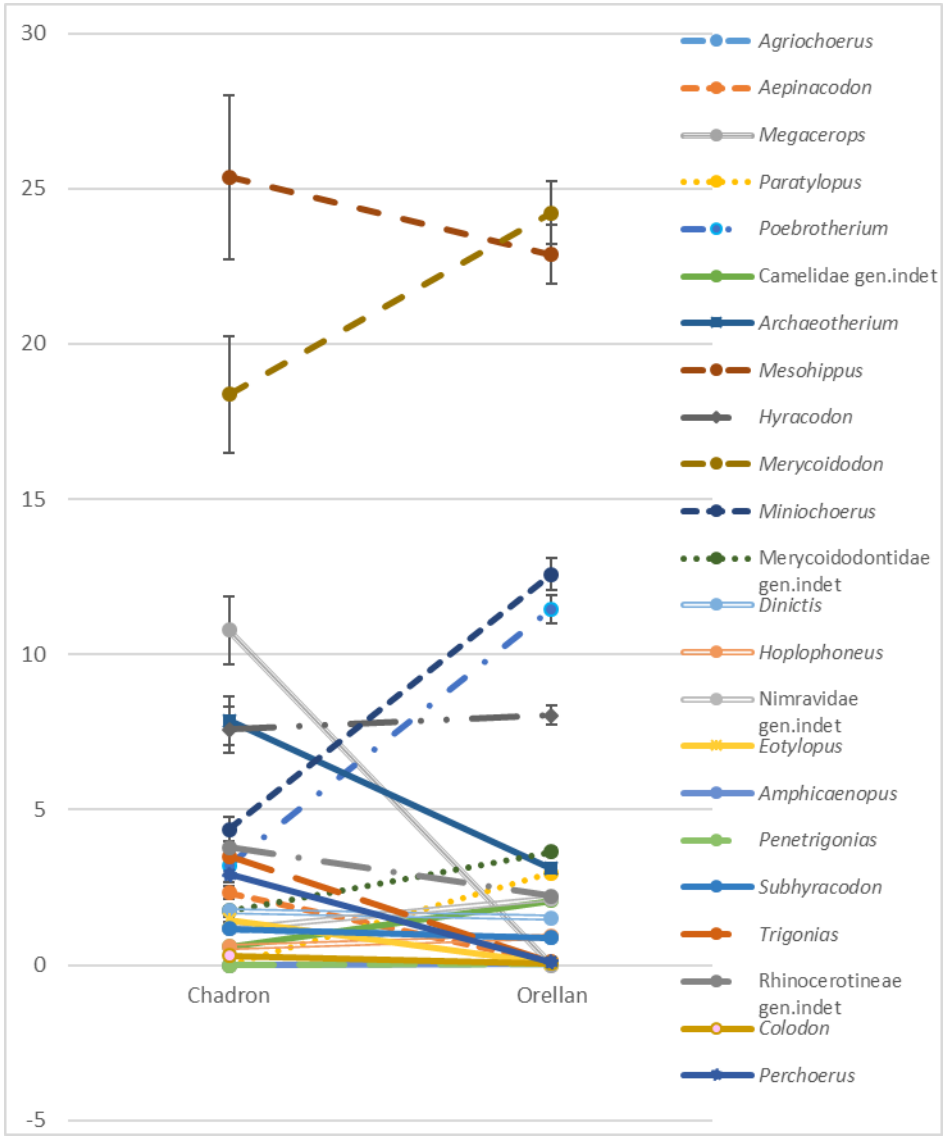

Figure D1. Change in relative abundance of mammalian genera from the Chadronian NALMA to the Orellan NALMA as defined in Schultz and Stout (1955). Error bars are 95% confidence intervals.

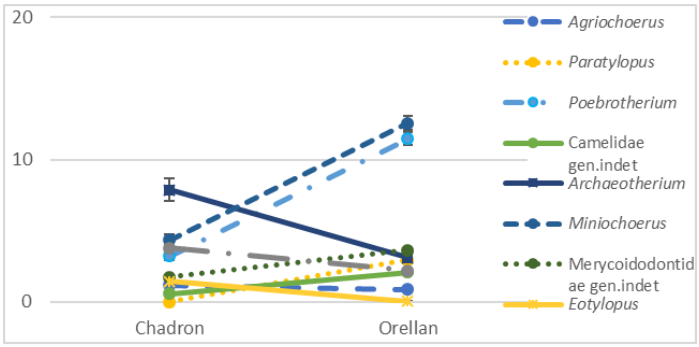

Figure D2. Change in relative abundance of Camelidae, Entelodontidae, Oromerycidae, and Merycoidodontoidea genera (except for *Merycoidodon)* from the Chadronian NALMA to the Orellan NALMA as defined in Schultz and Stout (1955). Error bars are 95% confidence intervals.

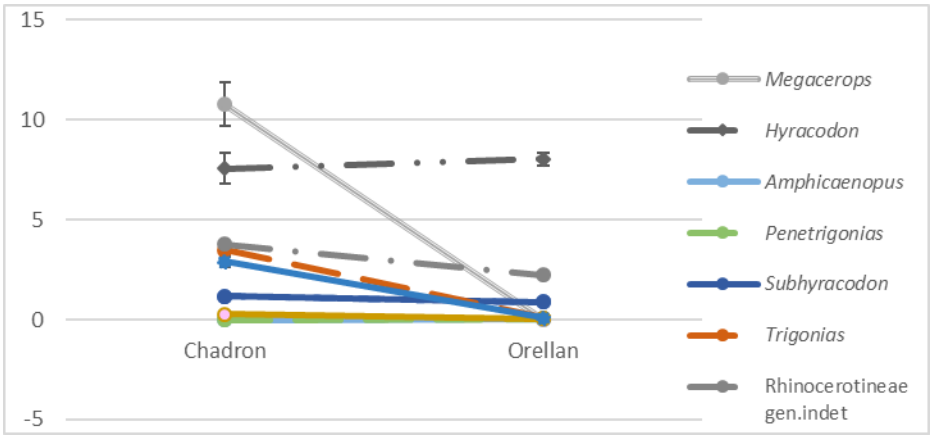

Figure D3. Change in relative abundance of Perissodactyl genera (Except for *Mesohippus*) from the Chadronian NALMA to the Orellan NALMA as defined in Schultz and Stout (1955). Error bars are 95% confidence intervals.

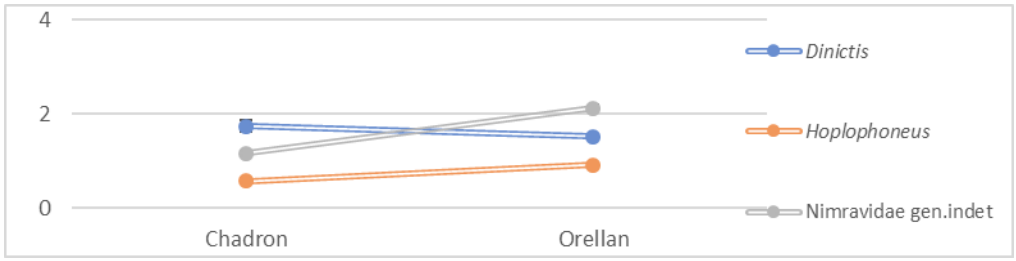

Figure D4. Change in relative abundance of Nimravid genera from the Chadronian NALMA to the Orellan NALMA as defined in Schultz and Stout (1955). Error bars are 95% confidence intervals.

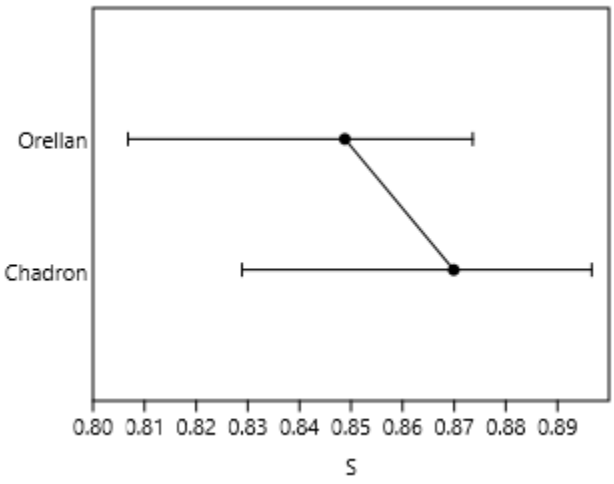

Figure D5. Measure of diversity using Simpson-D diversity index generated in Past 3.23 across the NALMAs showing 95% confidence intervals. This index measures 'evenness' of the community from 0 (one taxon dominates the zone entirely) to 1 (all taxa equally present).

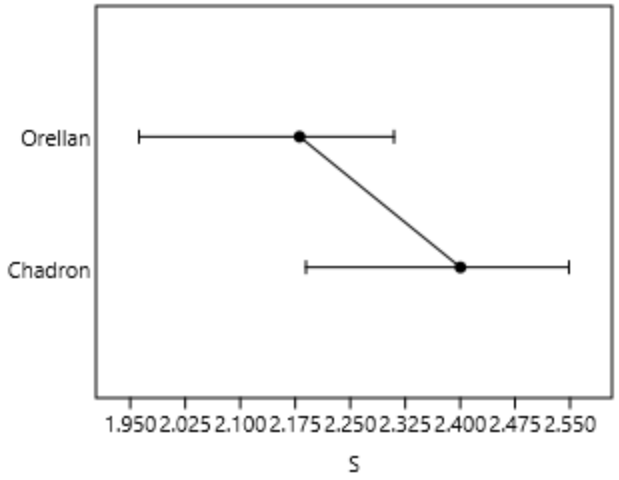

Figure D6. Measure of diversity using Shannon H index generated in Past 3.23 across the NALMAs showing 95% confidence intervals. The Shannon H index is H=-sum((ni/n)ln(ni/n)) where ni is number of individuals of taxon i. This index measures diversity considering the number of individuals as well as number of taxa. This index varies from 0 for communities with just one taxon to high values for communities with many relatively rare taxa.

Appendix E: Combined Fourth Series Bins Before and After Climate Shift

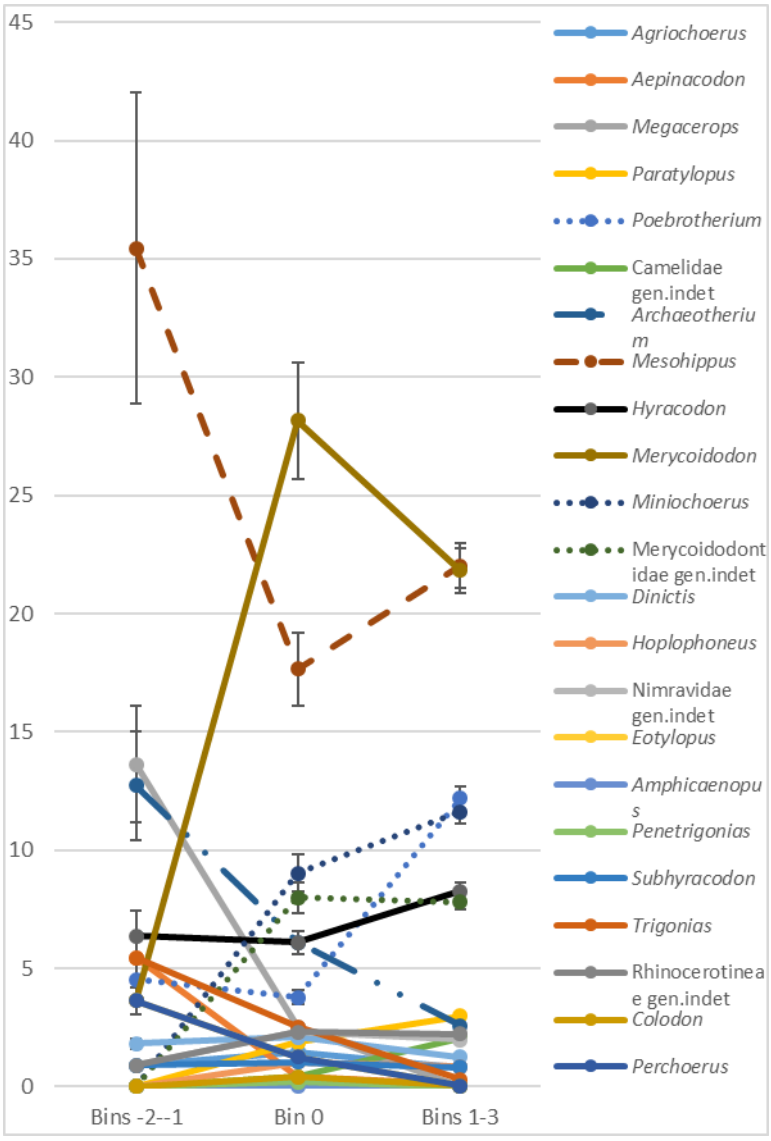

Figure E1. Combined bins before and after the climate shift of the fourth bin series showing 95% confidence interval bars.

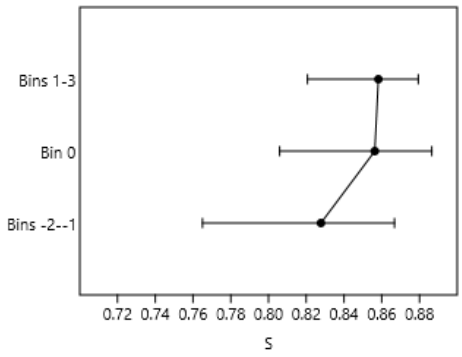

Figure E2. Measure of diversity using Simpson-D diversity index generated in Past 3.23 across the combined bins of the fourth series showing 95% confidence intervals. This index measures 'evenness' of the community from 0 (one taxa dominates the zone entirely) to 1 (all taxa equally present).

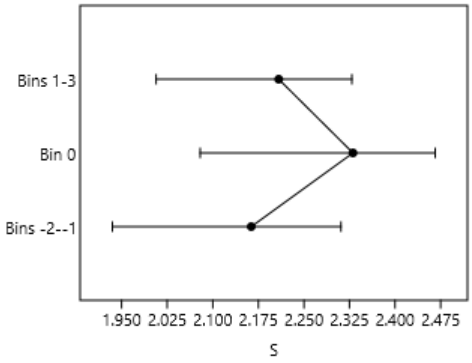

Figure E3. Measure of diversity using Shannon H index generated in Past 3.23 across the combined bins of the fourth series showing 95% confidence intervals. This index measures diversity considering the number of individuals as well as number of taxa. This index varies from 0 for communities with just one taxon to high values for communities with many relatively rare taxa.

Results

Table 1. List of *Merycoidodon* samples used for stable isotope analysis.

ID	Spec. UNSM #	Spec. Field #	Locality	δ13C (VPDB)	δ18O (VPDB)	δ18O (VSMOW)
RG1-37		1-22-8-37 SP	Sx-18 0-15' above UPW	**-9.2**	**-2.7**	**28.1**
RG1-38		2123-73	Sx-26 0-15' above UPW	**-9.8**	**-10.1**	**20.5**
RG1-39		171-54	Sx-0 just west of Sx-32 7' above base of UPW	**-9.0**	**-8.8**	**21.9**
RG1-40		122-52	Sx-18 6' above base of UPW	**-9.2**	**-7.3**	**23.4**
RG1-42		3-29-8-35 SP	Dw- S1/2 S 33 T 33N R52W 4' above UPW	**-8.5**	**-8.7**	**21.9**
RG1-43		605-38	Sx-29 3.5' above Upw	**-8.7**	**-6.6**	**24.1**
RG1-44		400-72	Sx-29 2.5' above UPW	**-8.9**	**-9.0**	**21.6**
RG1-45		2551-63	Sx-29 2' above Upw	**-8.8**	**-8.6**	**22.1**
RG1-46		MES		**-9.7**	**-7.5**	**23.1**
RG1-47		MES		**-9.8**	**-7.6**	**23.1**
RG1-48		2034-53	Sx-32 1' above UPW	**-9.4**	**-8.3**	**22.3**
RG1-49		2549-63	Sx-29 in UPW	**-9.6**	**-7.7**	**23.0**
RG1-50		602-38	Sx-29 Zone 0 3' below UPW	**-8.6**	**-6.9**	**23.8**
RG1-51	132084	609-38	Sx-29 3' below UPW	**-9.1**	**-6.6**	**24.1**
RG1-53		207-53	Dw-104 from the base of the UPW	**-9.4**	**-8.3**	**22.4**
RG1-54		3004-56	Sx-35 5' below PW	**-8.9**	**-6.8**	**24.0**
RG1-55		205-53	Dw-104 5' below UPW	**-10.2**	**-3.8**	**27.0**
RG1-56		3223-63	Sx-32 0-10' below UPW	**-8.3**	**-6.2**	**24.5**
RG1-58		MES		**-9.8**	**-7.4**	**23.2**
RG1-59		MES		**-9.8**	**-7.5**	**23.1**
RG1-60		19-15-8-35 SP	Sx-11 or Sx-12 5' below Upw	**-8.4**	**-3.9**	**26.9**
RG1-61		1550-62	Sx-20 8' below UPW	**-10.3**	**-7.5**	**23.2**
RG1-62		721-38	Sx-34 Zone 0 0-20' below UPW	**-9.0**	**-5.7**	**25.0**
RG1-63		604-38	Sx-29 10' below UPW	**-8.5**	**-8.6**	**22.0**
RG1-64		175-47	Sx-0 12-14' below UPW	**-8.9**	**-0.6**	**30.3**
RG1-65		176-54	Sx-32 15' below base of UPW	**-10.1**	**-5.4**	**25.3**
RG1-66	131812	3-3-9-34 SP	Sx-29 15' below UPW	**-9.3**	**-6.1**	**24.7**
RG1-67		719-38	Sx-34 25' below UPW	**-10.1**	**-6.3**	**24.4**
RG1-68		11-22-8-37 SP	Sx-18 12' SW of Soddie toadstool Park 25' below PW	**-9.8**	**-9.8**	**20.8**
RG1-69	132083	603-77	Dw-104 5' above lower purple white	**-9.5**	**-3.2**	**27.6**
RG1-70	131812	3-3-9-34 SP	Sx-29 15' below UPW	**-9.1**	**-6.4**	**24.3**

Table 2. Tooth width and length measurements to calculate area. Average value for each taxa on rightmost column. Note that *Leptomeryx* was not included in the tooth area size histograms.

	Museum #	Field #	Labial-Post. Length	Lingual-Buccal Width	Tooth Area	Average
Nimravid	25750		16.1	7.1	113.9	121.1
Nimravid	25515		18.6	7.6	140.7	
Nimravid	"-"		16.4	6.6	108.6	
Hyracodon	132092		21.0	23.9	500.9	447.4
Hyracodon	11012		19.6	19.8	387.3	
Hyracodon		1500-65	21.3	21.3	453.9	
Trigonias		2131-38	34.7	40.4	1400.4	1290.2
Trigonias		46-38	32.6	36.2	1180.0	
Archaeotherium		1-25-7-33	19.5	19.2	375.8	417.0
Archaeotherium		401-54	18.6	19.2	358.2	
Archaeotherium		210-54	22.7	22.7	516.9	
Aepinacodon	132055		18.6	25.4	473.5	383.7
Aepinacodon		2533-60	18.2	22.6	410.7	
Aepinacodon	1059		14.3	18.7	266.8	
Colodon		2613-76 A	10.6	12.7	135.3	135.3
Agriochoerus		1895-38	10.0	13.4	134.1	140.7
Agriochoerus		40-52	10.2	14.3	145.8	
Agriochoerus	46052		11.0	12.9	142.1	
Leptomeryx		13-28-7-34	4.9	5.0	24.4	29.4
Leptomeryx	64762		5.2	5.1	26.6	
Leptomeryx	64778		6.1	6.1	37.2	
Merycoidodon		40-22-8-34	9.5	11.8	111.3	160.0
Merycoidodon		2584-63	12.8	14.0	179.7	
Merycoidodon	28334		12.6	15.0	189.0	
Miniochoerus	28501		8.7	8.7	76.1	73.6
Miniochoerus	28130		7.6	9.4	71.8	
Miniochoerus	2811		7.9	9.3	73.0	
Megacerops		3287-91	59.7	60.5	3613.6	3613.6
Tayassuidae	123701		8.1	10.5	85.4	85.4
Eotylopus		20-151-8-36	9.3	9.2	85.5	92.4
Eotylopus	125463		9.2	10.8	99.4	
Poebrotherium		1-6-8-33	9.4	9.7	91.1	86.7
Poebrotherium		52-13-8-36	8.5	9.7	82.4	
Paratylopus		8-7-9-37	9.2	10.3	94.8	94.8
Mesohippus		18-8-33 SP	7.8	9.7	75.7	75.7

Table 3. chord distance (CRD) between zones without *Leptomeryx* for each Schultz and Stout(1955) zone.

	Chadron B&C	Orella A	Orella B	Orella C
Chadron B&C	0.00	0.97	0.69	1.07
Orella A	0.97	0.00	0.49	0.19
Orella B	0.69	0.49	0.00	0.55
Orella C	1.07	0.19	0.55	0.00

Table 4. chord distance (CRD) between without *Leptomeryx* for the fourth bin series.

	Bin -2	Bin -1	Bin 0	Bin 1	Bin 2	Bin 3
Bin -2	0.00	0.58	0.93	0.71	0.95	0.98
Bin -1	0.58	0.00	0.93	0.85	1.05	1.09
Bin 0	0.93	0.93	0.00	0.40	0.40	0.55
Bin 1	0.71	0.85	0.40	0.00	0.41	0.51
Bin 2	0.95	1.05	0.40	0.41	0.00	0.39
Bin 3	0.98	1.09	0.55	0.51	0.39	0.00

Table 5. chord distance (CRD) between without Leptomeryx for the sixth bin series.

	Bin -2	Bin -1	Bin 0	Bins 1	Bins 2
Bin -2	0.00	0.85	0.95	0.88	1.06
Bin -1	0.85	0.00	1.07	0.81	1.13
Bin 0	0.95	1.07	0.00	0.48	0.19
Bins 1	0.88	0.81	0.48	0.00	0.57
Bins 2	1.06	1.13	0.19	0.57	0.00

Table 6. Abundance of genera within the Shultz and Stout (1955) Zones.

	Chadron B&C	Orella A	Orella B	Orella C
Paratylopus	0	17	24	23
Poebrotherium	11	72	81	95
Archaeotherium	27	36	12	19
Mesohippus	87	251	134	110
Hyracodon	26	49	54	71
Merycoidodon	63	213	115	196
Miniochoerus	15	73	77	122

Table 7. Relative abundance of genera without *Leptomeryx* for each Schultz and Stout (1955) zone. Relative abundance is calculated by number of specimens of that genus from that interval divided by total number of specimens in the zone multiplied by 100.

Relative Abundance	Chadron B&C	Orella A	Orella B	Orella C
Paratylopus	0	2	5	4
Poebrotherium	5	10	16	15
Archaeotherium	12	5	2	3
Mesohippus	38	35	27	17
Hyracodon	11	7	11	11
Merycoidodon	28	30	23	31
Miniochoerus	7	10	15	19

Table 8. 95% confidence intervals with mean values for each Schultz and Stout(1955) zone.

	Chadron B&C	Orella A	Orella B	Orella C
Paratylopus	0.0 ± <0.001	2.4 ± <0.001	4.8 ± <0.001	3.6 ± <0.001
Poebrotherium	4.8 ± -0.55	10.1 ± -0.55	16.3 ± -0.55	14.9 ± -0.55
Archaeotherium	11.8 ± -1.46	5.1 ± -1.46	2.4 ± -1.46	3.0 ± -1.46
Mesohippus	38.0 ± -4.87	35.3 ± -4.87	27.0 ± -4.87	17.3 ± -4.87
Hyracodon	11.4 ± -1.41	6.9 ± -1.41	10.9 ± -1.41	11.2 ± -1.41
Merycoidodon	27.5 ± -3.51	30.0 ± -3.51	23.1 ± -3.51	30.8 ± -3.51
Miniochoerus	6.6 ± -0.78	10.3 ± -0.78	15.5 ± -0.78	19.2 ± -0.78

Table 9. Percent change from one interval to the next without *Leptomeryx*. Intervals from Schultz and Stout(1955). % decrease = Decrease ÷ Original Number × 100. % increase = Increase ÷ Original Number × 100.

Percent change	Chadron B&C to Orella A	Orella A to B	Orella B to C
Paratylopus		102	-25
Poebrotherium	111	61	-8
Archaeotherium	-57	-52	24
Mesohippus	-7	-24	-36
Hyracodon	-39	58	3
Merycoidodon	9	-23	33
Miniochoerus	57	51	24

Table 10. Diversity Indices for Schultz and Stout(1955) zones without *Leptomeryx*

	Chadron B	Lower	Upper	Chadron C	Lower	Upper	Orella A	Lower	Upper	Orella B	Lower	Upper	Orella C	Lower	Upper
Taxa_S	16.00	14.00	16.00	20.00	17.00	20.00	20.00	13.00	19.00	18.00	12.00	18.00	15.00	11.00	15.00
Individuals	92.00	92.00	92.00	88.00	88.00	88.00	92.00	92.00	92.00	93.00	93.00	93.00	92.00	92.00	92.00
Dominance_D	0.19	0.13	0.22	0.14	0.08	0.15	0.17	0.11	0.19	0.15	0.11	0.16	0.15	0.11	0.16
Simpson_1-D	0.81	0.78	0.87	0.86	0.85	0.92	0.83	0.81	0.89	0.85	0.84	0.89	0.85	0.84	0.89
Shannon_H	2.06	1.76	2.15	2.36	2.00	2.36	2.16	1.83	2.24	2.16	1.92	2.25	2.14	1.86	2.17
Evenness_e^H/S	0.49	0.38	0.54	0.53	0.39	0.54	0.43	0.40	0.56	0.48	0.46	0.61	0.57	0.49	0.65
Brillouin	1.48	1.50	1.85	1.56	1.66	1.98	1.57	1.57	1.93	1.63	1.67	1.95	1.58	1.62	1.89
Menhinick	1.60	1.40	1.60	2.00	1.70	2.00	2.00	1.30	1.90	1.80	1.20	1.80	1.50	1.10	1.50
Margalef	3.32	2.88	3.32	4.24	3.57	4.24	4.20	2.65	3.98	3.75	2.43	3.75	3.10	2.21	3.10
Equitability_J	0.74	0.65	0.78	0.79	0.68	0.79	0.72	0.67	0.79	0.75	0.72	0.81	0.79	0.73	0.83
Fisher_alpha	5.38	4.60	5.60	7.52	6.27	8.08	7.52	4.13	7.27	6.41	3.67	6.65	4.89	3.26	5.09
Berger-Parker	0.35	0.24	0.42	0.29	0.18	0.33	0.29	0.22	0.35	0.23	0.17	0.30	0.26	0.18	0.32
Chao-1	16.00	15.50	37.00	20.00	19.75	42.50	20.00	14.00	44.00	18.00	14.00	43.00	15.00	11.33	30.00

Table 11. Percent change from one interval to the next of the fourth bin series without *Leptomeryx*. % decrease = Decrease ÷ Original Number × 100. % increase = Increase ÷ Original Number × 100. Blank cells are those with divide by zero errors.

Percent change	Bin -2 to -1	Bin -1 to 0	Bin 0 to Bi	Bin 1 to 2	Bin 2 to 3
Paratylopus			-6.69	128.54	-59.34
Poebrotherium	-100.00		182.27	-5.56	57.23
Archaeotherium	3.45	-59.49	-56.56	-28.05	14.82
Mesohippus	18.23	-60.89	38.97	-41.08	2.13
Hyracodon	-44.83	21.53	2.80	34.12	10.61
Merycoidodon	313.79	274.37	-29.49	-3.51	-2.98
Miniochoerus			-22.86	110.54	-29.23

Table 12. Abundance of genera within the fourth bin series.

	Bin -2	Bin -1	Bin 0	Bin 1	Bin 2	Bin 3
Paratylopus	*0*	*0*	*9*	*20*	*36*	*3*
Poebrotherium	*5*	*0*	*18*	*121*	*90*	*29*
Archaeotherium	*8*	*6*	*29*	*30*	*17*	*4*
Mesohippus	*21*	*18*	*84*	*278*	*129*	*27*
Hyracodon	*5*	*2*	*29*	*71*	*75*	*17*
Merycoidodon	*1*	*3*	*134*	*225*	*171*	*34*
Miniochoerus	*0*	*0*	*43*	*79*	*131*	*19*

Table 13. Relative abundance of genera without *Leptomeryx* for within the fourth bin series. Relative abundance is calculated by number of specimens of that genus from that interval divided by total number of specimens in the zone multiplied by 100.

Relative Abundance	Bin -2	Bin -1	Bin 0	Bin 1	Bin 2	Bin 3
Paratylopus	0	0	3	2	6	2
Poebrotherium	13	0	5	15	14	22
Archaeotherium	20	21	8	4	3	3
Mesohippus	53	62	24	34	20	20
Hyracodon	13	7	8	9	12	13
Merycoidodon	3	10	39	27	26	26
Miniochoerus	0	0	12	10	20	14

Table 14. 95% confidence intervals with mean values for the fourth bin series.

	Bin -2	Bin -1	Bin 0	Bin 1	Bin 2	Bin 3
Paratylopus	0 ± <0.001	0.00 ± <0.001	2.60 ± -0.22	2.43 ± -0.13	5.55 ± -0.39	2.26 ± 0.29
Poebrotherium	13 ± -3.76	0.00 ± <0.001	5.20 ± -0.49	14.68 ± -0.97	13.87 ± -1.03	21.80 ± -3.63
Archaeotherium	20 ± -6.12	20.69 ± -7.48	8.38 ± -0.83	3.64 ± -0.21	2.62 ± -0.16	3.01 ± -0.42
Mesohippus	53 ± -16.32	62.07 ± -22.80	24.28 ± -2.51	33.74 ± -2.27	19.88 ± -1.49	20.30 ± -3.38
Hyracodon	13 ± -3.76	6.90 ± -2.36	8.38 ± -0.83	8.62 ± -2.09	11.56 ± -0.85	12.78 ± -2.09
Merycoidodon	3 ± -0.61	10.34 ± -3.64	38.73 ± -4.03	27.31 ± -1.99	26.35 ± -1.99	25.56 ± -4.27
Miniochoerus	0 ± <0.001	0.00 ± <0.001	12.43 ± -1.26	9.59 ± -1.52	20.18 ± -1.52	14.29 ± -2.35

Table 15. Diversity Indices for the fourth bin series without *Leptomeryx* in the dataset. It is divided in two pieces for increased legibility.

	Bin 1	Lower	Upper	Bin 2	Lower	Upper	Bin 3	Lower	Upper
Taxa_S	20.00	14.00	20.00	16.00	11.00	15.00	15.00	13.00	15.00
Individuals	90.00	90.00	90.00	92.00	92.00	92.00	94.00	94.00	94.00
Dominance_D	0.16	0.10	0.16	0.14	0.11	0.15	0.13	0.10	0.14
Simpson_1-D	0.84	0.84	0.90	0.86	0.85	0.89	0.87	0.86	0.90
Shannon_H	2.20	1.90	2.28	2.14	1.89	2.16	2.25	2.05	2.30
Evenness_e^H/S	0.45	0.41	0.56	0.53	0.52	0.68	0.63	0.53	0.67
Brillouin	1.52	1.61	1.94	1.58	1.65	1.88	1.77	1.80	2.02
Menhinick	2.00	1.40	2.00	1.60	1.10	1.50	1.50	1.30	1.50
Margalef	4.22	2.89	4.22	3.32	2.21	3.10	3.08	2.64	3.08
Equitability_J	0.74	0.69	0.79	0.77	0.75	0.84	0.83	0.77	0.85
Fisher_alpha	7.52	4.64	7.97	5.38	3.26	5.09	4.89	4.09	5.04
Berger-Parker	0.27	0.19	0.32	0.22	0.16	0.28	0.17	0.15	0.25
Chao-1	20.00	15.20	47.50	16.00	11.00	29.00	15.00	15.00	30.00

	Bin -2	Lower	Upper	Bin -1	Lower	Upper	Bin 0	Lower	Upper
Taxa_S	12.00	11.00	12.00	13.00	12.00	13.00	22.00	17.00	22.00
Individuals	92.00	92.00	92.00	93.00	93.00	93.00	92.00	92.00	92.00
Dominance_D	0.21	0.13	0.24	0.18	0.13	0.21	0.14	0.09	0.15
Simpson_1-D	0.79	0.76	0.87	0.82	0.79	0.87	0.86	0.85	0.91
Shannon_H	1.96	1.67	2.02	2.05	1.76	2.10	2.41	2.08	2.47
Evenness_e^H/S	0.59	0.45	0.63	0.60	0.45	0.63	0.51	0.42	0.57
Brillouin	1.42	1.44	1.76	1.54	1.52	1.84	1.78	1.78	2.11
Menhinick	1.20	1.10	1.20	1.30	1.20	1.30	2.20	1.70	2.20
Margalef	2.43	2.21	2.43	2.65	2.43	2.65	4.64	3.54	4.64
Equitability_J	0.79	0.68	0.81	0.80	0.69	0.82	0.78	0.71	0.81
Fisher_alpha	3.56	3.26	3.68	3.99	3.67	4.11	8.72	6.13	9.16
Berger-Parker	0.38	0.27	0.45	0.32	0.23	0.39	0.28	0.18	0.34
Chao-1	12.00	12.00	18.00	13.00	13.00	19.00	22.00	19.50	49.50

Table 16. Abundance of genera within the sixth bin series.

	Bin -2	Bin -1	Bin 0	Bin 1	Bin 2
Paratylopus	0	0	21	21	20
Poebrotherium	0	5	85	68	67
Archaeotherium	6	11	40	12	13
Mesohippus	16	23	279	109	82
Hyracodon	2	17	57	53	47
Merycoidodon	3	44	246	93	181
Miniochoerus	0	6	94	70	99

Table 17. Relative abundance of genera without *Leptomeryx* for within the sixth bin series. Relative abundance is calculated by number of specimens of that genus from that interval divided by total number of specimens in the zone multiplied by 100.

Relative Abundance	Bin -2	Bin -1	Bin 0	Bin 1	Bin 2
Paratylopus	0	0	3	5	4
Poebrotherium	0	5	10	16	13
Archaeotherium	22	10	5	3	3
Mesohippus	59	22	34	26	16
Hyracodon	7	16	7	12	9
Merycoidodon	11	42	30	22	36
Miniochoerus	0	6	11	16	19

Table 18. 95% confidence intervals with mean values for the sixth bin series.

	Bin -2	Bin -1	Bin 0	Bin 1	Bin 2
Paratylopus	0.00 ± <0.001	0.00 ± <0.001	2.55 ± 0.14	4.93 ± 0.42	3.93 ± 0.30
Poebrotherium	0.00 ± <0.001	4.72 ± 0.80	10.34 ± 0.67	15.96 ± 1.47	13.16 ± 1.10
Archaeotherium	22.22 ± 8.35	10.38 ± 1.89	4.87 ± 0.30	2.82 ± 0.22	2.55 ± 0.17
Mesohippus	59.26 ± 22.59	21.70 ± 4.05	33.94 ± 2.29	25.59 ± 2.38	16.11 ± 1.36
Hyracodon	7.41 ± 2.65	16.04 ± 2.97	6.93 ± 0.44	12.44 ± 1.13	9.23 ± 0.76
Merycoidodon	11.11 ± 4.07	41.51 ± 7.84	29.93 ± 2.01	21.83 ± 2.03	35.56 ± 3.05
Miniochoerus	0.00 ± <0.001	5.66 ± 0.98	11.44 ± 0.75	16.43 ± 1.51	19.45 ± 1.65

Table 19. Percent change from one interval to the next of the sixth bin series without *Leptomeryx*. % decrease = Decrease ÷ Original Number × 100. % increase = Increase ÷ Original Number × 100. Blank cells are those with divide by zero errors.

Percent change	Bin -2 to -1	Bin -1 to Bin 0	Bin 0 to 1	Bin 1 to 2
Paratylopus			92.96	-20.29
Poebrotherium		119.22	54.37	-17.54
Archaeotherium	-53.30	-53.11	-42.11	-9.33
Mesohippus	-63.38	56.43	-24.62	-37.04
Hyracodon	116.51	-56.76	79.42	-25.78
Merycoidodon	273.58	-27.90	-27.05	62.89
Miniochoerus		102.03	43.69	18.37

Table 20. Diversity Indices for the sixth bin series without *Leptomeryx* in the dataset.

	Bin -2	Lower	Upper	Bin -1	Lower	Upper	Bin 0	Lower	Upper	Bins 1	Lower	Upper	Bins 2	Lower	Upper
Taxa_S	12.00	12.00	12.00	20.00	17.00	20.00	16.00	12.00	16.00	14.00	11.00	14.00	11.00	10.00	11.00
Individuals	101.00	101.00	101.00	100.00	100.00	100.00	100.00	100.00	100.00	99.00	99.00	99.00	99.00	99.00	99.00
Dominance_D	0.16	0.14	0.21	0.13	0.10	0.18	0.26	0.19	0.33	0.14	0.12	0.18	0.32	0.24	0.40
Simpson_1-D	0.84	0.79	0.86	0.87	0.82	0.90	0.74	0.67	0.81	0.86	0.82	0.88	0.68	0.60	0.76
Shannon_H	2.09	1.89	2.19	2.41	2.18	2.56	1.85	1.61	2.06	2.18	1.97	2.28	1.62	1.41	1.82
Evenness_e^H/S	0.67	0.55	0.75	0.56	0.48	0.67	0.40	0.36	0.53	0.63	0.58	0.75	0.46	0.38	0.57
Brillouin	1.90	1.72	2.01	2.15	1.95	2.29	1.65	1.45	1.85	1.98	1.80	2.08	1.47	1.27	1.66
Menhinick	1.19	1.19	1.19	2.00	1.70	2.00	1.60	1.20	1.60	1.41	1.11	1.41	1.11	1.01	1.11
Margalef	2.38	2.38	2.38	4.13	3.47	4.13	3.26	2.39	3.26	2.83	2.18	2.83	2.18	1.96	2.18
Equitability_J	0.84	0.76	0.88	0.80	0.75	0.86	0.67	0.62	0.76	0.83	0.79	0.88	0.68	0.59	0.76
Fisher_alpha	3.55	3.55	3.55	7.52	5.88	7.52	5.38	3.56	5.38	4.45	3.17	4.45	3.17	2.78	3.17
Berger-Parker	0.29	0.22	0.38	0.28	0.19	0.36	0.46	0.35	0.55	0.23	0.18	0.31	0.53	0.42	0.61
Chao-1	12.00	12.00	15.00	29.33	19.00	38.00	25.33	12.50	34.00	14.60	11.00	23.00	12.50	10.25	17.00

Appendix A: Biostratigraphy

Appendix B: Datasets with *Leptomeryx* Included

Schultz and Stout (1955) Zones

Table B1. Abundance of genera within the Shultz and Stout (1955) Zones.

	Chadron B	Chadron C	Orella A	Orella B	Orella C
Paratylopus	0	0	17	24	23
Poebrotherium	7	4	72	81	95
Archaeotherium	15	12	36	12	19
Mesohippus	50	37	251	134	110
Hyracodon	7	19	49	54	71
Leptomeryx	19	4	786	182	790
Merycoidodon	4	59	213	115	196
Miniochoerus	0	15	73	77	122

Table B2. Relative abundance of genera with *Leptomeryx* for each Schultz and Stout(1955) zone. Relative abundance is calculated by number of specimens of that genus from that interval divided by total number of specimens in the zone multiplied by 100.

Relative Abundance	Chadron B	Chadron C	Orella A	Orella B	Orella C
Paratylopus	0	0	1	4	2
Poebrotherium	7	3	5	12	7
Archaeotherium	15	8	2	2	1
Mesohippus	49	25	17	20	8
Hyracodon	7	13	3	8	5
Leptomeryx	19	3	53	27	55
Merycoidodon	4	39	14	17	14
Miniochoerus	0	10	5	11	9

Table B3. 95% confidence intervals with mean values for each Schultz and Stout(1955) zone.

	Chadron B	Chadron C	Orella A	Orella B	Orella C
Paratylopus	0.0 ± 0.00	0.0 ± 0.00	1.1 ± 0.02	3.5 ± 0.23	1.6 ± 0.05
Poebrotherium	6.9 ± 1.24	2.7 ± 0.34	4.8 ± 0.22	11.9 ± 0.86	6.7 ± 0.32
Archaeotherium	14.7 ± 2.77	8.0 ± 1.20	2.4 ± 0.09	1.8 ± 0.09	1.3 ± 0.03
Mesohippus	49.0 ± 9.46	24.7 ± 3.88	16.8 ± 0.82	19.7 ± 1.45	7.7 ± 0.37
Hyracodon	6.9 ± 1.24	12.7 ± 1.95	3.3 ± 0.14	8.0 ± 0.56	5.0 ± 0.23
Leptomeryx	18.6 ± 3.53	2.7 ± 0.34	52.5 ± 2.64	26.8 ± 1.98	55.4 ± 2.85
Merycoidodon	3.9 ± 0.66	39.3 ± 6.23	14.2 ± 0.70	16.9 ± 1.24	13.7 ± 0.69
Miniochoerus	0.0 ± 0.00	10.0 ± 1.52	4.9 ± 0.22	11.3 ± 0.82	8.6 ± 0.42

Table B4. chord distance (CRD) between zones with *Leptomeryx* for each Schultz and Stout(1955) zone.

	Chadron B	Chadron C	Orella A	Orella B	Orella C
Chadron B	0.00	0.92	0.96	0.84	1.08
Chadron C	0.92	0.00	1.07	0.77	1.13
Orella A	0.96	1.07	0.00	0.48	0.19
Orella B	0.84	0.77	0.48	0.00	0.54
Orella C	1.08	1.13	0.19	0.54	0.00

Table B5. Diversity Indices for Schultz and Stout1955 zones with *Leptomeryx*

	Chadron B	Lower	Upper	Chadron C	Lower	Upper	Orella A	Lower	Upper	Orella B	Lower	Upper	Orella C	Lower	Upper
Taxa_S	17.00	14.00	17.00	21.00	18.00	21.00	21.00	12.00	18.00	19.00	13.00	18.00	16.00	11.00	15.00
Individuals	91.00	91.00	91.00	87.00	87.00	87.00	92.00	92.00	92.00	92.00	92.00	92.00	92.00	92.00	92.00
Dominance_D	0.17	0.11	0.18	0.14	0.08	0.14	0.28	0.17	0.30	0.14	0.10	0.15	0.30	0.18	0.33
Simpson_1-D	0.84	0.82	0.89	0.86	0.86	0.92	0.72	0.70	0.83	0.86	0.85	0.90	0.70	0.67	0.82
Shannon_H	2.18	1.86	2.23	2.41	2.03	2.39	1.81	1.51	1.97	2.19	1.94	2.26	1.73	1.46	1.89
Evenness_e^H/S	0.52	0.41	0.56	0.53	0.39	0.53	0.29	0.32	0.47	0.47	0.47	0.61	0.35	0.34	0.51
Brillouin	1.55	1.59	1.92	1.55	1.68	1.99	1.25	1.28	1.69	1.61	1.68	1.96	1.19	1.23	1.63
Menhinick	1.70	1.40	1.70	2.10	1.80	2.10	2.10	1.20	1.80	1.90	1.30	1.80	1.60	1.10	1.50
Margalef	3.55	2.88	3.55	4.48	3.81	4.48	4.42	2.43	3.76	3.98	2.65	3.76	3.32	2.21	3.10
Equitability_J	0.77	0.68	0.79	0.79	0.69	0.79	0.60	0.58	0.71	0.74	0.73	0.81	0.62	0.58	0.73
Fisher_alpha	5.88	4.62	6.17	8.11	6.89	8.79	8.11	3.68	6.69	6.95	4.13	6.69	5.38	3.26	5.09
Berger-Parker	0.31	0.21	0.37	0.28	0.17	0.32	0.48	0.34	0.52	0.24	0.17	0.30	0.51	0.37	0.55
Chao-1	17.00	16.43	44.00	21.00	20.75	43.50	21.00	13.00	44.00	19.00	14.00	44.00	16.00	12.20	34.00

Table B6. Percent change from one interval to the next with *Leptomeryx*. Intervals from Schultz and Stout(1955). % decrease = Decrease ÷ Original Number × 100. % increase = Increase ÷ Original Number × 100. Blank cells are those with divide by zero errors.

Percent change	Chadron B to C	Chadron C to Orella A	Orella A to B	Orella B to C
Paratylopus			211.25	-54.37
Poebrotherium	-61.14	80.36	148.03	-44.15
Archaeotherium	-45.60	-69.94	-26.51	-24.61
Mesohippus	-49.68	-32.03	17.70	-60.91
Hyracodon	84.57	-74.16	142.97	-37.39
Leptomeryx	-85.68	1868.94	-48.95	106.68
Merycoidodon	903.00	-63.83	19.03	-18.85
Miniochoerus		-51.24	132.55	-24.56

NALMA Bin Results

Table B7. Abundance of genera within the NALMA.

	Chadron	Orellan
Paratylopus	0	64
Poebrotherium	11	248
Archaeotherium	27	67
Mesohippus	87	495
Hyracodon	26	174
Leptomeryx	23	1758
Merycoidodon	63	524
Miniochoerus	15	272

Table B8. Relative abundance of well sampled genera with *Leptomeryx* for each NALMA. Relative abundance is calculated by number of specimens of that genus from that interval divided by total number of specimens in the zone multiplied by 100.

	Chadron	Orellan	Decrease in %
Paratylopus	0.00	1.78	-100.00
Poebrotherium	4.37	6.89	-36.60
Archaeotherium	10.71	1.86	476.01
Mesohippus	34.52	13.74	151.22
Hyracodon	10.32	4.83	113.58
Leptomeryx	9.13	48.81	-81.30
Merycoidodon	25.00	14.55	71.85
Miniochoerus	5.95	7.55	-21.17

Table B9. 95% confidence intervals with mean values for each NALMA.

	Chadron	Orellan
Paratylopus	0.0 ± 0.00	1.8 ± 0.04
Poebrotherium	4.4 ± 0.47	6.9 ± 0.21
Archaeotherium	10.7 ± 1.26	1.9 ± 0.04
Mesohippus	34.5 ± 4.21	13.7 ± 0.43
Hyracodon	10.3 ± 1.21	4.8 ± 0.14
Leptomeryx	9.1 ± 1.07	48.8 ± 1.58
Merycoidodon	25.0 ± 3.03	14.5 ± 0.46
Miniochoerus	6.0 ± 0.67	7.6 ± 0.23

Table B10. chord distance (CRD) between with *Leptomeryx* for each NALMA.

Chord Distance	Chadron	Orellan
Chadron	0.00	0.50
Orellan	0.50	0.00

Table B11. Diversity Indices of well sampled taxa for each NALMA with *Leptomeryx* in the dataset.

	Chadron	Lower	Upper	Orellan	Lower	Upper
Taxa_S	20.00	17.00	20.00	22.00	13.00	20.00
Individuals	90.00	90.00	90.00	92.00	92.00	92.00
Dominance_D	0.13	0.08	0.14	0.15	0.10	0.16
Simpson_1-D	0.87	0.86	0.92	0.85	0.84	0.90
Shannon_H	2.41	2.06	2.42	2.20	1.91	2.29
Evenness_e^H/S	0.55	0.43	0.57	0.41	0.44	0.59
Brillouin	1.69	1.74	2.05	1.61	1.65	1.97
Menhinick	2.00	1.70	2.00	2.20	1.30	2.00
Margalef	4.22	3.56	4.22	4.64	2.65	4.20
Equitability_J	0.80	0.71	0.81	0.71	0.71	0.80
Fisher_alpha	7.52	6.20	7.97	8.72	4.13	7.87
Berger-Parker	0.25	0.17	0.30	0.24	0.18	0.30
Chao-1	20.00	19.50	42.50	22.00	14.20	46.50

Fourth Bin Series Results

Table B12. Abundance of genera within the fourth bin series with *Leptomeryx.*

	Bin -2	Bin -1	Bin 0	Bin 1	Bin 2	Bin 3
Paratylopus	0	0	9	20	36	3
Poebrotherium	5	0	18	121	90	29
Archaeotherium	8	6	29	30	17	4
Mesohippus	21	18	84	278	129	27
Hyracodon	5	2	29	71	75	17
Leptomeryx	1	16	80	849	692	160
Merycoidodon	1	3	134	225	171	34
Miniochoerus	0	0	43	79	131	19

Table B13. Relative abundance of genera with *Leptomeryx* for within the fourth bin series. Relative abundance is calculated by number of specimens of that genus from that interval divided by total number of specimens in the zone multiplied by 100.

Relative Abundance	Bin -2	Bin -1	Bin 0	Bin 1	Bin 2	Bin 3
Paratylopus	0	0	2	1	3	1
Poebrotherium	12	0	4	7	7	10
Archaeotherium	20	13	7	2	1	1
Mesohippus	51	40	20	17	10	9
Hyracodon	12	4	7	4	6	6
Leptomeryx	2	36	19	51	52	55
Merycoidodon	2	7	31	13	13	12
Miniochoerus	0	0	10	5	10	6

Table B14. 95% confidence intervals with mean values for the fourth bin series.

	Bin -2	Bin -1	Bin 0	Bin 1	Bin 2	Bin 3
Paratylopus	0 ± 0.00	2.60 ± 0.00	9.00 ± 0.15	20.00 ± 0.02	36.00 ± 0.11	3.00 ± 0.02
Poebrotherium	7 ± 3.62	5.20 ± 0.00	18.00 ± 0.35	121.00 ± 0.32	90.00 ± 0.33	29.00 ± 1.08
Archaeotherium	20 ± 5.89	8.38 ± 3.79	29.00 ± 0.60	30.00 ± 0.06	17.00 ± 0.03	4.00 ± 0.08
Mesohippus	57 ± 15.72	24.28 ± 11.67	84.00 ± 1.83	278.00 ± 0.77	129.00 ± 0.49	27.00 ± 1.00
Hyracodon	10 ± 3.62	8.38 ± 1.16	29.00 ± 0.60	71.00 ± 0.18	75.00 ± 0.27	17.00 ± 0.61
Leptomeryx	6 ± 0.58	38.73 ± 10.36	80.00 ± 1.74	849.00 ± 2.41	692.00 ± 2.74	160.00 ± 6.21
Merycoidodon	0 ± 0.58	12.43 ± 1.82	134.00 ± 2.94	225.00 ± 0.62	171.00 ± 0.66	34.00 ± 1.27
Miniochoerus	1 ± 0.00	13.43 ± 0.00	43.00 ± 0.91	79.00 ± 0.20	131.00 ± 0.50	19.00 ± 0.68

Table B15. chord distance (CRD) between with *Leptomeryx* for the fourth bin series.

	Bin -2	Bin -1	Bin 0	Bin 1	Bin 2	Bin 3
Bin -2	0.00	0.76	0.96	1.12	1.23	1.23
Bin -1	0.76	0.00	0.82	1.14	0.83	0.85
Bin 0	0.96	0.82	0.00	0.51	0.77	0.80
Bin 1	1.12	1.14	0.51	0.00	1.13	1.15
Bin 2	1.23	0.83	0.77	1.13	0.00	0.15
Bin 3	1.23	0.85	0.80	1.15	0.15	0.00

Table B16. Diversity Indices for the fourth bin series with *Leptomeryx* in the dataset.

	Bin -2	Lower	Upper	Bin -1	Lower	Upper	Bin 0	Lower	Upper
Taxa_S	13.00	12.00	13.00	14.00	13.00	14.00	23.00	17.00	23.00
Individuals	93.00	93.00	93.00	96.00	96.00	96.00	90.00	90.00	90.00
Dominance_D	0.20	0.13	0.23	0.16	0.12	0.19	0.12	0.08	0.13
Simpson_1-D	0.80	0.77	0.87	0.84	0.81	0.88	0.88	0.87	0.92
Shannon_H	2.02	1.72	2.08	2.12	1.87	2.20	2.48	2.13	2.49
Evenness_e^H/S	0.58	0.44	0.62	0.60	0.48	0.65	0.52	0.43	0.57
Brillouin	1.51	1.49	1.82	1.74	1.66	1.96	1.74	1.80	2.11
Menhinick	1.30	1.20	1.30	1.40	1.30	1.40	2.30	1.70	2.30
Margalef	2.65	2.43	2.65	2.85	2.63	2.85	4.89	3.56	4.89
Equitability_J	0.79	0.68	0.81	0.80	0.72	0.83	0.79	0.72	0.81
Fisher_alpha	3.99	3.67	4.11	4.43	4.06	4.51	9.35	6.20	9.98
Berger-Parker	0.38	0.26	0.45	0.25	0.20	0.33	0.24	0.15	0.29
Chao-1	13.00	12.50	23.00	14.00	13.25	24.00	23.00	19.50	55.00

	Bin 1	Lower	Upper	Bin 2	Lower	Upper	Bin 3	Lower	Upper
Taxa_S	21.00	13.00	20.00	17.00	12.00	15.00	16.00	12.00	16.00
Individuals	92.00	92.00	92.00	93.00	93.00	93.00	92.00	92.00	92.00
Dominance_D	0.28	0.17	0.30	0.26	0.16	0.30	0.24	0.15	0.27
Simpson_1-D	0.72	0.70	0.83	0.74	0.70	0.84	0.76	0.73	0.86
Shannon_H	1.84	1.57	2.04	1.82	1.56	1.96	1.92	1.64	2.07
Evenness_e^H/S	0.30	0.31	0.46	0.36	0.38	0.55	0.43	0.36	0.52
Brillouin	1.27	1.32	1.74	1.32	1.34	1.71	1.36	1.39	1.78
Menhinick	2.10	1.30	2.00	1.70	1.20	1.50	1.60	1.20	1.60
Margalef	4.42	2.65	4.20	3.53	2.43	3.09	3.32	2.43	3.32
Equitability_J	0.60	0.58	0.72	0.64	0.62	0.76	0.69	0.62	0.76
Fisher_alpha	8.11	4.13	7.87	5.88	3.67	5.06	5.38	3.68	5.60
Berger-Parker	0.48	0.34	0.52	0.47	0.34	0.52	0.45	0.31	0.50
Chao-1	21.00	15.00	51.00	17.00	12.25	29.00	16.00	13.50	44.00

Table B17. Percent change from one interval to the next of the fourth bin series with *Leptomeryx*. % decrease = Decrease ÷ Original Number × 100. % increase = Increase ÷ Original Number × 100. Blank cells are those with divide by zero errors.

Percent change	Bin -2 to -1	Bin -1 to 0	Bin 0 to Bi	Bin 1 to 2	Bin 2 to 3
Paratylopus			-43.42	124.56	-61.86
Poebrotherium	-100.00		71.17	-7.21	47.47
Archaeotherium	-31.67	-48.94	-73.66	-29.30	7.69
Mesohippus	-21.90	-50.70	-15.73	-42.11	-4.21
Hyracodon	-63.56	53.17	-37.66	31.79	3.74
Leptomeryx	1357.78	-47.18	170.23	1.69	5.82
Merycoidodon	173.33	371.83	-57.24	-5.18	-9.00
Miniochoerus			-53.22	106.88	-33.62

Fourth Combined Bin Series

Table B18. Abundance of genera within the fourth combined bin series.

	Bins -2-0	Bin 1	Bins 2-3
Paratylopus	*9*	20	39
Poebrotherium	*23*	121	119
Archaeotherium	*43*	30	21
Mesohippus	*123*	278	156
Hyracodon	*36*	71	92
Leptomeryx	*97*	849	852
Merycoidodon	*138*	225	205
Miniochoerus	*43*	79	150

Table B19. Relative abundance of genera with *Leptomeryx* for within the fourth combined bin series. Relative abundance is calculated by number of specimens of that genus from that interval divided by total number of specimens in the zone multiplied by 100.

	Bins -2-0	Bin 1	Bins 2-3
Paratylopus	1.76	1.20	2.39
Poebrotherium	4.49	7.23	7.28
Archaeotherium	8.40	1.79	1.29
Mesohippus	24.02	16.62	9.55
Hyracodon	7.03	4.24	5.63
Leptomeryx	18.95	50.75	52.14
Merycoidodon	26.95	13.45	12.55
Miniochoerus	8.40	4.72	9.18

Table B20. 95% confidence intervals with mean values for the fourth combined bin series.

	Bins -2-0	Bin 1	Bins 2-3
Paratylopus	0 ± 0.10	2.60 ±	3.67 ± 0.09
Poebrotherium	7 ± 0.34	5.20 ±	14.94 ± 0.33
Archaeotherium	20 ± 0.68	8.38 ±	3.18 ± 0.03
Mesohippus	57 ± 2.04	24.28 ±	27.02 ± 0.44
Hyracodon	10 ± 0.56	8.38 ±	10.15 ± 0.25
Leptomeryx	6 ± 1.60	38.73 ±	26.77 ± 2.50
Merycoidodon	0 ± 2.29	12.43 ±	14.26 ± 0.58
Miniochoerus	1 ± 0.68	13.43 ±	15.26 ± 0.42

Table B21. chord distance (CRD) between with *Leptomeryx* for the fourth combined bin series.

	Bins -2-0	Bin 1	Bins 2-3
Bins -2-0	0.00	0.60	0.77
Bin 1	0.60	0.00	1.13
Bins 2-3	0.77	1.13	0.00

Table B22. Diversity Indices for the fourth combined bin series with *Leptomeryx* in the dataset.

	Bins -2-0	Lower	Upper	Bin 1	Lower	Upper	Bins 2-3	Lower	Upper
Taxa_S	23.00	17.00	23.00	21.00	13.00	19.00	18.00	12.00	16.00
Individuals	90.00	90.00	90.00	92.00	92.00	92.00	94.00	94.00	94.00
Dominance_D	0.11	0.07	0.12	0.25	0.15	0.27	0.26	0.16	0.30
Simpson_1-D	0.89	0.88	0.93	0.75	0.73	0.85	0.74	0.70	0.84
Shannon_H	2.53	2.17	2.52	1.89	1.62	2.07	1.86	1.59	2.01
Evenness_e^H/S	0.55	0.45	0.58	0.31	0.33	0.49	0.36	0.38	0.56
Brillouin	1.79	1.84	2.14	1.31	1.37	1.77	1.39	1.37	1.75
Menhinick	2.30	1.70	2.30	2.10	1.30	1.90	1.80	1.20	1.60
Margalef	4.89	3.56	4.89	4.42	2.65	3.98	3.74	2.42	3.30
Equitability_J	0.81	0.73	0.82	0.62	0.60	0.73	0.64	0.63	0.77
Fisher_alpha	9.35	6.20	9.98	8.11	4.13	7.27	6.41	3.65	5.54
Berger-Parker	0.20	0.14	0.25	0.45	0.31	0.49	0.47	0.34	0.52
Chao-1	23.00	19.67	55.00	21.00	14.50	51.00	18.00	12.25	35.00

Sixth Bin Series Results

Table B23. Abundance of genera within the sixth bin series with *Leptomeryx.*

	Bin -2	Bin -1	Bin 0	Bin 1	Bin 2
Paratylopus	0	0	21	21	20
Poebrotherium	0	5	85	68	67
Archaeotherium	6	11	40	12	13
Mesohippus	16	23	279	109	82
Hyracodon	2	17	57	53	47
Leptomeryx	7	3	840	142	636
Merycoidodon	3	44	246	93	181
Miniochoerus	0	6	94	70	99

Table B24. Relative abundance of genera with *Leptomeryx* for within the sixth bin series. Relative abundance is calculated by number of specimens of that genus from that interval divided by total number of specimens in the zone multiplied by 100.

Relative Abundance	Bin -2	Bin -1	Bin 0	Bin 1	Bin 2
Paratylopus	0	0	1	4	2
Poebrotherium	0	5	5	12	6
Archaeotherium	18	10	2	2	1
Mesohippus	47	21	17	19	7
Hyracodon	6	16	3	9	4
Leptomeryx	21	3	51	25	56
Merycoidodon	9	40	15	16	16
Miniochoerus	0	6	6	12	9

Table B25. 95% confidence intervals with mean values for the sixth bin series.

	Bin -2	Bin -1	Bin 0	Bin 1	Bin 2
Paratylopus	0.00 ± 0.00	0.00 ± 0.00	1.26 ± 0.03	3.70 ± 0.26	1.75 ± 0.07
Poebrotherium	0.00 ± 0.00	4.59 ± 0.77	5.11 ± 0.22	11.97 ± 0.94	5.85 ± 0.31
Archaeotherium	17.65 ± 5.85	10.09 ± 1.81	2.41 ± 0.09	2.11 ± 0.13	1.14 ± 0.02
Mesohippus	47.06 ± 15.88	21.10 ± 3.88	16.79 ± 0.78	19.19 ± 1.54	7.16 ± 0.38
Hyracodon	5.88 ± 1.83	15.60 ± 2.85	3.43 ± 0.14	9.33 ± 0.73	4.10 ± 0.21
Leptomeryx	20.59 ± 6.85	2.75 ± 0.41	50.54 ± 2.41	25.00 ± 2.02	55.55 ± 3.19
Merycoidodon	8.82 ± 2.83	40.37 ± 7.52	14.80 ± 0.69	16.37 ± 1.31	15.81 ± 0.89
Miniochoerus	0.00 ± 0.00	5.50 ± 0.94	5.66 ± 0.25	12.32 ± 0.97	8.65 ± 0.47

Table B26. chord distance (CRD) between with *Leptomeryx* for the sixth bin series.

	Bin -2	Bin -1	Bin 0	Bin 1	Bin 2
Bin -2	0.00	0.88	0.83	0.73	0.99
Bin -1	0.88	0.00	1.06	0.77	1.12
Bin 0	0.83	1.06	0.00	0.49	0.19
Bin 1	0.73	0.77	0.49	0.00	0.58
Bin 2	0.99	1.12	0.19	0.58	0.00

Appendix C: All Taxa Plotted Together

Schultz and Stout (1955) Zones

Table C1. Abundance of genera within the Shultz and Stout (1955) Zones.

	Chadron B	Chadron C	Orella A	Orella B	Orella C
Agriochoerus	1	3	13	1	5
Aepinacodon	6	2	0	2	0
Megacerops	28	9	0	0	0
Paratylopus	0	0	17	24	23
Poebrotherium	7	4	72	81	95
Camelidae gen.indet	0	2	9	14	22
Archaeotherium	15	12	36	12	19
Mesohippus	50	37	251	134	110
Hyracodon	7	19	49	54	71
Leptomeryx	19	4	786	182	790
Merycoidodon	4	59	213	115	196
Miniochoerus	0	15	73	77	122
Merycoidodontidae gen.indet	0	6	16	17	46
Dinictis	2	4	23	6	4
Hoplophoneus	1	1	13	2	5
Nimravidae gen.indet	1	3	23	14	9
Eotylopus	2	3	0	1	0
Amphicaenopus	0	0	1	0	0
Penetrigonias	0	0	1	0	0
Subhyracodon	1	3	11	4	4
Trigonias	7	5	2	0	0
Rhinocerotineae gen.indet	1	12	26	9	13
Colodon	0	1	1	0	0
Perchoerus	6	4	1	1	0

Table C2. Relative abundance of genera without *Leptomeryx* for each Schultz and Stout(1955) zone. Relative abundance is calculated by number of specimens of that genus from that interval divided by total number of specimens in the zone multiplied by 100.

Relative Abundance	Chadron B	Chadron C	Orella A	Orella B	Orella C
Agriochoerus	1	1	1	0	0
Aepinacodon	4	1	0	0	0
Megacerops	18	4	0	0	0
Paratylopus	0	0	1	3	1
Poebrotherium	4	2	4	11	6
Camelidae gen.indet	0	1	1	2	1
Archaeotherium	9	6	2	2	1
Mesohippus	32	18	15	18	7
Hyracodon	4	9	3	7	5
Leptomeryx	12	2	48	24	51
Merycoidodon	3	28	13	15	13
Miniochoerus	0	7	4	10	8
Merycoidodontidae gen.indet	0	3	1	2	3
Dinictis	1	2	1	1	0
Hoplophoneus	1	0	1	0	0
Nimravidae gen.indet	1	1	1	2	1
Eotylopus	1	1	0	0	0
Amphicaenopus	0	0	0	0	0
Penetrigonias	0	0	0	0	0
Subhyracodon	1	1	1	1	0
Trigonias	4	2	0	0	0
Rhinocerotineae gen.indet	1	6	2	1	1
Colodon	0	0	0	0	0
Perchoerus	4	2	0	0	0

Table C3. 95% confidence intervals with mean values for each Schultz and Stout(1955) zone.

	Chadron B	Chadron C	Orella A	Orella B	Orella C
Agriochoerus	0.6 ± 0.08	1.4 ± 0.15	0.8 ± 0.02	0.1 ± 0.02	0.3 ± 0.02
Aepinacodon	3.8 ± 0.52	1.0 ± 0.04	0.0 ± 0.00	0.3 ± 0.03	0.0 ± 0.00
Megacerops	17.7 ± 2.75	4.3 ± 0.63	0.0 ± 0.00	0.0 ± 0.00	0.0 ± 0.00
Paratylopus	0.0 ± 0.00	0.0 ± 0.00	1.0 ± 0.02	3.2 ± 0.22	1.5 ± 0.05
Poebrotherium	4.4 ± 0.62	1.9 ± 0.23	4.4 ± 0.20	10.8 ± 0.83	6.2 ± 0.31
Camelidae gen.indet	0.0 ± 0.00	1.0 ± 0.03	0.5 ± 0.02	1.9 ± 0.09	1.4 ± 0.04
Archaeotherium	9.5 ± 1.43	5.8 ± 0.87	2.2 ± 0.09	1.6 ± 0.08	1.2 ± 0.03
Mesohippus	31.6 ± 4.97	17.8 ± 2.84	15.3 ± 0.77	17.9 ± 1.39	7.2 ± 0.37
Hyracodon	4.4 ± 0.62	9.1 ± 1.42	3.0 ± 0.13	7.2 ± 0.54	4.6 ± 0.23
Leptomeryx	12.0 ± 1.84	1.9 ± 0.23	48.0 ± 2.47	24.3 ± 1.91	51.5 ± 2.80
Merycoidodon	2.5 ± 0.32	28.4 ± 4.57	13.0 ± 0.65	15.3 ± 1.19	12.8 ± 0.67
Miniochoerus	0.0 ± 0.00	7.2 ± 1.11	4.5 ± 0.21	10.3 ± 0.78	8.0 ± 0.41
Merycoidodontidae g	0.0 ± 0.00	2.9 ± 0.32	1.0 ± 0.01	2.3 ± 0.12	3.0 ± 0.12
Dinictis	1.3 ± 0.09	1.9 ± 0.15	1.4 ± 0.04	0.8 ± 0.03	0.3 ± 0.02
Hoplophoneus	0.6 ± 0.08	0.5 ± 0.07	0.8 ± 0.02	0.3 ± 0.03	0.3 ± 0.02
Nimravidae gen.inde	0.6 ± 0.08	1.4 ± 0.11	1.4 ± 0.04	1.9 ± 0.09	0.6 ± 0.02
Eotylopus	1.3 ± 0.09	1.4 ± 0.15	0.0 ± 0.00	0.1 ± 0.02	0.0 ± 0.00
Amphicaenopus	0.0 ± 0.00	0.0 ± 0.00	0.1 ± 0.01	0.0 ± 0.00	0.0 ± 0.00
Penetrigonias	0.0 ± 0.00	0.0 ± 0.00	0.1 ± 0.01	0.0 ± 0.00	0.0 ± 0.00
Subhyracodon	0.6 ± 0.08	1.4 ± 0.15	0.7 ± 0.02	0.5 ± 0.04	0.3 ± 0.02
Trigonias	4.4 ± 0.62	2.4 ± 0.31	0.1 ± 0.02	0.0 ± 0.00	0.0 ± 0.00
Rhinocerotineae gen	0.6 ± 0.08	5.8 ± 0.72	1.6 ± 0.05	1.2 ± 0.04	0.8 ± 0.02
Colodon	0.0 ± 0.00	0.5 ± 0.07	0.1 ± 0.01	0.0 ± 0.00	0.0 ± 0.00
Perchoerus	3.8 ± 0.52	1.9 ± 0.23	0.1 ± 0.01	0.1 ± 0.02	0.0 ± 0.00

Table C4. Percent change from one interval to the next without *Leptomeryx*. Intervals from Schultz and Stout(1955). % decrease = Decrease ÷ Original Number × 100. % increase = Increase ÷ Original Number × 100.

Percent change	Chadron B to C	Chadron C to Orella A	Orella A to B	Orella B to C
Agriochoerus	127.88	-44.94	-83.21	144.46
Aepinacodon	-74.68	-100.00		-100.00
Megacerops	-75.58	-100.00		
Paratylopus			208.14	-53.15
Poebrotherium	-56.59	128.71	145.55	-42.66
Camelidae gen.indet		-42.82	239.53	-23.17
Archaeotherium	-39.23	-61.88	-27.24	-22.59
Mesohippus	-43.79	-13.80	16.52	-59.86
Hyracodon	106.18	-67.23	140.54	-35.72
Leptomeryx	-84.01	2396.76	-49.46	112.22
Merycoidodon	1020.43	-54.13	17.84	-16.67
Miniochoerus		-38.16	130.23	-22.54
Merycoidodontidae gen.indet		-66.12	131.91	32.30
Dinictis	51.92	-26.94	-43.06	-67.41
Hoplophoneus	-24.04	65.18	-66.42	22.23
Nimravidae gen.indet	127.88	-2.59	32.86	-68.57
Eotylopus	13.94	-100.00		-100.00
Amphicaenopus			-100.00	
Penetrigonias			-100.00	
Subhyracodon	127.88	-53.41	-20.63	-51.11
Trigonias	-45.74	-94.92	-100.00	
Rhinocerotineae gen.indet	811.54	-72.47	-24.45	-29.38
Colodon		-87.29	-100.00	
Perchoerus	-49.36	-96.82	118.27	-100.00

Fourth Bin Series Results

Table C5. Abundance of genera within the fourth bin series.

	Bin -2	Bin -1	Bin 0	Bin 1	Bin 2	Bin 3
Agriochoerus	*1*	*0*	*7*	*9*	*5*	*2*
Aepinacodon	*5*	*1*	*2*	*2*	*0*	*0*
Megacerops	*2*	*13*	*12*	*0*	*0*	*0*
Paratylopus	*0*	*0*	*9*	*20*	*36*	*3*
Poebrotherium	*5*	*0*	*18*	*121*	*90*	*29*
Camelidae gen.indet	*0*	*0*	*2*	*19*	*16*	*6*
Archaeotherium	*8*	*6*	*29*	*30*	*17*	*4*
Miohippus	*21*	*18*	*84*	*278*	*129*	*27*
Hyracodon	*5*	*2*	*29*	*71*	*75*	*17*
Merycoidodon	*1*	*3*	*134*	*225*	*171*	*34*
Miniochoerus	*0*	*0*	*43*	*79*	*131*	*19*
Merycoidodontidae gen.indet	*0*	*0*	*38*	*50*	*71*	*33*
Dinictis	*1*	*1*	*10*	*21*	*3*	*1*
Hoplophoneus	*0*	*0*	*5*	*11*	*4*	*2*
Nimravidae gen.indet	*0*	*1*	*11*	*29*	*7*	*3*
Eotylopus	*1*	*3*	*6*	*1*	*0*	*0*
Amphicaenopus	*0*	*0*	*0*	*1*	*0*	*0*
Penetrigonias	*0*	*0*	*1*	*0*	*0*	*0*
Subhyracodon	*0*	*1*	*5*	*10*	*5*	*1*
Trigonias	*3*	*3*	*12*	*1*	*5*	*0*
Rhinocerotineae gen.indet	*0*	*1*	*11*	*32*	*0*	*12*
Colodon	*0*	*0*	*2*	*1*	*0*	*0*
Perchoerus	*1*	*3*	*6*	*0*	*1*	*0*

Table C6. Relative abundance of genera without *Leptomeryx* for within the fourth bin series. Relative abundance is calculated by number of specimens of that genus from that interval divided by total number of specimens in the zone multiplied by 100.

Relative Abundance	Bin -2	Bin -1	Bin 0	Bin 1	Bin 2	Bin 3
Agriochoerus	2	0	1	1	1	1
Aepinacodon	9	2	0	0	0	0
Megacerops	4	23	3	0	0	0
Paratylopus	0	0	2	2	5	2
Poebrotherium	9	0	4	12	12	15
Camelidae gen.indet	0	0	0	2	2	3
Archaeotherium	15	11	6	3	2	2
Miohippus	39	32	18	27	17	14
Hyracodon	9	4	6	7	10	9
Merycoidodon	2	5	28	22	22	18
Miniochoerus	0	0	9	8	17	10
Merycoidodontidae gen.indet	0	0	8	5	9	17
Dinictis	2	2	2	2	0	1
Hoplophoneus	0	0	1	1	1	1
Nimravidae gen.indet	0	2	2	3	1	2
Eotylopus	2	5	1	0	0	0
Amphicaenopus	0	0	0	0	0	0
Penetrigonias	0	0	0	0	0	0
Subhyracodon	0	2	1	1	1	1
Trigonias	6	5	3	0	1	0
Rhinocerotineae gen.indet	0	2	2	3	0	6
Colodon	0	0	0	0	0	0
Perchoerus	2	5	1	0	0	0

Table C7. 95% confidence intervals with mean values for the fourth bin series.

	Bin -2	Bin -1	Bin 0	Bin 1	Bin 2	Bin 3
Agriochoerus	2 ± 0.34	0.00 ± 0.00	1.47 ± 0.07	0.89 ± 0.02	0.65 ± 0.03	1.04 ± 0.03
Aepinacodon	9 ± 2.35	1.79 ± 0.31	0.42 ± 0.04	0.20 ± 0.02	0.00 ± 0.00	0.00 ± 0.00
Megacerops	4 ± 0.85	23.21 ± 6.00	2.52 ± 0.18	0.00 ± 0.00	0.00 ± 0.00	0.00 ± 0.00
Paratylopus	0 ± 0.00	0.00 ± 0.00	1.89 ± 0.12	1.98 ± 0.09	4.70 ± 0.30	1.55 ± 0.13
Poebrotherium	9 ± 2.35	0.00 ± 0.00	3.78 ± 0.29	11.97 ± 0.71	11.75 ± 0.80	15.03 ± 2.05
Camelidae gen.in	0 ± 0.00	0.00 ± 0.00	0.42 ± 0.04	1.88 ± 0.08	2.09 ± 0.11	3.11 ± 0.36
Archaeotherium	15 ± 3.85	10.71 ± 2.70	6.09 ± 0.50	2.97 ± 0.15	2.22 ± 0.12	2.07 ± 0.21
Miohippus	39 ± 10.33	32.14 ± 8.36	17.65 ± 1.54	27.50 ± 1.66	16.84 ± 1.16	13.99 ± 1.91
Hyracodon	9 ± 2.35	3.57 ± 0.80	6.09 ± 0.50	7.02 ± 1.17	9.79 ± 0.66	8.81 ± 1.17
Merycoidodon	2 ± 0.34	5.36 ± 1.28	28.15 ± 2.49	22.26 ± 1.55	22.32 ± 1.55	17.62 ± 2.42
Miniochoerus	0 ± 0.00	0.00 ± 0.00	9.03 ± 0.77	7.81 ± 1.18	17.10 ± 1.18	9.84 ± 1.32
Merycoidodontid	0 ± 0.00	0.00 ± 0.00	7.98 ± 0.67	4.95 ± 0.27	9.27 ± 0.62	17.10 ± 2.35
Dinictis	2 ± 0.34	1.79 ± 0.31	2.10 ± 0.14	2.08 ± 0.09	0.39 ± 0.03	0.52 ± 0.07
Hoplophoneus	0 ± 0.00	0.00 ± 0.00	1.05 ± 0.02	1.09 ± 0.02	0.52 ± 0.04	1.04 ± 0.03
Nimravidae gen.i	0 ± 0.00	1.79 ± 0.31	2.31 ± 0.16	2.87 ± 0.14	0.91 ± 0.02	1.55 ± 0.13
Eotylopus	2 ± 0.34	5.36 ± 1.28	1.26 ± 0.05	0.10 ± 0.02	0.00 ± 0.00	0.00 ± 0.00
Amphicaenopus	0 ± 0.00	0.00 ± 0.00	0.00 ± 0.00	0.10 ± 0.02	0.00 ± 0.00	0.00 ± 0.00
Penetrigonias	0 ± 0.00	0.00 ± 0.00	0.21 ± 0.04	0.00 ± 0.00	0.00 ± 0.00	0.00 ± 0.00
Subhyracodon	0 ± 0.00	1.79 ± 0.31	1.05 ± 0.02	0.99 ± 0.01	0.65 ± 0.03	0.52 ± 0.07
Trigonias	6 ± 1.35	5.36 ± 1.28	2.52 ± 0.18	0.10 ± 0.02	0.65 ± 0.03	0.00 ± 0.00
Rhinocerotineae	0 ± 0.00	1.79 ± 0.31	2.31 ± 0.16	3.17 ± 0.16	0.00 ± 0.00	6.22 ± 0.81
Colodon	0 ± 0.00	0.00 ± 0.00	0.42 ± 0.04	0.10 ± 0.02	0.00 ± 0.00	0.00 ± 0.00
Perchoerus	2 ± 0.34	5.36 ± 1.28	1.26 ± 0.05	0.00 ± 0.00	0.13 ± 0.02	0.00 ± 0.00

Table C8. Percent change from one interval to the next of the fourth bin series without *Leptomeryx*. % decrease = Decrease ÷ Original Number × 100. % increase = Increase ÷ Original Number × 100. Blank cells are those with divide by zero errors.

Relative Abundance	Bin -2	Bin -1	Bin 0	Bin 1	Bin 2	Bin 3
Agriochoerus	2	0	1	1	1	1
Aepinacodon	9	2	0	0	0	0
Megacerops	4	23	3	0	0	0
Paratylopus	0	0	2	2	5	2
Poebrotherium	9	0	4	12	12	15
Camelidae gen.indet	0	0	0	2	2	3
Archaeotherium	15	11	6	3	2	2
Miohippus	39	32	18	27	17	14
Hyracodon	9	4	6	7	10	9
Merycoidodon	2	5	28	22	22	18
Miniochoerus	0	0	9	8	17	10
Merycoidodontidae gen.indet	0	0	8	5	9	17
Dinictis	2	2	2	2	0	1
Hoplophoneus	0	0	1	1	1	1
Nimravidae gen.indet	0	2	2	3	1	2
Eotylopus	2	5	1	0	0	0
Amphicaenopus	0	0	0	0	0	0
Penetrigonias	0	0	0	0	0	0
Subhyracodon	0	2	1	1	1	1
Trigonias	6	5	3	0	1	0
Rhinocerotineae gen.indet	0	2	2	3	0	6
Colodon	0	0	0	0	0	0
Perchoerus	2	5	1	0	0	0

Appendix D: NALMA Abundance Figures

Table D1. Abundance of genera within the NALMA.

	Chadron	Orellan
Agriochoerus	4	19
Aepinacodon	8	2
Megacerops	37	0
Paratylopus	0	64
Poebrotherium	11	248
Camelidae gen.indet	2	45
Archaeotherium	27	67
Mesohippus	87	495
Hyracodon	26	174
Merycoidodon	63	524
Miniochoerus	15	272
Merycoidodontidae gen.indet	6	79
Dinictis	6	33
Hoplophoneus	2	20
Nimravidae gen.indet	4	46
Eotylopus	5	1
Amphicaenopus	0	1
Penetrigonias	0	1
Subhyracodon	4	19
Trigonias	12	2
Rhinocerotineae gen.indet	13	48
Colodon	1	1
Perchoerus	10	2

Table D2. Relative abundance of well sampled genera without *Leptomeryx* for each NALMA. Relative abundance is calculated by number of specimens of that genus from that interval divided by total number of specimens in the zone multiplied by 100.

	Chadron	Orellan	Decrease in %
Agriochoerus	1	1	33
Aepinacodon	2	0	2422
Megacerops	11	0	
Paratylopus	0	3	-100
Poebrotherium	3	11	-72
Camelidae gen.indet	1	2	-72
Archaeotherium	8	3	154
Mesohippus	25	23	11
Hyracodon	8	8	-6
Merycoidodon	18	24	-24
Miniochoerus	4	13	-65
Merycoidodontidae gen.indet	2	4	-52
Dinictis	2	2	15
Hoplophoneus	1	1	-37
Nimravidae gen.indet	1	2	-45
Eotylopus	1	0	3053
Amphicaenopus	0	0	-100
Penetrigonias	0	0	-100
Subhyracodon	1	1	33
Trigonias	3	0	3684
Rhinocerotineae gen.indet	4	2	71
Colodon	0	0	531
Perchoerus	3	0	3053

Table D3. 95% confidence intervals with mean values for each NALMA.

	Chadron	Orellan
Agriochoerus	0.6 ± 1.17	0.9 ± 0.01
Aepinacodon	3.8 ± 2.33	0.1 ± 0.01
Megacerops	17.7 ± 10.79	0.0 ± 0.00
Paratylopus	0.0 ± 0.00	3.0 ± 0.10
Poebrotherium	4.4 ± 3.21	11.5 ± 0.46
Camelidae gen.indet	0.0 ± 0.58	2.1 ± 0.06
Archaeotherium	9.5 ± 7.87	3.1 ± 0.11
Mesohippus	31.6 ± 25.36	22.9 ± 0.94
Hyracodon	4.4 ± 7.58	8.0 ± 0.32
Merycoidodon	12.0 ± 18.37	24.2 ± 1.00
Miniochoerus	2.5 ± 4.37	12.6 ± 0.51
Merycoidodontidae g	0.0 ± 1.75	3.7 ± 0.13
Dinictis	0.0 ± 1.75	1.5 ± 0.04
Hoplophoneus	1.3 ± 0.58	0.9 ± 0.01
Nimravidae gen.inde	0.6 ± 1.17	2.1 ± 0.07
Eotylopus	0.6 ± 1.46	0.0 ± 0.01
Amphicaenopus	1.3 ± 0.00	0.0 ± 0.01
Penetrigonias	0.0 ± 0.00	0.0 ± 0.01
Subhyracodon	0.0 ± 1.17	0.9 ± 0.01
Trigonias	0.6 ± 3.50	0.1 ± 0.01
Rhinocerotineae gen	4.4 ± 3.79	2.2 ± 0.07
Colodon	0.6 ± 0.29	0.0 ± 0.01
Perchoerus	0.0 ± 2.92	0.1 ± 0.01

Table D4. chord distance (CRD) between without *Leptomeryx* for each NALMA.

Chord Distance	Chadron	Orellan
Chadron	0.00	0.96
Orellan	0.96	0.00

Table D5. Diversity Indices of well sampled taxa for each NALMA without *Leptomeryx* in the dataset.

	Chadron	Lower	Upper	Orellan	Lower	Upper
Taxa_S	20.00	17.00	20.00	22.00	13.00	20.00
Individuals	90.00	90.00	90.00	92.00	92.00	92.00
Dominance_D	0.13	0.08	0.14	0.15	0.10	0.16
Simpson_1-D	0.87	0.86	0.92	0.85	0.84	0.90
Shannon_H	2.41	2.06	2.42	2.20	1.91	2.29
Evenness_e^H/S	0.55	0.43	0.57	0.41	0.44	0.59
Brillouin	1.69	1.74	2.05	1.61	1.65	1.97
Menhinick	2.00	1.70	2.00	2.20	1.30	2.00
Margalef	4.22	3.56	4.22	4.64	2.65	4.20
Equitability_J	0.80	0.71	0.81	0.71	0.71	0.80
Fisher_alpha	7.52	6.20	7.97	8.72	4.13	7.87
Berger-Parker	0.25	0.17	0.30	0.24	0.18	0.30
Chao-1	20.00	19.50	42.50	22.00	14.20	46.50

Appendix E: Combined Bins Before and After Climate Shift

Fourth Combined Bin Series

Table E1. Abundance of genera within the fourth combined bin series.

	Bins -2--1	Bin 0	Bins 1-3
Paratylopus	0	9	59
Poebrotherium	5	18	240
Archaeotherium	14	29	51
Mesohippus	39	84	434
Hyracodon	7	29	163
Merycoidodon	4	134	430
Miniochoerus	0	43	229

Table E2. Relative abundance of genera without *Leptomeryx* for within the fourth combined bin series. Relative abundance is calculated by number of specimens of that genus from that interval divided by total number of specimens in the zone multiplied by 100.

	Bins -2--	Bin 0	Bins 1-3
Paratylopus	0	3	4
Poebrotherium	7	5	15
Archaeotherium	20	8	3
Mesohippus	57	24	27
Hyracodon	10	8	10
Merycoidodon	6	39	27
Miniochoerus	0	12	14

Table E3. 95% confidence intervals with mean values for the fourth combined bin series.

	Bins -2-0	Bin 1	Bins 2-3
Paratylopus	0 ± 0.00	2.60 ±	3.67 ± 0.15
Poebrotherium	7 ± 1.60	5.20 ±	14.94 ± 0.71
Archaeotherium	20 ± 4.70	8.38 ±	3.18 ± 0.13
Mesohippus	57 ± 13.31	24.28 ±	27.02 ± 1.30
Hyracodon	10 ± 2.29	8.38 ±	10.15 ± 0.47
Merycoidodon	6 ± 1.25	38.73 ±	26.77 ± 1.29
Miniochoerus	0 ± 0.00	12.43 ±	14.26 ± 0.67

Table E4. chord distance (CRD) between without *Leptomeryx* for the fourth combined bin series.

	Bins -2--1	Bin 0	Bins 1-3
Bins -2--1	0.00	0.90	0.85
Bin 0	0.90	0.00	0.35
Bins 1-3	0.85	0.35	0.00

Table E5. Diversity Indices for the fourth combined bin series without *Leptomeryx* in the dataset

	Bins -2--1	Lower	Upper	Bin 0	Lower	Upper	Bins 1-3	Lower	Upper
Taxa_S	15.00	14.00	15.00	22.00	17.00	22.00	21.00	13.00	20.00
Individuals	90.00	90.00	90.00	92.00	92.00	92.00	91.00	91.00	91.00
Dominance_D	0.18	0.11	0.20	0.14	0.09	0.15	0.14	0.10	0.15
Simpson_1-D	0.82	0.80	0.89	0.86	0.85	0.91	0.86	0.85	0.90
Shannon_H	2.14	1.81	2.17	2.41	2.09	2.47	2.23	1.95	2.30
Evenness_e^H/S	0.57	0.42	0.59	0.51	0.42	0.57	0.44	0.45	0.60
Brillouin	1.48	1.53	1.86	1.78	1.78	2.12	1.60	1.68	1.97
Menhinick	1.50	1.40	1.50	2.20	1.70	2.20	2.10	1.30	2.00
Margalef	3.11	2.89	3.11	4.64	3.54	4.64	4.43	2.66	4.21
Equitability_J	0.79	0.68	0.80	0.78	0.71	0.81	0.73	0.72	0.81
Fisher_alpha	4.89	4.64	5.14	8.72	6.13	9.16	8.11	4.15	7.92
Berger-Parker	0.35	0.23	0.41	0.28	0.18	0.33	0.22	0.17	0.28
Chao-1	15.00	14.25	29.00	22.00	19.43	48.50	21.00	14.50	46.50

Appendix F: Principle Components Analysis
Schultz and Stout

Table F1. Principle components analysis of Schultz and Stout Zones without *Leptomeryx* in dataset.

	PC 1	PC 2	PC 3	PC 4	PC 5		PC	Eigenvalu	% variance
Agriochoerus	-7.5795	-0.58982	0.84809	-1.2409	-0.47668		1	204.739	75.954
Aepinacodon	-7.4881	2.9714	0.26278	0.38822	0.099313		2	51.8248	19.226
Megacerops	-0.37438	16.531	2.408	5.1725	-0.35904		3	9.30428	3.4517
Paratylopus	-5.3017	-2.59	-3.0307	-0.86598	0.40887		4	3.36722	1.2492
Poebrotherium	9.6387	-4.0039	-9.081	0.92993	-0.07377		5	0.319854	0.11866
Camelidae gen.indet	-6.2528	-2.4054	-1.2901	0.031732	-0.05965				
Archaeotherium	1.1423	6.5408	2.5259	1.1384	-0.57425				
Mesohippus	44.222	18.177	-2.2496	-3.2115	0.062903				
Hyracodon	7.7756	-3.0667	0.034723	2.7538	1.8066				
Merycoidodon	37.834	-16.971	7.1171	0.21541	-0.35932				
Miniochoerus	11.42	-10.696	-4.9221	2.6072	-0.33265				
Merycoidodontidae gen.indet	-3.3369	-4.1212	-0.6949	1.5616	-1.0708				
Dinictis	-6.1362	-0.13461	0.80736	-1.9591	-0.14374				
Hoplophoneus	-7.9223	-0.46195	-0.03326	-1.433	-0.68105				
Nimravidae gen.indet	-5.6715	-1.1748	-0.46419	-1.9183	0.35711				
Eotylopus	-8.4121	0.36346	0.89649	-0.26266	0.38759				
Amphicaenopus	-9.5927	-0.66258	-0.11016	-1.0006	-0.13849				
Penetrigonias	-9.5927	-0.66258	-0.11016	-1.0006	-0.13849				
Subhyracodon	-7.5212	-0.60647	0.58406	-1.1509	0.036557				
Trigonias	-6.6276	3.4261	1.6103	0.6848	0.19062				
Rhinocerotineae gen.indet	-3.7589	-1.9629	3.4578	-1.0209	0.77772				
Colodon	-9.382	-0.73895	0.28425	-0.90785	0.021708				
Perchoerus	-7.0821	2.8403	1.1494	0.48893	0.25899				

Table F2. Principle components analysis of Schultz and Stout Zones with *Leptomeryx* in dataset.

	PC 1	PC 2	PC 3	PC 4	PC 5		PC	Eigenvalu	% variance
Agriochoerus	-7.2597	-2.9236	-0.16596	-0.84593	-0.60206		1	262.489	73.877
Aepinacodon	-7.265	-0.81824	-2.5761	-0.44321	0.19061		2	59.2754	16.683
Megacerops	-3.7312	10.56	-9.8382	-2.6158	2.5955		3	28.6579	8.0657
Paratylopus	-5.5557	-4.1086	-0.03642	2.1485	-0.41233		4	4.01646	1.1304
Poebrotherium	3.6697	-0.71771	-0.22149	6.234	0.59938		5	0.864844	0.24341
Camelidae gen.indet	-6.2637	-3.6736	0.36829	0.78299	0.053167				
Archaeotherium	-2.6044	5.4127	-3.0136	-2.1124	0.55822				
Mesohippus	22.268	26.583	-7.2294	2.0943	-1.7977				
Hyracodon	1.5397	3.7452	4.0254	1.0983	1.306				
Leptomeryx	66.081	-15.501	-4.9905	-1.3352	0.074667				
Merycoidodon	18.491	11.247	19.747	-2.6743	0.020383				
Miniochoerus	4.4299	-1.2295	6.3734	3.7973	1.4482				
Merycoidodontidae gen.indet	-4.5607	-3.0548	1.7818	0.079929	0.90198				
Dinictis	-6.4483	-2.1457	-0.1776	-0.62757	-1.0107				
Hoplophoneus	-7.3528	-3.479	-0.79622	-0.37555	-0.67674				
Nimravidae gen.indet	-6.0484	-2.7888	0.17572	0.46572	-0.9983				
Eotylopus	-7.8127	-2.2596	-0.54554	-0.60968	-0.15933				
Amphicaenopus	-8.3299	-4.0201	-0.70274	-0.1531	-0.48639				
Penetrigonias	-8.3299	-4.0201	-0.70274	-0.1531	-0.48639				
Subhyracodon	-7.2254	-2.8084	-0.06852	-0.45191	-0.59255				
Trigonias	-6.9328	0.41118	-2.0852	-1.2669	0.31879				
Rhinocerotineae gen.indet	-5.3678	-0.40878	3.001	-1.779	-0.61249				
Colodon	-8.2566	-3.7297	-0.37202	-0.32702	-0.45418				
Perchoerus	-7.1348	-0.27166	-1.9509	-0.93023	0.22232				

Fourth Bin Series Principle Components Analysis

Table F3. Principle components analysis with *Leptomeryx* in dataset.

	PC 1	PC 2	PC 3	PC 4	PC 5	PC 6		PC	Eigenvalu	% variance
Agriochoerus	-8.0979	-0.28744	-1.4023	-1.4424	0.52293	0.15413		1	208.316	66.344
Aepinacodon	-5.2378	-6.1439	-5.2266	-2.1893	-0.01205	1.9564		2	77.0266	24.531
Megacerops	1.0135	-15.243	12.322	5.3802	-1.409	-0.30466		3	16.6416	5.3
Paratylopus	-6.56	2.7338	-0.23012	-1.1201	-2.2615	-0.69773		4	6.6482	2.1173
Poebrotherium	10.377	8.1257	-8.6123	4.1751	-0.27041	-2.2293		5	3.1182	0.99307
Camelidae gen.indet	-7.686	1.8781	-1.1322	0.71229	-0.03893	-1.2505		6	2.24435	0.71477
Archaeotherium	5.8317	-10.457	-1.5052	-1.7795	0.5712	3.9342				
Mesohippus	51.058	-17.581	-2.9288	-0.5899	0.25535	-1.5966				
Hyracodon	7.5144	2.728	-3.9145	0.85222	-1.6311	1.3518				
Merycoidodon	28.22	22.37	8.4346	-4.6946	1.9391	0.30541				
Miniochoerus	6.4542	13.713	0.78081	0.4991	-5.8096	0.44294				
Merycoidodontidae gen.indet	3.9894	12.638	-0.79783	6.9282	2.3184	2.9282				
Dinictis	-6.8706	-1.2578	-0.03077	-1.7942	0.86787	-0.73083				
Hoplophoneus	-9.0901	0.51608	-0.4157	-0.97718	0.54065	-0.75994				
Nimravidae gen.indet	-6.754	0.46619	0.98441	-0.99233	1.0681	-1.5808				
Eotylopus	-7.1008	-4.2482	2.042	-0.04229	-0.08559	-0.00729				
Amphicaenopus	-10.506	-0.53991	-0.5908	-1.0194	0.012075	-0.71165				
Penetrigonias	-10.472	-0.4982	-0.49452	-1.0959	0.05886	-0.52753				
Subhyracodon	-8.573	-0.68944	0.78382	-0.70379	0.04789	-0.91615				
Trigonias	-4.6068	-5.5242	0.20975	-1.2643	-0.21115	1.7418				
Rhinocerotineae gen.indet	-5.4612	1.938	0.088231	2.3941	3.5915	-1.0802				
Colodon	-10.343	-0.42338	-0.41304	-1.2211	0.15255	-0.50153				
Perchoerus	-7.0983	-4.2136	2.0492	-0.01496	-0.21718	0.079813				

Table F4. Principle components analysis without *Leptomeryx* in dataset.

	PC 1	PC 2	PC 3	PC 4	PC 5	PC 6		PC	Eigenvalu	% variance
Agriochoerus	-8.1882	-1.468	-1.2337	-1.1116	0.07857	-0.12194		1	243.335	54.924
Aepinacodon	-7.3762	1.0155	5.1908	-3.7063	-0.9009	-0.77566		2	108.865	24.572
Megacerops	-2.4081	-0.57415	9.1382	12.621	-0.55173	0.38253		3	76.5225	17.272
Paratylopus	-6.7749	-2.4428	-3.1279	-0.46035	0.45548	-1.3069		4	11.8527	2.6753
Poebrotherium	3.7485	1.6483	-0.218	-6.9002	-2.9846	0.17612		5	1.37947	0.31136
Camelidae gen.indet	-7.5436	-2.6238	-2.9156	-0.47698	-1.0847	-0.23483		6	1.08664	0.24527
Archaeotherium	-0.64042	4.6425	11.151	-1.1927	1.4085	0.43603				
Mesohippus	25.749	21.594	27.892	-1.4543	0.19535	0.039407				
Hyracodon	1.7612	1.5933	2.6353	-3.9632	0.59181	-0.17473				
Leptomeryx	55.459	-30.467	-1.0588	0.80151	-0.41642	-0.39135				
Merycoidodon	29.73	31.755	-24.381	2.6171	-0.34653	-0.21783				
Miniochoerus	2.7333	-2.3898	-6.3315	-1.99	3.6567	-1.3811				
Merycoidodontidae gen.indet	1.5523	-3.9093	-5.4412	-2.4068	1.5491	3.8614				
Dinictis	-7.525	-0.64214	-0.89251	0.15255	0.2205	-0.0904				
Hoplophoneus	-8.6318	-2.1146	-2.5882	-0.13921	-0.17829	-0.12905				
Nimravidae gen.indet	-7.1545	-1.2258	-2.5455	0.99046	0.13339	0.15985				
Eotylopus	-7.5754	-1.5147	1.1104	2.3794	-0.12223	-0.1674				
Amphicaenopus	-9.6109	-2.4667	-2.1537	-0.03909	-0.55236	-0.52737				
Penetrigonias	-9.5739	-2.4655	-2.1472	-0.03998	-0.37875	-0.46071				
Subhyracodon	-8.3181	-2.069	-1.8659	1.0285	-0.17043	-0.32603				
Trigonias	-6.3691	-0.03427	3.6515	0.43558	0.63662	-0.19951				
Rhinocerotineae gen.indet	-5.9928	-1.8806	-2.8057	0.52157	-0.90002	2.0664				
Colodon	-9.4931	-2.3772	-2.1925	-0.03214	-0.24929	-0.40772				
Perchoerus	-7.5569	-1.5837	1.13	2.365	-0.08971	-0.20924				